UCLA
UCLA Electronic Theses and Dissertations

Title

How and Why We Comfort Others: Neural Mechanisms of Prosocial Allogrooming

Permalink

https://escholarship.org/uc/item/71d962ns

Author

Lim, Kayla Y

Publication Date

2025

Peer reviewed|Thesis/dissertation

eScholarship.org Powered by the California Digital Library
University of California

UNIVERSITY OF CALIFORNIA
Los Angeles

How and Why We Comfort Others:
Neural Mechanisms of Prosocial Allogrooming

A dissertation submitted in partial satisfaction of the requirements for the degree
Doctor of Philosophy in Molecular, Cellular, and Integrative Physiology

by

Kayla Ying Yan Lim

2025

© Copyright by

Kayla Ying Yan Lim

2025

ABSTRACT OF THE DISSERTATION

How and Why We Comfort Others: Neural Mechanisms of Prosocial Allogrooming

by

Kayla Ying Yan Lim

Doctor of Philosophy in Molecular, Cellular, and Integrative Physiology

University of California, Los Angeles, 2025

Professor Weizhe Hong, Chair

Comforting is a critical form of prosocial behavior, expressed as affiliative social touch directed toward distressed individuals. These behaviors play a key role in promoting emotional recovery and maintaining social cohesion. While extensively studied in humans, comforting has only recently been examined in rodents, where it offers a tractable model system for dissecting the underlying neural mechanisms.

Chapters 1 and 2 establish the conceptual and methodological framework for this dissertation. Chapter 1 outlines the conceptual frameworks and roots of comforting behavior. Chapter 2 focuses on the behavioral expression of comforting in mice, characterizing its core features and motivational underpinnings, and synthesizes emerging evidence from rodent models regarding the neurobiology of how animals detect and respond to the distress of conspecifics and the mechanisms mediating social buffering effect of comforting behavior.

Subsequent chapters present a series of experimental findings that reveal a shared behavioral and neural architecture supporting comforting behavior in mice. Individual differences in parenting behavior predict variation in adult-directed prosocial comforting, measured as

allogrooming toward stressed conspecifics. These two behaviors recruit partially overlapping neuronal populations in the MPOA. Through calcium imaging and a series of functional manipulation experiments, a shared MPOA-to-ventral tegmental area (VTA) projection is identified as a critical circuit element supporting both pup grooming and adult-directed prosocial behavior. Neuronal ensembles engaged during pup interaction are shown to be functionally necessary for allogrooming, suggesting that evolutionarily conserved caregiving circuits may be recruited to support broader forms of prosocial behavior. The final chapter extends this framework to examine how mice respond to social partners experiencing other negative internal states, including immune-induced sickness and nausea-like visceral malaise. Across all conditions, subject animals display increased allogrooming and sustained physical proximity (huddling) toward affected partners. Furthermore, the distribution of grooming across different body regions varies depending on the conspecific's condition, suggesting that mice may be sensitive to somatic cues and capable of modulating their affiliative responses accordingly.

Together, these findings advance understanding of the neural basis of comforting behavior and highlight the MPOA as a central integrator of caregiving responses across multiple social contexts. This work provides a foundation for further studies into the biological mechanisms of prosociality and the capacity for social animals to respond flexibly to the needs of others.

The dissertation of Kayla Ying Yan Lim is approved.

Mark R. Frye

Laura A. Denardo

Carlos Portera-Cailliau

Weizhe Hong, Committee Chair

University of California, Los Angeles

2025

“Tell Stories Filled With Facts.

Make People Touch and Taste and KNOW.

Make People FEEL! FEEL! FEEL!”

– Octavia E. Butler

TABLE OF CONTENTS

LIST OF TABLES AND FIGURES viii

ACKNOWLEDGEMENTS xi

PREFACE xiv

VITA xv

CHAPTER 1: Introduction 1

CHAPTER 2: Foundations of prosocial comforting in mice 10

CHAPTER 3: Shared neural substrates of comforting and parenting 25

CHAPTER 4: MPOA→VTA circuit controls prosocial allogrooming and parenting 49

CHAPTER 5: Extending comforting towards other distressed states.....82

CHAPTER 6: Conclusions and future directions 97

APPENDIX: Statistical Methods.....108

REFERENCES 109

LIST OF FIGURES

Chapter 1

Figure 1-1: Conceptual differences between empathy and prosocial behavior

Figure 1-2: Comforting touch feedback loop

Chapter 3

Figure 3-1: Behavioral paradigms for measuring prosocial and parenting responses to stressed adults or pups.

Figure 3-2: Parenting and prosocial behaviors are positively correlated in male and female mice.

Figure 3-3: Parenting and prosocial behaviors are positively correlated in mothers and fathers.

Figure 3-4: Pup grooming accounts for the positive correlation between parenting and prosocial allogrooming.

Figure 3-5: Prosocial allogrooming in females does not depend on estrous stage.

Figure 3-6. MPOA neurons represent pups more similarly to stressed adults than to unstressed adults.

Figure 3-7. Prosocial allogrooming and pup grooming engage partially overlapping MPOA neuron populations.

Figure 3-8. Allogrooming and pup grooming elicit partially shared neural representations in the MPOA in males and females.

Chapter 4

Figure 4-1: Chemogenetic inhibition of MPOA^{Vgat+} neurons

Figure 4-2: Photo-inhibition of MPOA^{Vgat+} neurons

Figure 4-3: Photo-activation of MPOA^{Vgat+} neurons

Figure 4-4: Functional manipulations of the MPOA in pup grooming

Figure 4-5: Summary of photo-stimulation of additional molecularly defined MPOA cell types

Figure 4-6: Dopamine release during allogrooming and pup grooming

Figure 4-7: Activation of MPOA^{Vgat+} is associated with positive valence

Figure 4-8: An MPOA^{Vgat+}-VTA pathway controls both allogrooming and parenting behaviors.

Figure 4-9: Selective activation of VTA-projecting MPOA^{Vgat+} neurons drives allogrooming and pupgrooming

Figure 4-10: Activation of MPOA^{Vgat+}-VTA is associated with positive valence

Figure 4-11: Activation of MPOA-PAG pathway promotes pup grooming, but not allogrooming

Figure 4-12: MPOA^{Vgat+}-VTA induced allogrooming is modulated by partner stress state

Figure 4-13: Pup-activated MPOA neurons are required for allogrooming

Chapter 5

Figure 5-1: Validation of LPS-induced sickness and LiCl-induced malaise in mice

Figure 5-2: Behavioral paradigms and body targets of allogrooming

Figure 5-3: Mice display prosocial allogrooming towards sick (LPS) and nauseous (LiCl) partners

Figure 5-4: Mice show increased huddling during interaction with sick, nauseous, and stressed conspecifics

ACKNOWLEDGEMENTS

I would like to express my sincere thanks to my advisor, Dr. Weizhe Hong, for his unwavering patience, support, and guidance throughout my graduate training. Over the past five years, Weizhe has helped me grow as a scholar and a person, challenging me to improve across so many domains. His insight, rigor, and enthusiasm have profoundly shaped my development as a scientist and has showed me that I was capable of more than I ever believed. For that, I am deeply grateful.

I am also immensely thankful to past and present members of the Hong lab for their camaraderie and support. I am especially grateful to Fangmiao for her immense experimental prowess, and to Emily for her sharp thinking and poise. To my undergraduate mentees, Daniel and Lily, thank you for your energy and for reminding me of the joy of seeing science with fresh eyes. I've also learned so much from Tara and Mingmin, whose clarity and thoughtfulness continue to inspire me. And to Nguyen, Ryan, James, and Linfan, thank you for the laughter and friendship that made the hard days easier and the good days better. Nguyen and Ryan: we started in the lab together and I feel incredibly lucky to have shared this chapter of my life with both of you. I also thank all other members of the Hong lab and CHS 7th floor neuroscience community, whose presence shaped this chapter of my scientific life in ways both big and small.

I am deeply grateful to my dissertation committee: Dr. Mark Frye, Dr. Carlos Portera-Cailliau, and Dr. Laura DeNardo. Your thoughtful feedback, encouragement, and support have shaped this dissertation, my graduate training, and my scientific thinking in lasting ways. I especially thank Dr. Frye, who also served as program director for MCIP, and Yesenia for going above and beyond in her steadfast student support throughout the program.

In addition to my work in the lab, I am beyond thankful to have found community in spaces that embrace science as a practice rooted in communication, equity, and social responsibility. Through the Science Policy Group at UCLA, NeuroComm, Knowing Neurons, and more, it has been uniquely fulfilling to work with so many others who share a commitment to bridging science and society in meaningful ways. I am immensely grateful to everyone who shaped these spaces, and especially to Erin, Natalie, Yuki, Bineh, Caitlin, Melis, and Megan for being some of the brightest lights I've had the privilege of leading alongside, whose collaboration and friendship has been a source of joy and growth. I also thank the UCLA Brain Research Institute and Dr. Felix Schweizer for their generous support of these efforts.

I am incredibly grateful to the UCLA-CDU Dana Center for the opportunity to deeply engage with the social and ethical dimensions of science. This fellowship has been a rare and transformative experience that broadened my perspective and strengthened my commitment to community-rooted, reflective science. As a Dana Fellow, I had the joy of learning alongside a cohort of brilliant, thoughtful, and passionate individuals – Erin, Akila, Ana Sofia, Anna, Lily, John, Paola, Sydney, Torrence, Shantee, and Hafifa – I could not have asked for a better group of people to grow with, and I am deeply grateful for each of you. My heartfelt thanks also go to Dr. Ashley Feinsinger and Dr. Amy Woods for their mentorship and kindness. Their care and vision made the fellowship a uniquely transformative part of my graduate training. I also extend my sincere thanks to Rin, Sabrina, Kimberly and everyone at the Center whose steady support and warmth made this experience so memorable and meaningful.

My path into neuroscience was shaped by mentors who believed in me long before I believed in myself – especially Drs. Chiye Aoki, Adrienne Santiago, and Nick Stavropoulos. They welcomed me into the lab and gave me the freedom, encouragement, and confidence to grow as a researcher. I carry the lessons I learned from them with me every day.

To my dear friends and family near and far, thank you for every shared meal, craft night, video call, spontaneous outing, and moment of quiet company. Your steady presence and love anchored me, even when I got lost in the fog. You are too many to name, and too wonderful for my words to capture. I love you all so much, thank you thank you thank you. And to the artist spaces and creative communities that offered moments of grounding and inspiration along the way, I am eternally grateful.

And finally, to Matt (and Bunsen), thank you for being my anchor and my soft place to land. I could not have done this without you.

This work was supported by F31 MH134495 (NIH-NIMH), a Bouchet Scholar Award in 2023, and a Dana Center Fellowship in 2024 awarded to me. This work was also supported by the following grants and fellowships: a Marion Bowen Postdoctoral Grant awarded to Fangmiao Sun, and National Institutes of Health grants R01 MH130941, R01 NS113124, R01 MH132736, RF1 NS132912, and UF1 NS122124, as well as a Vallee Scholar Award and a Mallinckrodt Scholar Award awarded to Weizhe Hong.

PREFACE

Part of the work I present in this thesis has been modified from the following manuscripts:

Some components of Chapter 1, Chapter 2, and the discussion are taken from a review I authored with my advisor Dr. Weizhe Hong published in *Hormones and Behavior* in 2023, titled "Neural mechanisms of comforting: prosocial touch and stress buffering".

Chapter 3 includes some experiments and data generated by other members of the lab, including Fangmiao Sun and Emily Wu. I performed all behavioral experiments included in this chapter. Fangmiao Sun performed all miniscope calcium imaging experiments presented in this chapter (Figs 3-6, 3-7, 3-8). Emily Wu analyzed the imaging data presented in these figures (Figs 3-6, 3-7, 3-8). Lily McLeod and Daniel Fillet performed some of the behavioral annotations presented in this Chapter. Part of Chapter 3, as well as components of the discussion and appendix, are included in a manuscript currently under revision, titled "Shared neural substrates of prosocial and parenting behaviors." I am co-first author on this manuscript with Dr. Fangmiao Sun. Additional co-authors are Dr. James Dang, Dr. Emily Wu, and my advisor, Dr. Weizhe Hong.

Chapter 4 also includes some experiments and data generated by other members of the lab, including Fangmiao Sun and James Dang. I performed all behavioral experiments and all but one of the optogenetic experiments in this chapter. Fangmiao Sun performed and analyzed the data for the fiber photometry, chemogenetic manipulations, and TRAP experiments presented in this Chapter (Figs. 4-1, 4-4a–f, 4-6, 4-11a–c, 4-13). I conducted pilot chemogenetic and TRAP experiments during early stages of the project. James Dang assisted with some of the optogenetics experiments in Chapter 4 (Figs. 4-2 – 4-5). Lily McLeod and Daniel Fillet performed some of the behavioral annotations presented in this Chapter. Part of Chapter 4, as well as components of the discussion and appendix, are also included in the same manuscript.

VITA

EDUCATION

University of California, Los Angeles — 2020 – present
PhD Candidate: Molecular, Cellular, and Integrative Physiology
GPA: 4.00

New York University — 2014 – 2018
Bachelor of Science: Neuroscience, Bachelor of Arts: Psychology
GPA: 3.86

HONORS & AWARDS

UCLA-CDU-Dana Center for Neuroscience and Society Fellow	2024 – present
NIH F31 Ruth L. Kirschstein National Research Service Award	2023 – present
Research! America Civic Engagement Micrograntee	2024
Bouchet Graduate Honors Scholar	2023 – 2024
Science for Public Good Grantee, Union for Concerned Scientists	2023
AAAS Catalyzing Advocacy in Science and Technology (CASE) Fellow	2023
UCLA Graduate Division Dean's Scholar Award	2020 – 2022
NYU University Honors Scholar	2018
Sherrington Award for Neural Science Undergraduate Research	2018

PUBLICATIONS

Sun F*, **Lim KY***, Dang JX, Zhang LI, Wu Y, Hong W. (In revision). Common and distinct neural substrates of prosocial and parenting behaviors. (*Equal contributions)

Raam T., Li Q., Gu L., Elagio G., **Lim KY.**, Zhang X, Correa S., Hong W. (Under review). Neural basis of collective response to environmental challenge.

Li QL, **Lim KY,** Altawell R, Verderose F, Li X, Dong W, Martinez J, Dickman D,, Stavropoulos N. (2025). The Cul3 ubiquitin ligase engages Insomniac as an adaptor to impact sleep and synaptic homeostasis. *PLOS Genetics* 21(1): e1011574. doi: 10.1371/journal.pgen.1011574

Giovanniello, J.R., Paredes, N., Wiener, A. …, **Lim KY,** …, Wassum KM. (2025). A dual-pathway architecture for stress to disrupt agency and promote habit. *Nature* 640, 722–731 doi: 10.1038/s41586-024-08580-w

Herrera S, Sarac C, Vaidya S, …, **Lim KY**, … Corcoran CM, Landa Y. (2024). A Feasibility and Pilot Trial of the Brief Educational Guide for Individuals in Need (BEGIN): Psychoeducation for Individuals at Risk for Psychosis. *Psychological Services*. doi: 10.1037/ser0000843

Lim KY, Hong WZ. (2023). Comforting behavior: prosocial touch and stress buffering. *Hormones and Behavior* 153, 105391. doi: 10.1016/j.yhbeh.2023.105391

Hebner Y, **Lim KY,** Gehred N, Guttman Z. (2023). The Growing Presence of Faith-Based Hospitals in California Restricts Access to Sexual and Reproductive Healthcare. *California Journal of Politics and Policy*. doi: 10.5070/P2cjpp15160083

Li QL, Jang HS, **Lim KY,** Lessing A, Stavropoulos N. (2021) insomniac links the development and function of a sleep regulatory circuit*. eLife.* doi: 10.7554/eLife.65437

Santiago AN, **Lim KY**, Opendak M, Sullivan RM, Aoki C. (2018) Early life trauma increases threat response of peri-weaning rats, reduction of axo-somatic synapses formed by parvalbumin cells and perineuronal net in the basolateral nucleus of amygdala. Journal of Comparative Neurology. doi: 10.1002/cne.24522

SELECT TALKS & PRESENTATIONS

Invited Workshops: UCLA Brain Research Institute, Physiology Department, NSIDP Seminar, Women in Neuroscience (2025)
"Science as Dialogue: Communicating With, Not At"
Los Angeles, CA

Invited Talk: Bouchet National Graduate Honors Society Local Chapter Conference (2024)
"Affiliative caregiving: Hypothalamic regulation of prosocial and parenting behaviors"
Los Angeles, CA

SELECT SERVICE & LEADERSHIP

Co-Director, Neuroscience Communication Affinity Group	2023 – present
President (formerly VP Outreach '21-22), Science Policy Group at UCLA	2022 – 2024
Contributing Illustrator & Editor, Knowing Neurons	2021 – 2024
Volunteer Scientist, Skype a Scientist	2020 – 2022

CHAPTER ONE

Introduction

Why study comforting?

A pat on the shoulder, a gentle embrace; comforting behavior can have a profound impact on mitigating an individual's negative emotional state. Comforting, or consoling, is commonly characterized by affiliative social touch aimed at relieving the distress of others and is an important form of prosocial behavior that is essential for fostering social cohesion and improving the physical and emotional health of social species[1–5]. In recent decades, adults have reported experiencing more frequent and severe daily stressors, with greater emotional distress and perceived impacts on their well-being[6]. Prosocial actions that provide comfort and support are therefore of growing importance for alleviating distress and fostering healthier, more connected communities.

Across cultures and species, extensive research has shown that offering comfort through physical contact is a powerful form of social support[7–9] In humans, comforting behavior appears early in childhood[10–12] and may involve various forms of gentle social touch, such as patting, caressing and hugging. These forms of gentle touch are often seen as an expression of empathic or sympathetic concern for the other [13,14] and may serve to reduce stress in the recipient[15].

Empathy and prosocial behavior: related but distinct

Prosocial behavior refers broadly to any behavior that benefits another individual. In both human and non-human species, this can include a range of actions such as comforting (addressing emotional distress), targeted helping (assisting in goal-directed tasks), and sharing (providing material support) – each corresponding to different categories of recipient need[2].

It is important to note that although empathy and prosocial behavior are inter-connected, they are distinct concepts that do not always co-occur and should not be conflated.

Empathy broadly refers to the process of feeling, recognizing, and understanding others' emotional states and perspectives, whereas prosocial behavior refers to the behavioral actions that address others' needs and improve their conditions (Fig. 1-1). Prosocial behavior is an essential step beyond feeling and understanding others – simply experiencing and understanding others emotional states provides limited value to those in need if the observers do not take action to provide assistance and address those needs. While empathic processes may motivate prosocial responses in many contexts, prosocial behaviors can also arise through reflexive, socially learned, or goal-directed mechanisms that do not rely on empathy.

Although several recent reviews have provided comprehensive discussions of empathy-related processes—including the perception and social transfer of negative emotional states[1,16–20], there has been limited attention to prosocial comforting behavior. This dissertation focuses on the expression and mechanisms of comforting, with primary emphasis on recent advances in rodent models, to help fill this gap in the literature.

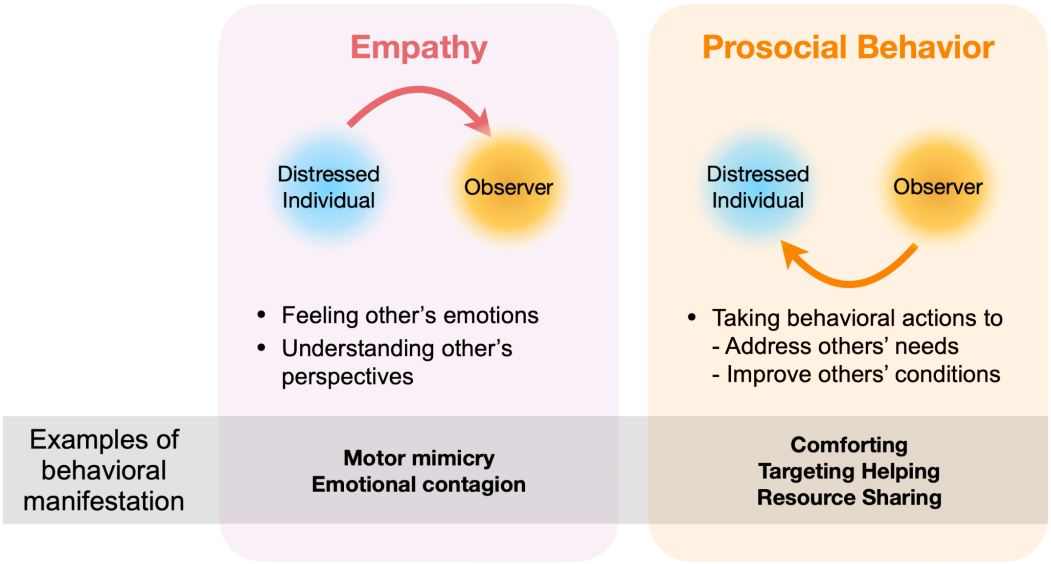

Figure 1-1. Conceptual differences between empathy and prosocial behavior. Empathy involves feeling, recognizing, and understanding others' emotional states and perspectives, while prosocial behavior encompasses the crucial step of taking actions to address their needs and improve their conditions.

Behavioral motivations

In order to engage in comforting behavior, a helper must first perceive the distress signals that an animal in distress produces. The distressed state, which is characterized by experiencing anxiety and emotional or physical discomfort, activates the neuroendocrine sympatho-adrenomedullary and hypothalamic-pituitary-adrenal systems and produces physiological and behavioral changes in response to stress[21]. These changes may then be sensed by the helper through multiple sensory modalities. For example, stress information can be transmitted through volatile chemical signals in rats and mice through feces, urine, saliva, tear, and other bodily fluids largely produced by facial or anogenital glands[22–25]. Chemical signals released by a distressed animal are sufficient to trigger an increase in comforting behavior[26]. In addition to olfactory cues, visual inputs may also contribute to observational contagious pain and consolation behavior[27]. In humans, others' stress is largely communicated by visual and auditory cues, where negative emotional facial expressions can elicit a prosocial response[28] and watching other people experience pain increased the helper's effort to alleviate their partner's pain through hand holding[29].

After perceiving distress signals, this perception of another's distressed state may elicit a behavioral and physiological affective state-matching between the helper and distressed target (emotional contagion), then potentially followed by other-oriented empathic concern[1,13,30]. Indeed, helpers exposed to a distressed conspecific show more anxiety-like behaviors and elevated plasma corticosterone that match the recipient's responses[31–33]. Similarly, helpers exposed to a conspecific that received surgery exhibit more anxiety-like

behaviors and increased serum and brain pro-inflammatory cytokines matching the recipient's responses[34].

Although the phenomenon of emotional contagion has been well-documented in animal studies, it can be difficult to distinguish an other-oriented empathic motivation to relieve others' distress, from a self-serving motivation (e.g., self-soothing) aimed at alleviating the personal unpleasantness of sharing the distress of the other (Fig. 1-2, helper). Instead, considering prosocial comforting from a consequentialist perspective may allow us to assess comforting without imposing assumptions of intentions. Specifically, a behavioral action can be defined as prosocial comforting as long as 1) the action is induced by another's distress and 2) helps to alleviate stress or improve the negative state of the recipient individual, regardless of the motivations or intentions behind it. In rodents, the fact that prosocial allogrooming reduces behavioral measures of anxiety[26,31,34] suggests that the behavior is indeed beneficial to the recipient. In multiple non-human primate and ungulate species, receiving allogrooming induces behavioral and physiological changes indicative of stress reduction. Being groomed reduces heart rates[35–38] and behavioral measures of stress[39]. In monkeys, receiving allogrooming can also release beta-endorphins in cerebrospinal fluid that in humans are reported to be pleasurable and released during social touch activities such as massage[40–42]. In fact, even experimental imitation of allogrooming can similarly reduce heart rate[43] and promotes behavioral cues and facial expressions reflective of a positive emotional state[44].

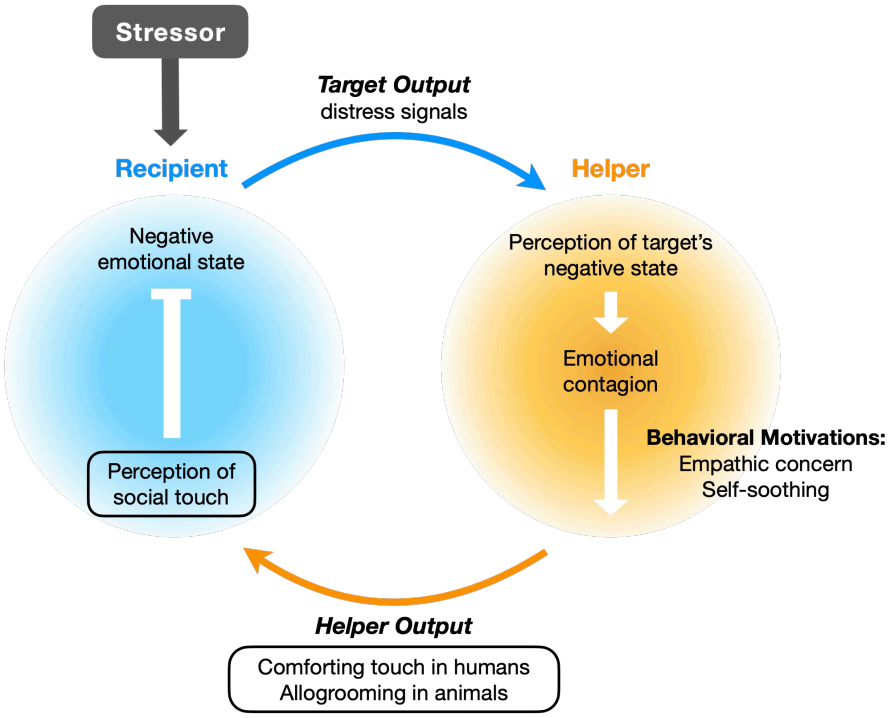

Figure 1-2. Comforting touch feedback loop. A stressor commences the loop, activating distress circuits and stress responses in the recipient. This triggers perception of distress signals by the helper, leading to emotional contagion driving behavioral motivations like empathic concern or self-soothing for a behavioral decision. The helper initiates social touch/allogrooming, which is perceived by the recipient and reducing its distress. This cycle may continue as the helper detects changes in the recipient's distress levels, adapting behavioral responses based on feedback from the recipient.

Evolution of comforting behavior

Conceptual Foundations: Proximate and Ultimate Explanations

Understanding the origins and functions of comforting behavior requires integrating both mechanistic and evolutionary perspectives. A foundational framework in ethology for

addressing both how a behavior works and why it exists involves four key questions: mechanism (causation), development (ontogeny), function (adaptive value), and evolutionary history (phylogeny)[45,46]. The four types of questions operate at two different levels. Proximate explanations focus on explaining how a behavior is produced, while ultimate explanations focus on explaining why it evolved[47,48]. In neuroscience, research has typically focused on proximate mechanisms: the neural, hormonal, and developmental processes that enable comforting behavior. In contrast, fields like behavioral ecology and anthropology emphasize ultimate explanations, such as kin selection, group fitness, and the ecological demands that shape social organization. Importantly, these are not competing views, but complementary perspectives that together offer a fuller understanding of prosocial behavior.

This dissertation primarily engages with proximate explanations, identifying neural substrates and behavioral correlates of prosocial comforting in rodents. However, these findings also speak to broader ultimate questions: why comforting behavior evolved, what selective pressures shaped it, and how it may enhance survival and reproductive success. Framing comforting within both axes is critical for understanding its biological significance and its role in shaping complex social behavior.

Comparative evidence across species

Across species, comforting behavior often involves related forms of social touch such as allogrooming in mammals or allopreening in birds. Allogrooming (or allopreening) is typically characterized by scratching, stroking, licking or nibbling and is directed toward the outer body surface (fur, feathers, or bare skin)[49–51]. Affiliative allogrooming plays a crucial role in the formation and maintenance of social relationships across diverse social species[4,50,52]. While a baseline amount of allogrooming occurs between animals as part of general affiliation, a significant increase in allogrooming can be observed in a prosocial context when a helper

responds to another distressed animal – we refer to the former as *affiliative allogrooming* and the latter as *prosocial allogrooming.*

First described in great apes[53,54], prosocial allogrooming has been studied extensively in several non-human primate species, where it is one of the primary mechanisms of conflict resolution for maintaining peace and providing social comfort in groups[49,55–57]. Other field studies have also observed affiliative allogrooming as important for social cohesion and improving the welfare of distressed conspecifics in other mammals, including elephants[58], cattle[59,60], horses[37,61,62], bats[63], and felines[64–66]. Several highly social avian species have also been observed to display post-conflict bystander affiliation through allopreening[67–71].

Evolutionary pressures and adaptive functions

Prosocial comforting behavior likely evolved in response to multiple, context-dependent selective pressures that promoted individual fitness through social mechanisms[72,73]. Kin selection provides an adaptive framework to explain the evolution of comforting behaviors toward genetically related individuals. By improving the well-being or survival of kin, individuals indirectly enhance the propagation of shared genes. Comforting behaviors may thus confer inclusive fitness benefits, especially in species with high within-group relatedness. However, the presence of comforting behaviors directed toward non-kin suggests that other evolutionary forces are also at play. Reciprocal altruism and indirect reciprocity offer complementary models for explaining prosocial behavior toward unrelated individuals. In these cases, comforting may help establish or reinforce social bonds and increase the likelihood of future cooperative interactions. Previous studies have shown that individuals who engage in prosocial affiliative behaviors like allogrooming, are more likely to receive support or reciprocal grooming later, either immediately or in delayed contexts[57,67].

Comforting behavior may also serve as a mechanism of stress buffering and emotional regulation, benefitting both individuals and social groups. In rodents, receiving allogrooming reduces anxiety-like behaviors[26, 31, 74] and in primates, grooming leads to decreased heart rate and cortisol levels as well as promotes behavioral signs of relaxation[35,39]. These physiological effects may facilitate more rapid recovery from aversive states and improve behavioral flexibility. By mitigating individual distress, comforting may reduce the disruption caused by stress-related social withdrawal or defensive behaviors that impair group coordination. More broadly at the group level, these stress-buffering effects may enhance group survival by reducing emotional contagion and preventing escalation of distress within the group. Beyond its regulatory effects, one might speculate that prosocial comforting behavior may also carry social signaling value in addition to maintaining affiliative bonds. While its evolutionary roots may lie in parental caregiving, its persistence likely reflects a wider range of adaptive functions that support social groups.

CHAPTER TWO

Foundations of prosocial comforting in mice

In rodents, prosocial allogrooming was only first experimentally demonstrated less than a decade ago in the socially monogamous prairie vole[31]. This behavior has a comforting effect on the recipient and occurs more frequently toward familiar partners, which is consistent with the familiarity bias in human and non-human primate consolation literature[1]. Similarly, laboratory mice were recently shown to exhibit prosocial allogrooming behavior toward distressed conspecifics subjected to acute stressors such as footshock and physical restraint[26], offering opportunities for employing the versatile genetic tools available in mice to dissect the neural mechanisms underlying this behavior. Since then, the phenomenon of prosocial allogrooming has been consistently observed in mice in subsequent studies[32,74]. Other rodent species including mandarin voles and rats also show increased allogrooming towards a distressed other, although their stress buffering effects have not been formally demonstrated yet[33,75].

Rodents display increased allogrooming toward distressed conspecifics subjected to acute stressors including footshock, physical restraint, inflammatory pain, and social defeat[26,31,33,75]. Additionally, mice also display increased allogrooming towards their partner when cohoused with a chronically-restrained stressed partner compared to a naive partner[32]. These effects are stronger toward familiar partners, consistent with the familiarity bias in human and non-human primate consolation literature[1]. Notably, the scent of a distressed conspecific alone can trigger an increase in allogrooming behavior[26]. Rodents also exhibit distinctive facial expressions for pain and stress[76–79] characterized by tightened orbital muscles, squinted eyes, flattened cheeks, and retracted ears. While the role of visual cues in triggering allogrooming is less well established, actors with visual deficits induced by chemical ablation of rods and cones show impaired consolation behavior toward a conspecific in pain, without impairments in other general social or non-social behaviors[27]. Together, these suggest

that integrating multimodal sensory cues of a target's distress is important for expressing prosocial allogrooming.

Although prosocial allogrooming has been demonstrated in several rodent species over the past decade, this behavior is often discussed only briefly within broader reviews of empathy, social touch, or prosocial behavior, with limited attention to its behavioral diversity or underlying mechanisms. This chapter provides a comprehensive synthesis of allogrooming in rodents, not only in prosocial and comforting contexts, but also as it occurs in affiliative, hygienic, hierarchical, and reproductive settings. In addition to this ethological overview, I focus extensively on the neurobiological basis of comforting behavior, including the circuits, neuroendocrine pathways, and sensory systems that support allogrooming and related forms of social touch, such as huddling. To the best of my knowledge, there has not yet been a focused synthesis that integrates both the behavioral diversity and neural underpinnings of allogrooming across multiple social contexts in rodents. This chapter aims to fill that gap by providing an overview of the distinct social functions of allogrooming and reviewing recent progress in identifying the neural circuits and mechanisms that support comforting behavior.

Operationalizing comforting in rodent models

Prosocial allogrooming

Although providing comfort through allogrooming is widely observed in a variety of social species, recent studies of prosocial allogrooming in rodents enable us to gain new insights into the neural mechanisms underlying comforting. Not only do rodent models demonstrate that prosocial comforting is not exclusive to cognitively complex species, they also offer unique experimental access to neural circuits. As discussed above, a primary effect of allogrooming toward a distressed other is the social buffering of stress. In both prairie voles and mice, distressed animals exhibited reduced anxiety-like behaviors after receiving

increased allogrooming compared to animals that did not receive any allogrooming[26,31,74], suggesting that allogrooming behavior produces a comforting effect on other individuals.

In rodents, additional social contexts like social hierarchy can modulate the effect of prosocial allogrooming. For example, the display and effects of prosocial allogrooming may differ depending on an individual's place in a social hierarchy. Interestingly, subordinate mice engaged in less prosocial allogrooming than dominant mice toward their respective stressed partners[80]. Additionally, the stress buffering effect is observed when naïve subordinate helper mice allogroom their stressed dominant partners, and not when dominant helpers allogroom stressed subordinate partners.

Although animals display increased allogrooming during prosocial interactions, increased social approach has also been commonly observed as a potential way to seek information about the other animal's negative state[81]. As stress information is largely transmitted through volatile chemical signals in rats and mice produced by facial or anogenital glands, these investigative behaviors (particularly those involving direct contact towards the anogenital region) allow helpers to obtain information about potential environmental threats, which is a vital component of survival[22,23,25,82,83]. By contrast, allogrooming typically occurs following investigative behavior and is largely directed toward the dorsal flank, neck and head regions[26,31,32]. Allogrooming is thus unlikely to serve as a risk assessment behavior, but rather primarily a comforting behavior.

Allogrooming in other social contexts

While allogrooming functions as a comforting behavior in prosocial interactions, it may also serve additional purposes depending on the social context[84,85]. Allogrooming is commonly associated with its role in general affiliation, where multiple rodent species, including pine voles, rats, and mice, have been observed to engage in social grooming in both observational

field studies and laboratory studies[86–89]. Several characteristics like body language, reciprocity, mutual care and familiarity bias support the general affiliative role of allogrooming. Amongst naïve rats, recipients of affiliative allogrooming typically adopt droopy eyelids characteristic of a relaxed body tone and may solicit grooming by nudging and pushing its head under the potential groomer[50]. In mice and rats, allogrooming within a group tends to be reciprocated, suggesting that perhaps this behavior may serve some mutually affiliative function between individuals[90–93]. Additionally, allogrooming can help maintain group hygiene by removing ectoparasites and improving hygienic benefits, as an extension of the hygienic benefits of self-grooming. In domesticated and wild-derived rats, animals directly groom localized difficult-to-reach regions for the groomee including the body trunk, shoulder region and back of head[94–97].

Moreover, allogrooming may serve multiple roles in social hierarchical structure depending on its directionality and specific temporal sequence. Allogrooming occurring between dominant and subordinate mice may support the social hierarchy through opposing approaches of maintaining dominance (dominant toward subordinate) and ameliorating aggression (subordinate toward dominant)[98], while allogrooming between mutually subordinate mice may provide social buffering after being attacked[89,93]. However, other studies have shown that allogrooming is not predictive of social rank or dominance hierarchy in males[93,99].

Finally, across male-female dyads in wood mice, herb-field mice, and singing short-tailed singing mice, males allogroom females more than vice versa, which is likely driven by males obtaining information on female reproductive receptivity and establishing mating access[100–103]. These distinct functions may be distinguished by dynamics of the allogrooming interaction and social context (e.g. vocalizations and receptivity of recipient), but are still largely ill-defined.

Other comforting touch

In addition to allogrooming in rodents, there is evidence that other prolonged affiliative body contact like huddling behavior and prolonged close side-by-side contact may also afford comforting and strengthen social bonding[84,104,105]. Huddling behavior is characterized by sustained, increased direct body surface contact, often with reduced overall movement and increased pressure toward each other[86,88,106]. Huddling has been observed frequently in multiple rodent species and is known for its role in regulating energy expenditure and reducing heat loss for participating individuals[107–110]. While huddling behavior is recognized for its role in social behavioral thermoregulation, it may also provide comfort by reducing HPA arousal and providing stress relief when cold distress is alleviated[52]. Although it has not been directly tested, there is evidence that huddling may also be a form of prosocial comforting. Several studies have reported that naive actors interacting with distressed conspecifics dramatically increased side-by-side time and huddling behavior[33,74,111–113]. Huddling may simply facilitate allogrooming by nature of increasing physical proximity, or it may have an independent role. Huddling as infant rodents can produce stress-buffering effects[114,115] whose mechanisms may apply similarly in adult affiliative huddling – although it important to note that huddling can also be considered a behavioral state comprising multiple sub-behaviors [86].

However, the functional significance of huddling is context-dependent – rodents also exhibit defensive huddling where groups exposed to a threat will aggregate for protection[113,116,117]. Open questions remain, such as how affiliative huddles with a distressed conspecific are different from thermoregulatory huddling, and whether thermoregulatory and other-distress huddling offer comfort through similar neural circuits. Although cold temperature is a source of stress, thermoregulatory huddles that are symmetrical in nature may be distinct from comfort huddles that are offered to another in distress, as the latter is asymmetric. Lastly,

since huddling often takes place in groups, it also raises the question of how the dynamics of prosocial comforting might differ in groups larger than dyads. Whether these prolonged affiliative body contacts may serve independently as a comforting behavior is an open question for future study.

Neurobiology of providing comforting in rodents

Neural circuits underlying allogrooming

Until recently, the direct physical interactions between bystanders and distressed individuals have rarely been studied, despite evidence of rodents demonstrating social transmission of emotions such as fear and stress[5,81,118]. While multiple brain regions have emerged from studies of perception and transfer of others' emotional states like observational fear and emotional contagion in rodents[119–122], only recently have regions specifically linked to prosocial comforting behavior been identified. Below, we discuss studies that directly examined the biological mechanisms of providing and/or receiving comforting.

In rodents, olfactory cues play a potent role in communicating emotional states and mediating social behaviors[123,124]. The odor of a distressed conspecific via an anogenital swab transfer to a naive conspecific is sufficient to elicit increased allogrooming[26]. Additionally, specific olfactory compounds from sweat, saliva, and urine are associated with allogrooming behavior in laboratory mice in a strain-specific manner[125,126]. The medial amygdala (MeA) is an important hub that receives chemosensory inputs from the olfactory system[127–129], and is a key node in bridging the perception of distress in others and the expression of comforting behavior[26]. *In vivo* calcium imaging shows that MeA neurons exhibit distinct responses to stressed versus unstressed animals, suggesting that the MeA is involved in the detection of conspecific stress. Additionally, MeA neurons that responded to distressed animals partially

overlap with neurons activated during allogrooming, implying a potential direct link between the perception of another's stress state and the regulation of allogrooming.

Interestingly, an intersectional genetic approach identified a molecularly defined neuronal population in the MeA—tachykinin-1-expressing ($Tac1^+$) GABAergic neurons—in regulating allogrooming behavior[26]. Optogenetic activation of these neurons directly evokes allogrooming, whereas silencing this population acutely suppresses this behavior. Moreover, activation of the axonal projections of these neurons to the medial preoptic area (MPOA) in the hypothalamus directly elicits allogrooming. These findings provide the first evidence that allogrooming behavior can be evoked by modulating a precise molecularly and anatomically defined neural circuit.

In addition, neurons in the posterior intralaminar thalamic nucleus (PIL) were recently identified as critical for allogrooming behavior in female rats through their projections to the MPOA[130], although it is unclear if they also function in a prosocial comforting context. While both the MeA and PIL appear to directly control allogrooming behavior through their projections to the MPOA, the functional relationship between these pathways and other brain regions in driving comforting remains to be characterized. In rats, the PIL acts as an information processing center, receiving multiple modalities of ascending sensory input (primarily auditory and somatosensory), with strong efferents to multiple subcortical and cortical regions[131–133]. Given that PIL neurons have yet to be well characterized in mice, whether or not the circuits underlying this allogrooming are the same in rats and mice also remains an open question. Another thalamic nucleus, the paraventricular thalamus (PVT), has also been implicated in increased allogrooming towards mice that received a surgical procedure[34]. The PVT is involved in both arousal and valence during affective behavior[134,135]. In a prosocial context, the PVT shows increased cFos expression in response to surgically treated mice and chemogenetic silencing of PVT neurons reduces allogrooming behavior[34].

Future experiments activating PVT neurons will allow us to gain better insight into whether it plays an instructive role in driving comforting behavior.

Beyond the subcortical regions, the anterior cingulate cortex (ACC) is a hub for emotion processing sharing, social transfer of affect, and the integration of emotional and cognitive processes[136]. Several studies have indicated that ACC neurons play an important role for prosocial allogrooming in prairie voles and mandarin voles[31,33], largely based on the evidence of immediate early gene activation. Consistent with this role, infusion of an oxytocin receptor antagonist into the ACC reduces allogrooming behavior in voles[31,33]. Additionally, a recent study in mice show that chemogenetically inhibiting the ACC reduces allogrooming towards a partner in pain, and opptogenetically activating the ACC increases allogrooming toward a partner in pain[138]. Given that the ACC is a large brain structure, it is noteworthy that studies linking ACC to prosocial allogrooming behavior range across rostral ACC[33,74,137] and caudal ACC[31] across several rodent species. This necessitates more comprehensive analyses of how each subregion contributes to various stages of the prosocial process.

Whether these brain regions play a role in detecting and sharing other's negative state, empathetic motivations, modulating prosocial behavior responses, or multiple of these roles – have yet to be disambiguated. For example, MeA neurons not only respond to conspecific stress, but also control allogrooming behavior[26]. How might the MeA orchestrate both stress perception and comforting behavior? Are there discrete neural computations for these processes? Moreover, specific subpopulations of MeA neurons have been found to regulate different behaviors – while Tac1-expressing GABAergic neurons evoke allogrooming, glutamatergic Tac1 neurons promote self-grooming. These findings emphasize the complexity of the MeA's role in regulating multiple types of behavior, and highlight the broader question of how a single brain region can regulate such a range of behaviors. Similarly, PVT neurons are crucial for both allogrooming and anxiety-like behaviors in the helper[34] and the ACC has

been implicated in both emotional contagion[119] and prosocial comforting[31,74,138]. Given the evidence for these regions multiplexed roles, this raises multiple questions for they facilitate prosocial comforting behavior. For example, do the PVT and ACC only mediate the initial stage of affective empathy (emotional contagion), or do they play a role in directly regulating affiliative allogrooming, or both? Are PVT or ACC neurons and circuits involved in each process discrete or overlapping? Additionally, allogrooming across social contexts may have similar motor patterns but differing motivations, thus raising the question of where the circuits diverge and converge in their dynamics.

Neuroendocrinological mechanisms underlying allogrooming

Prosocial affiliative allogrooming is orchestrated by a complex interplay of neuroendocrine mechanisms. Of the neuropeptidergic systems implicated, the one that has received the most attention is oxytocin. Oxytocin signaling is thought to play a major role in promoting a variety of affiliative social interactions and empathy-related phenomena[16,139,140], and has been implicated in comforting behavior. Oxytocin neurons in the PVN show increased cFos activity when interacting with a distressed conspecific[33]. Moreover, infusion of OT receptor antagonists in the brain or deletion of OT receptor appears to be necessary for prosocial allogrooming behavior in voles and mice[31,111,141]. Evidence from other mammalian species including vampire bats, pigs, and non-human primates, where intranasal oxytocin delivery increases allogrooming, suggests that oxytocin signaling within the brain indeed supports a conserved role in comforting across species[142–145]. However, given the diversity in oxytocinergic effects and marked differences in OTR distribution across rodent species and across sex[146,147], the precise roles of the oxytocin system in detecting and responding to the distress of others remain to be determined. Since OTR are also expressed in multiple regions involved in comforting like the MeA and PVT and are important for processing social cues in

mice[148–150], it is also possible that oxytocin may also exert its influence there to regulate comforting.

Serotonergic modulation may also regulate prosocial comforting behavior. The dorsal raphe nucleus is one of the major sources of serotonin (5-HT) in the brain[151]. Both serotonergic dorsal raphe neurons that project to the rostral ACC and serotonergic receptors within the ACC are required for prosocial allogrooming in mandarin voles[152]. Additionally, infusions of 5HT1A receptor agonist into the rostral ACC increases allogrooming behavior. Furthermore, fiber photometry evidence of increased neuronal activity of dorsal raphe serotonergic neurons and endogenous release of 5-HT in the ACC during natural allogrooming, social approach and investigation suggest that this circuit's role facilitates both general sociability and prosocial allogrooming. By contrast, in mice, experimentally inducing 5-HT increase in the ACC reduces observational fear responses[153] and systemic 5-HT3 receptor activation attenuates observational contagious pain[154]. The counterintuitive observation that 5-HT can both promote sociability and allogrooming, and also suppress emotional contagion, necessitates further investigation. The diversity of distribution, signaling pathways, and functions of 5-HT receptor subtypes in the brain make it essential to further explore the complex role of serotonin in regulating prosocial comforting behavior.

The vertebrate-specific parathyroid hormone 2 (PTH2) has also been implicated in allogrooming behavior[130], although it is unclear if it also plays a role in a prosocial comforting context. Interestingly, PTH2-expressing PIL neurons also innervate PVN oxytocin[155] and corticotropin-releasing hormone neurons[156], presenting an appealing intersection for how PTH2-PTH2R signaling may interact with other neuropeptide systems in modulating affiliative allogrooming behavior.

Additionally, D2 receptors in the ACC are important for allogrooming[141] and are required for observational fear learning[153], suggesting that dopamine signaling might play a role in emotional contagion to promote comforting behavior.

What role do these neuropeptides play in distress perception versus expression of comforting behavior and how do they act in concert? As neuropeptides can modulate the activity of co-released neurotransmitters to increase or decrease postsynaptic responses and can also exert influence over other peptidergic systems[157], the regulation of such complex social behavior likely requires the coordinated actions of multiple neuromodulators and neurotransmitters in an intertwined manner. Furthermore, given that physiological responses involved in emotional contagion may affect the expression of comforting behavior, neuropeptidergic action on peripheral systems should also be considered. Recent tool development for measuring endogenous peptide signaling[158] may allow us to begin building a more comprehensive understanding of the neuroendocrinology underlying prosocial comforting behavior.

Neural mechanisms mediating the social buffering effect of comforting behavior

A key attribute of comforting behavior is the other-benefitting feature of prosocial allogrooming. How and why is affiliative allogrooming comforting for the recipient? The neurophysiology of affiliative social touch may provide some insight into how receiving allogrooming can modulate a recipient's stress-buffering pathways in rodents.

Peripheral circuits of gentle touch perception

The peripheral pathways transmitting gentle touch signals starting with cutaneous sensory low-threshold mechanoreceptors (LTMRs) are classified based on their action

potential conduction velocities[159,160]. In rodents and other non-human mammals, gentle, pleasant touch information are primarily conveyed by a class of slow unmyelinated low-threshold mechanosensitive afferents called unmyelinated C-tactile LTMRs (C-LTMRs). C-LTMRs are attuned to low-velocity gentle touch and are found exclusively in the hairy skin, which are the predominant areas involved in social touch behaviors like allogrooming[161]. They are also thought to convey information about affiliative social touch. While there is currently no universal molecular marker for the overall C-LTMR population, several genetically-defined subtypes have been identified that are activated specifically to innocuous social-like touch stimuli mimicking stroking and allogrooming[159,162,163]. These neuronal subtypes include those expressing tyrosine hydroxylase[164], MrgprB4[165,166], TAFA4[167], Cav3.3[168], and VGLUT3[169]. Experiments characterizing these peripheral pathways have largely been performed with gentle somatosensory stimuli mimicking social touch, like gentle brushing or stroking stimuli presented by experimenters[170].

There is increasing evidence that gentle social touch can be anxiolytic and rewarding across species[171–175]. Endogenous activation of C-LTMRs through gentle stroking stimuli produces soothing and stress-buffering effects. Receiving massage-like gentle stroking is sufficient to lower heart rate[176], decrease anxiety behaviors and reduce plasma corticosterone levels following stress[177]. Chemogenetically activating C-LTMRs similarly reduces physiological markers of stress[178] and has been found to be rewarding[166,179] and can trigger dopamine release in the nucleus accumbens in female mice[162].

Convergence of gentle touch and stress circuits in the brain

One potential mechanism to explain the stress buffering effects of allogrooming is the convergence of gentle touch signals onto stress circuits in the brain. Peripheral inputs of gentle touch travel through a spinothalamic tract that transmits signals from the dorsal horn

of the spinal cord to the brain[176,180]. Several subcortical structures involved in touch-related responses also regulate autonomic stress responses. For example, hypothalamic nuclei (PVN, arcuate nucleus) which are implicated in beta-endorphin/mu-opioid- and oxytocinergic-mediated responses to gentle social touch stimulation, also regulate stress responses. The nucleus of the solitary tract (NTS) in the brainstem receives signals from these nuclei as well as touch-related signaling reflecting thermoreceptive and skin stimulation[181], influencing peripheral heart and vascular responses through the vagal nerve and sympathetic ganglia respectively[182]. Additionally, noradrenergic inputs to the PVN from the NTS and the ventral lateral medulla modulate the activity of corticotropin-releasing factor producing neurons, thereby regulating the expression of stress-associated behaviors and activating the HPA axis[183,184].

The anxiolytic effects of social touch are commonly attributed to oxytocin, a neuropeptide associated with general affiliative and prosocial behaviors[185–187]. Dynamic stroking cutaneous stimulation activates oxytocin neurons in the PVN and SON[174,188–190] and triggers oxytocin release and elevated plasma oxytocin levels[191]. Exogenous infusion of oxytocin into the brain has been linked with decreased anxiety, reduced blood pressure and stress-induced tachycardia, reduced stress-induced rises of circulating corticosterone and anxiety-like behavior[192–196]. This aligns with evidence from human research that receiving a massage is a pleasant and de-stressing experience that is associated with increased oxytocin release and a dampening of HPA response[197,198]. Given oxytocin's ability to increase the salience of both positive and negative social contexts, it is important to also consider the diversity in oxytocinergic effects. Although the mechanisms underlying both gentle touch and distress are complex with interactions between multiple neuropeptide systems, the shared components between the two provide some insight into how comforting behavior can provide stress-relief and comfort to an individual[199].

Comforting behavior via allogrooming is likely to be effective in generating calming effects to buffer the recipient's stress through these gentle touch neural circuits and endocrinological mechanisms, though many open questions remain. It has been previously shown that the mere presence of a conspecific can reduce stress[200]. However, there is evidence that that allogrooming provides additional stress buffering beyond just physical proximity. How do comforting social touch signals compound and integrate with olfactory communication-induced social buffering? Across species, gentle touch perception is modulated by additional available multisensory information/cues[201–204] – how are these signals integrated during comforting to attenuate stress? And how is receiving grooming from another more stress-relieving than self-grooming? Despite its explanatory potential, the neurophysiology of affiliative touch has been largely overlooked in studies of comforting behavior thus far. Future studies integrating prosocial behavior assays with experiments probing stress-buffering effects resulting specifically from social touch will begin to deepen our understanding of comforting. Additionally, the real-time physiological effects of prosocial allogrooming in a recipient mouse such as changes in respiratory and cardiovascular autonomic responses can be measured through wireless telemetry systems, allowing assessment of the temporal dynamics and sequence of comforting behavior and the resultant stress buffering.

CHAPTER THREE

Shared neural substrates of prosocial and parenting behavior

INTRODUCTION

Prosocial behaviors that assist and benefit other individuals play a pivotal role in fostering social cohesion[1,2,5,81]. These behaviors entail the ability to recognize the needs or negative states of others and the motivation to address them. This capacity to perceive and act upon the needs or distress of others is seen across diverse species, from humans to rodents. From an individual perspective, it might seem paradoxical for animals to exhibit behaviors that benefit others, given the prevailing notion that behaviors primarily evolve to enhance one's own reproductive fitness. This raises the fundamental question of what neural mechanisms motivate and enable animals to take prosocial actions and whether such mechanisms may reflect conserved biological systems originally shaped for caregiving. A long-standing hypothesis suggests that prosocial behavior may share a common foundation with parental care for helpless newborn offspring, a phenomenon that is ubiquitous across mammals[1,5,205]–and also observed in other taxa such as birds, reptiles, and invertebrates[206]. As vulnerable offspring are intrinsically linked to their parents' reproductive success, the act of caring for them directly stems from an animal's reproductive imperatives. Yet, both parenting and prosocial behaviors target a distressed or needy individual, prompting a response to aid or console, thereby mitigating adverse conditions. As species evolved nurturing behaviors toward their young, it is plausible that the need to care for vulnerable offspring shaped neural systems that are also responsive to the needs of adult conspecifics. Indeed, across multiple primate species including humans, the extent of allomaternal care is correlated with prosocial behavior among adults[207].

From a neurobiological standpoint, this evolutionary hypothesis raises the intriguing notion that the neural architecture underlying parenting behaviors may also, at least in part, contribute to adult-directed prosocial behaviors. However, the identity and nature of such shared neural elements have remained largely unclear. Previous studies have identified the

medial preoptic area (MPOA) as a key brain area for the regulation of parenting behaviors[208–212]. This raises the question of whether the MPOA may also control adult-directed prosocial behavior. Recent studies suggest that rodents, including mice, can display prosocial comforting behavior, in the form of allogrooming toward the distressed conspecifics[31,213]. Allogrooming is a common form of affiliative social touch across many species and can provide a stress-relieving effect[31,51]. While axonal projections from the medial amygdala (MeA) and the thalamus to the MPOA have been implicated in allogrooming[26,130], no previous studies have identified a role for the MPOA itself and its downstream circuitry in directly controlling allogrooming behavior and encoding the stress state of other individuals. Moreover, the potential relationship between the functions of the MPOA in allogrooming and parenting behaviors has not been explored.

Here, we show that neurons in the MPOA encode the perception of distressed adults and bidirectionally regulate prosocial allogrooming. Interestingly, although stressed adults and pups are associated with distinct sensory cues, the neural representation of pups more closely resembles that of stressed adults than that of unstressed adults. Moreover, allogrooming and parenting behaviors are positively correlated at the level of individual animals and recruit partially overlapping populations of MPOA neurons. While we do not directly investigate the biological mechanisms underlying this individual variability, this meaningful association between these two forms of affiliative behavior offers a window into shared motivational or neural mechanisms that coordinate caregiving across contexts.

RESULTS

Parenting and prosocial behaviors are positively correlated in mice

To explore the relationship between prosocial allogrooming and parenting behaviors in mice, I first examined the levels of prosocial behavior toward stressed adults and parenting behavior toward pups exhibited by the same animals (Fig. 3-1).

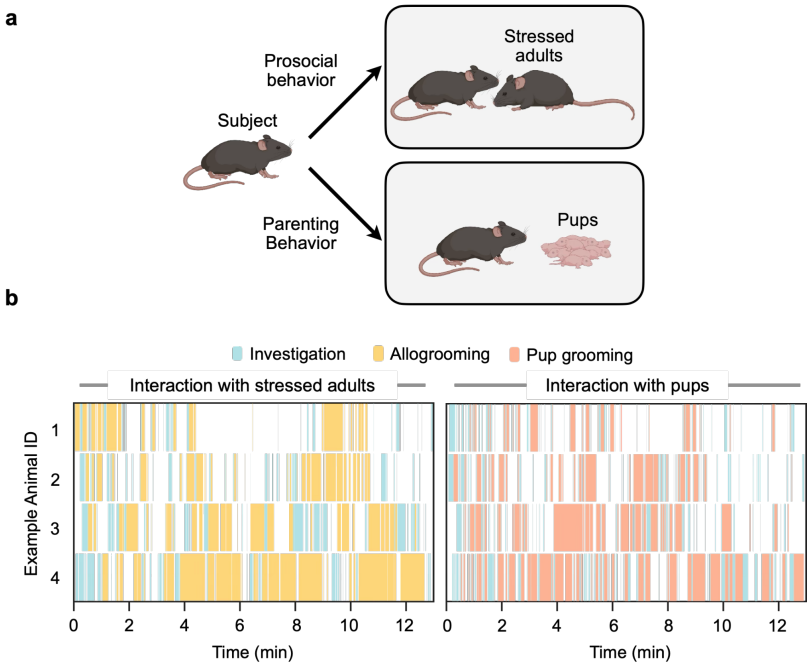

Figure 3-1. Behavioral paradigms for measuring prosocial and parenting responses to stressed adults or pups. a, Schematics of behavior paradigms for examining prosocial and parenting behaviors during interactions with stressed adults and pups. **b**, Example raster plots showing allogrooming, pup grooming, and social investigation behaviors during interactions with stressed adults or pups.

In virgin female mice, individual animals displayed varying levels of allogrooming and parenting behaviors (pup grooming, retrieval, and crouching). Interestingly, I found that the duration of allogrooming was positively correlated with that of parenting behavior, indicating that animals displaying a higher level of pup-directed care also exhibited more adult-directed prosocial behavior, and vice versa (Fig. 3-1b, 3-2-a, 3-2b). In virgin male mice, while some

individuals can exhibit aggressive behavior toward pups, a sizable fraction of animals show parenting behavior[214,215]. To investigate the relationship between allogrooming and parenting behavior, I first excluded males that exhibited pup attacks (n=2 of 16) in order to focus our analysis on animals that could express parenting behaviors. When examining male animals that exhibited parenting behavior without displaying pup attack, I also observed a positive correlation between allogrooming and parenting behaviors in males (Fig. 3-2e). Of note, the 2 animals excluded from correlation analysis also displayed allogrooming toward stressed adults, suggesting that pup-directed aggression and adult-directed prosocial behavior can coexist and may be regulated along orthogonal motivational or neural axes. In addition, I observed a significant correlation between allogrooming and pup grooming, a predominant form of parenting behavior (>90%, Fig. 3-3a).

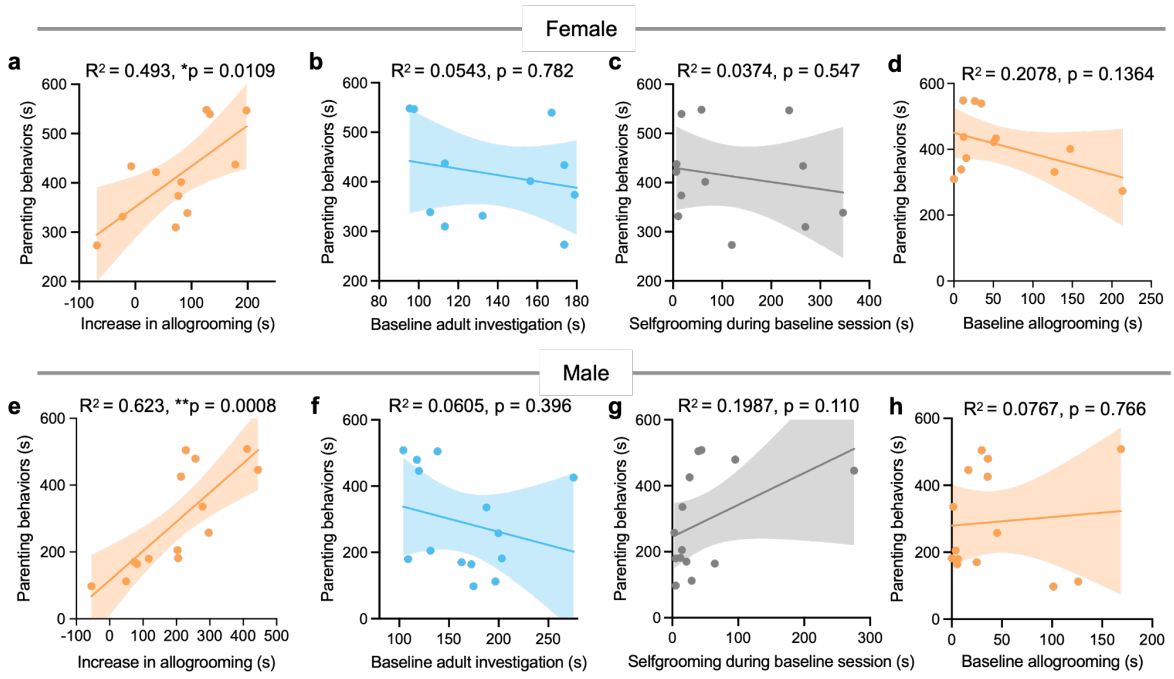

Figure 3-2. Parenting and prosocial behaviors are positively correlated in male and female mice. Correlation between the duration of parenting behaviors and the increase in allogrooming toward stressed adult conspecifics (**a, e**), the duration of baseline adult investigation (**b, f**), the duration of baseline self-grooming (**c, g**), and the duration of baseline

allogrooming (**d, h**), in female (**a-d**) and male (**e-h**) mice. The linear regression lines (solid lines) and 95% confidence intervals (shaded areas) are shown. n = 12 mice in (**a-d**), 14 mice in (**e-h**).

This relationship between allogrooming and parenting behaviors did not appear to reflect the animals' general social investigative behavior, as there was no significant correlation between the animals' investigative sniffing behavior toward adults and their parenting behavior (Fig. 3-2b, f). Additionally, I observed no significant correlation between the animals' general propensity to self-groom and the levels of parenting behavior (Fig. 3-2c, g). Moreover, when I examined spontaneous, baseline allogrooming toward non-stressed conspecifics, I found no correlation with pup grooming behavior (Fig 3-2d, h). This indicates that the positive correlation between natural prosocial allogrooming and parenting behavior is not a trait-driven phenomenon but is unique to allogrooming induced by others' stress state, supporting the notion that a distinct motivational drive underlies stress-induced prosocial behaviors. This specific correlation between prosocial allogrooming and parenting behavior raises the question of whether a common circuit supports caregiving responses across both social contexts.

While parenting behavior includes a composite of behaviors (e.g., pup grooming, retrieval, crouching), both virgin male and female animals predominantly engage in pup grooming in this assay (>94%, Fig. 3-3a). Accordingly, I show that the positive relationship between parenting behavior and prosocial allogrooming in virgin mice is driven by pup grooming (Fig 3-4a-f). Naturally, it follows that one might ask: what about parenting in parents? In this short homecage assay, mother and father mice display a more diverse repertoire of parenting behaviors (Fig. 3-3b). Do parental animals displaying a higher level of pup-directed care also exhibit more adult-directed prosocial behavior? Interestingly, these parental female and male animals also exhibited correlated levels of allogrooming and parenting behaviors

(Fig 3-3e), with no correlations between levels of parenting and investigative sniffing nor self-grooming (Fig 3-3f-g). Although their parenting behavioral composition is more varied (Fig 3-3-b), I find that the positive relationship between parenting behavior and prosocial allogrooming in parental mice is also driven by pup grooming (Fig 3-4g-i).

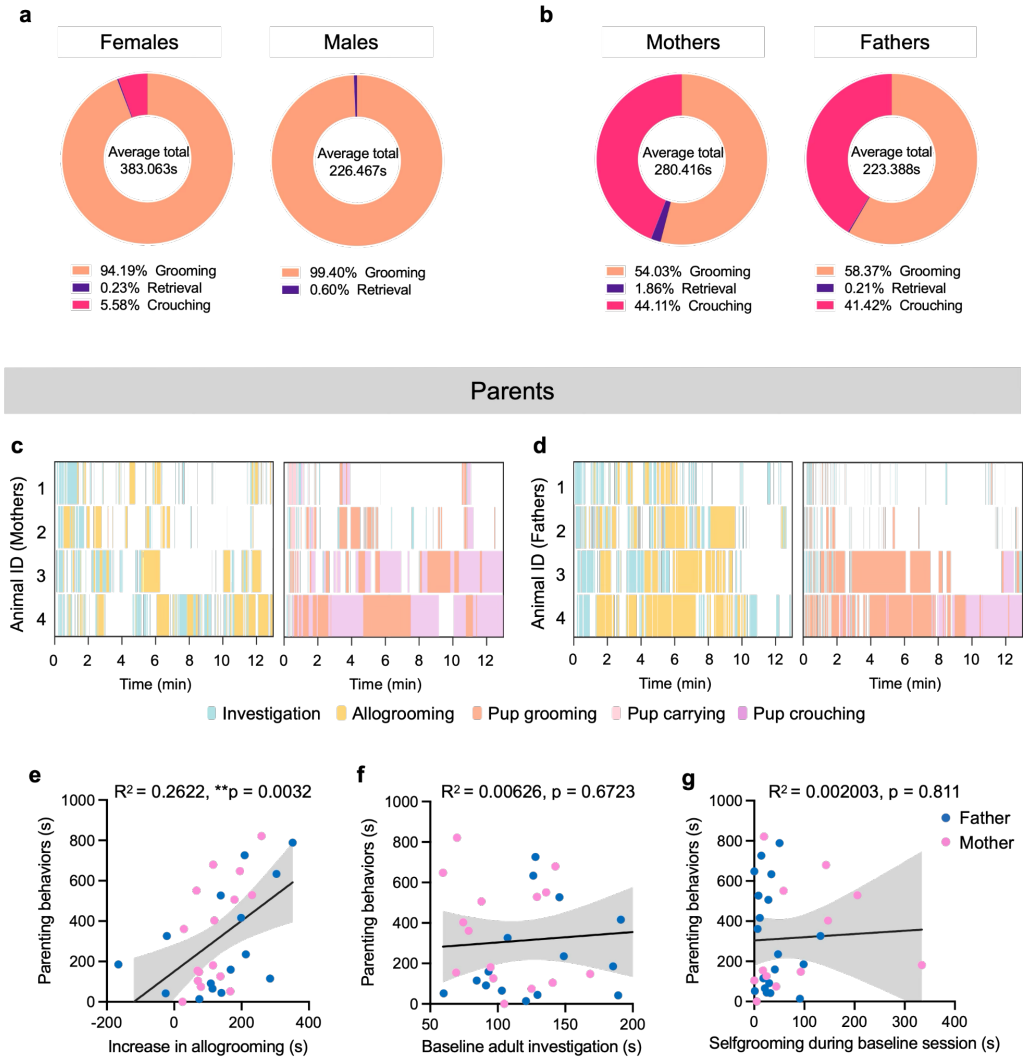

Figure 3-3. Parenting and prosocial behaviors are positively correlated in mothers and fathers. Average composition of parenting behaviors in virgin females and males (**a**) and in mothers and fathers (**b**). **c,d,** Example raster plots of different behaviors displayed by mother (**c**) or father (**d**) mice during interactions with stressed adults (left) or pups (right). **e-g**, Correlation between the duration of all parenting behaviors and the increase in allogrooming toward stressed adult conspecifics (**e**), the duration of baseline adult investigation (**f**), and the duration of baseline self-grooming (**g**) in mothers and fathers. The linear regression lines (solid lines) and 95% confidence intervals (shaded areas) are shown. n = 12 mice in (a, left), 14 mice in (a, right), 31 mice in (b-g).

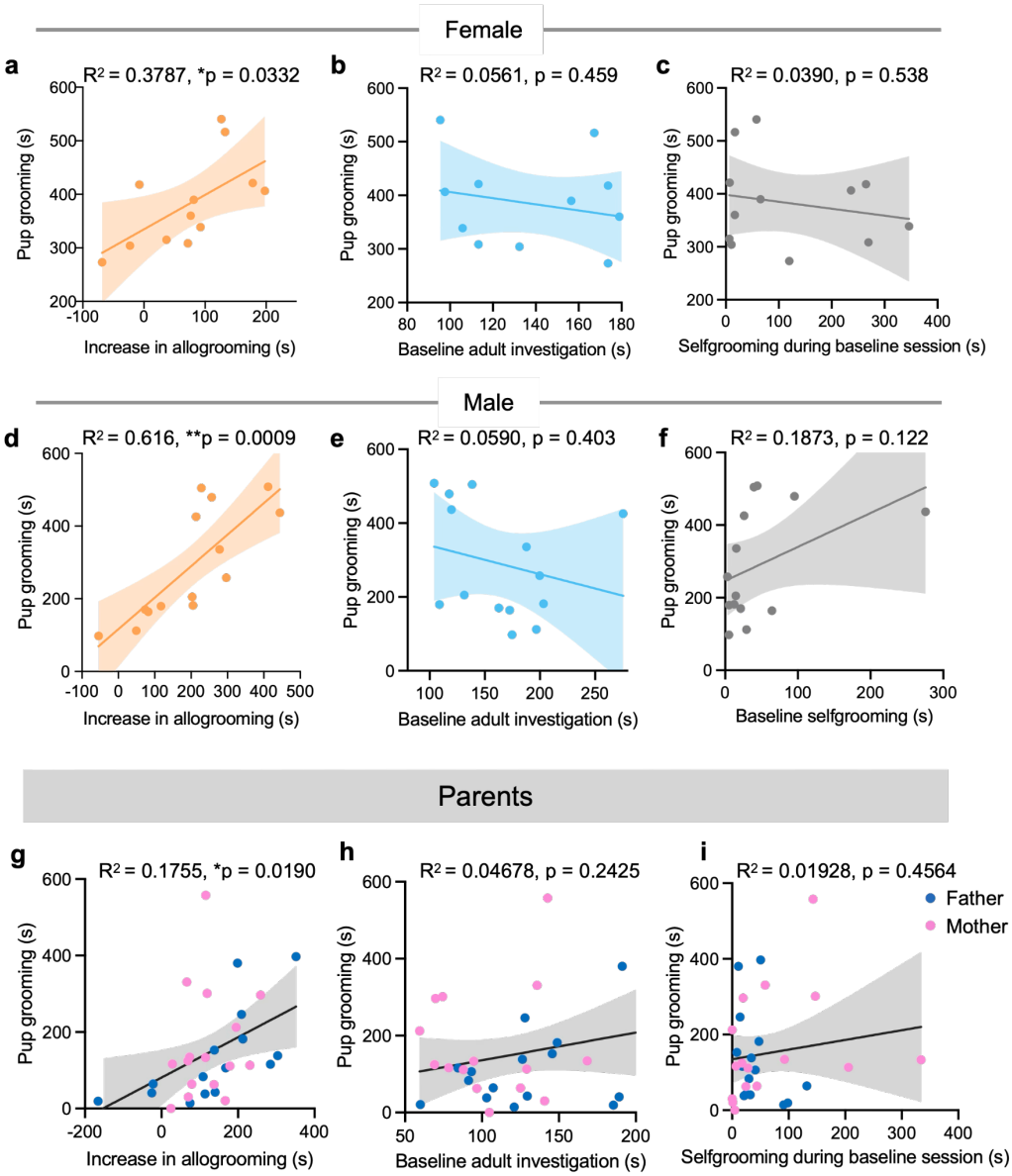

Figure 3-4. Pup grooming accounts for the positive correlation between parenting and prosocial allogrooming. Correlation between the duration of pup grooming and the increase in allogrooming toward stressed adult conspecifics (**a,d,g**), the duration of baseline adult investigation (**b,e,h**), and the duration of baseline self-grooming (**c,f,i**) in virgin females (**a-c**), virgin males (**d-f**) and mothers and fathers (**g-i**). The linear regression lines (solid lines) and 95% confidence intervals (shaded areas) are shown.
n = 12 mice in (a), 14 mice in (b), 31 mice in (g-i).

It is important to distinguish parenting behaviors (which even virgin mice are capable of performing) from parental status. In our experiments, parental animals (mothers and

fathers) are tested with their other-sex mate, which differs from the same-sex cage mates in experiments with virgin mice. Given that the neural mechanisms underlying allogrooming may be modulated differently for same-sex versus opposite-sex mates, we will focus on exploring the shared neural substrates of allogrooming and parenting in virgin mice. While the question of how parental status may modulate the relationship between prosocial allogrooming and parenting behavior remains open, we note that the predominant active parenting behavior in both male and female animals across parental status is pup grooming. Accordingly, the remainder of experiments in this dissertation focuses on the pup grooming component of the parenting behavioral repertoire in our microendoscopic imaging and functional manipulation experiments. Together, this specific correlation between allogrooming toward stressed adults and parenting toward pups at the behavioral level raises the possibility that these two types of caregiving behaviors could be co-regulated by shared neural circuits. Together, this specific correlation between allogrooming toward stressed adults and parenting toward pups at the behavioral level raises the possibility that these two types of caregiving behaviors could be co-regulated by shared neural circuits.

Before exploring the neural mechanisms underlying these behaviors, it is worth briefly addressing a potential biological variable that could influence the expression of prosocial behavior – estrous state. Both female and male mice were tested in this dissertation, and a common concern when assessing female behavior is the potential influence of estrous cycle on behavior. Prior studies have reported mixed findings on whether female social behaviors are modulated by estrous state[216,217]. To assess whether the expression of prosocial allogrooming depends on estrous stage, I performed daily monitoring of estrous state using the visual assessment method, a non-invasive approach that avoids the risk of inducing pseudopregnancy[218–220]. To increase confidence in estrous classification, I also collected

vaginal lavage samples following each experiment and confirmed estrous stage based on cytological analysis. I found no significant difference in allogrooming behavior between sexually receptive and non-receptive females. This finding aligns with recent work suggesting that individual variability accounts for more behavioral variation than estrous state in spontaneous social interactions[217] and is also consistent with previous findings showing that optogenetically induced parenting behaviors in female mice do not depend estrous state [208,209].

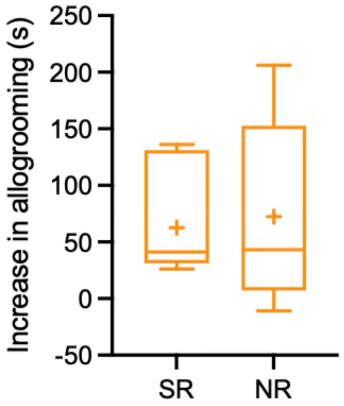

Figure 3-5. Prosocial allogrooming in females does not depend on estrous stage. Sexually receptive (SR) includes proestrus and estrus. Non-sexually receptie (NR) includes metestrus and diestrus.
n = 5-7 female mice. p=>0.9999

Partially overlapping representations of prosocial and parenting behaviors in the MPOA

Our observation that mice show correlated prosocial and parenting behaviors prompted us to investigate whether social cues from stressed adults and pups elicit similar or distinct neural responses in the MPOA. While there is much evidence that MPOA neurons respond to social cues[208,214,221]. it remains unclear how the encoding of others' stress state is related to that of pup-derived cues. To explore this question, I collaborated with co-authors FS and YW to examine the response of individual MPOA neurons during the investigation of stressed or unstressed adults or pups, or during self-stress (Fig. 3-6a). They show that MPOA

neurons exhibit diverse response patterns to various types of social or stress stimuli, with some neurons selectively activated by a single type of stimulus while others were responsive to multiple types of stimuli (Fig. 3-6b,c). Notably, neurons activated during investigation toward stressed adults or pups were largely distinct, with an overlap lower than the chance level (Fisher's exact test, odds ratio = 0.69, $p < 0.0005$. Fig. 3-6b). Moreover, these two types of investigation events could be decoded based on population activity with high performance (Fig. 3-6d, Fig. 3-8a). These findings are consistent with the notion that pups and stressed adults present largely distinct social cues.

Despite the distinct representation of adults and pups in the MPOA, the observation that animals exhibit caregiving behavior toward pups and stressed adults—but not toward unstressed adults—raises the question of whether animals may perceive pups more similarly to stressed adults (as both manifest a state of need) than to unstressed adults. To investigate this, they performed PCA on population responses in the MPOA during events of investigation toward stressed adults, unstressed adults, and pups (Fig. 3-6e). The Mahalanobis distances between these different types of events in the PC space was then computed. Interestingly, the distance between stressed adults and pups is significantly smaller than that between unstressed adults and pups (Fig. 3-6f, Fig. 3-8a-b). Additionally, within cells activated during investigation toward stressed adults, the proportion of cells also activated during pup investigation was significantly higher compared to that within cells activated during investigation toward unstressed adults (Fisher's exact test, odds ratio = 1.31, $p < 0.05$). These observations suggest that pups may be represented more similarly to stressed adults than to unstressed adults in the MPOA.

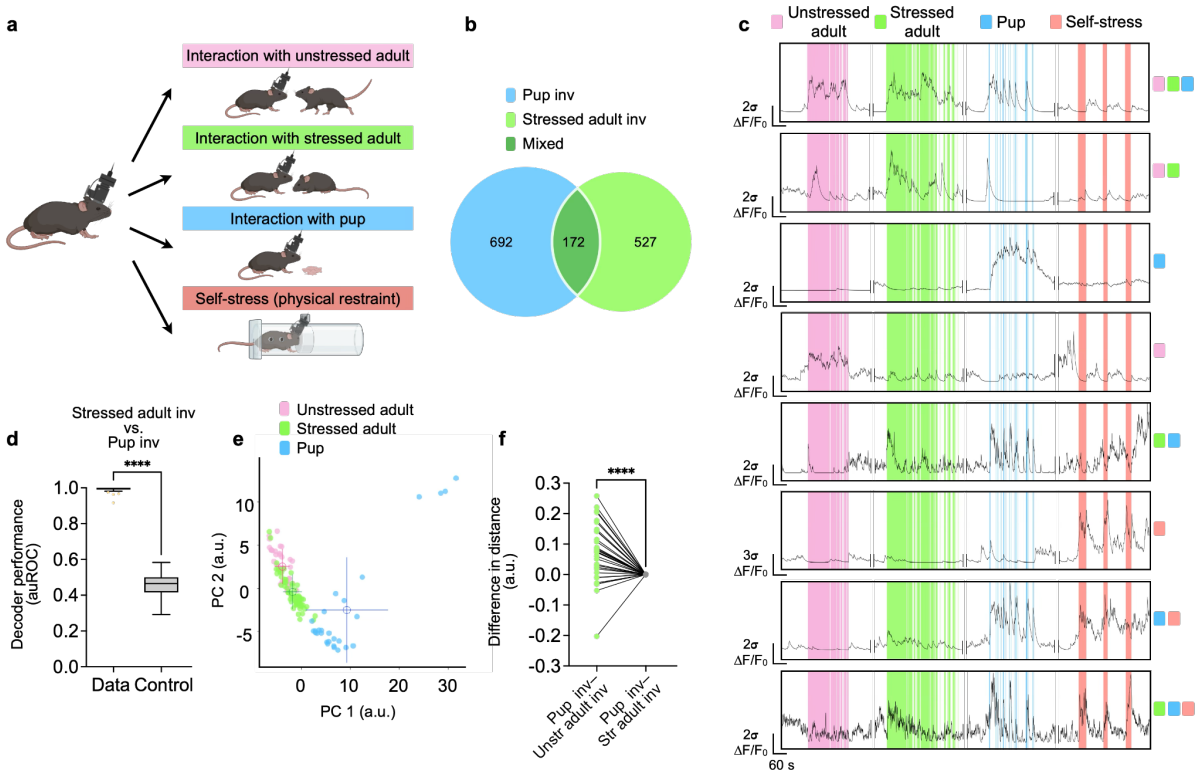

Figure 3-6. MPOA neurons represent pups more similarly to stressed adults than to unstressed adults. **a**, Schematic of microendoscopic imaging during interactions with unstressed adults, stressed adults, and pups and during the experience of self-stress. **b**, Venn diagram of MPOA neurons that are significantly activated during investigation toward stressed adults ("stressed adult inv") or pups ("pup inv"). **c**, Calcium traces of example MPOA neurons that are significantly activated in response to various social stimuli or self-stress. Color blocks on the right indicate the types of events during which the neurons are activated. **d**, Performance of decoders trained using MPOA population activities in differentiating between investigation events toward stressed adults versus pups. **e**, Principal component (PC) projections of MPOA population activity associated with episodes (individual dots) of investigation toward unstressed adults, stressed adults, and pups from one example imaging experiment. a.u., arbitrary units. **f**, Average Mahalanobis distances between investigation events toward pups and unstressed adults ("Pup inv–Unstr adult inv") and between investigation events toward pups and stressed adults ("Pup inv–Str adult inv"). The distances are calculated using the first 3 PCs of MPOA population activities. Within each animal (each pair of matched dots), the observed distances are normalized by subtracting the average distance between investigation events toward pups and stressed adults. In (d), decoders in the control groups (grey boxes or lines) are constructed using temporally permutated calcium traces. (d, f), two-sided Wilcoxon signed-rank test. n = 33 mice in (d, f).

These findings further raise the intriguing question of whether prosocial allogrooming and parenting behaviors engage any common neuronal ensembles in the MPOA. To investigate this, they performed microendoscopic imaging during interactions with adult conspecifics and pups (Fig. 3-7a) and compared the neural representation of allogrooming

with that of pup grooming, the predominant form of parenting behavior observed in both males and females, which we have shown to be correlated with allogrooming behavior (Fig. 3-4a-f). Neurons that were active during allogrooming or pup grooming were identified (Fig. 3-7b-d). Interestingly, a sizable fraction (42.4%) of allogrooming-activated MPOA neurons were also activated during pup grooming (Fig. 3-7b-g), with the overlap higher than chance level (Fisher's exact test, odds ratio = 1.33, $p < 0.05$). This indicates a partial overlap between neural representations of these two behaviors at the single-cell level.

To further examine whether the population code of allogrooming and pup grooming may contain shared information, they performed a mutual decoding analysis to determine whether population activity elicited by allogrooming behavior may predict pup grooming. Interestingly, models trained to distinguish allogrooming from baseline periods could also predict pup grooming, and decoders trained for pup grooming could also decode allogrooming (Fig. 3-7h,i). These results suggest shared information between the population code of allogrooming and pup grooming. By contrast, decoders trained for allogrooming could not decode self-grooming, and decoders trained for self-grooming could not decode allogrooming (Fig. 3-7j,k). Together, our findings suggest that allogrooming and pup grooming elicit partially overlapping neural representations in the MPOA. This neural activity pattern was similarly observed in both males and females (Fig. 3-8c,d).

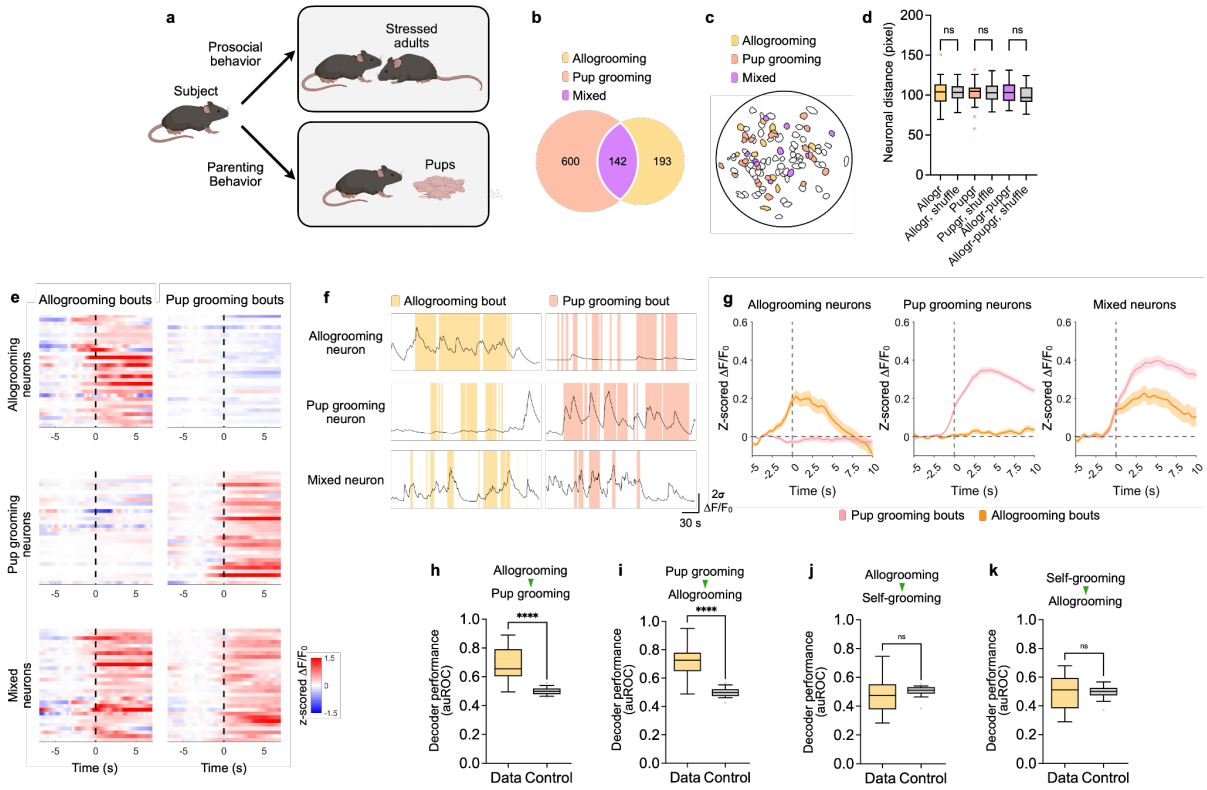

Figure 3-7. Prosocial allogrooming and pup grooming engage partially overlapping MPOA neuron populations. a, Schematic of microendoscopic imaging during prosocial and parenting behaviors. **b**, Venn diagram of neurons significantly activated during allogrooming or pup grooming. **c**, Example field of view showing the spatial distribution of neurons activated only during allogrooming, only during pup grooming, or during both types of behavior. **d**, Average pairwise distances between neurons within the same response type (i.e., allogrooming-activated or pup grooming-activated) or between these two different response types. The "shuffle" groups (grey boxes) are generated by calculating the distances after randomly shuffling cell type identity among all neurons. **e, f**, Heatmaps (**e**) and calcium traces (**f**) showing the responses of example neurons activated only during allogrooming, only during pup grooming, or during both types of behaviors. In (**e**) the heatmaps are aligned to the onset (time 0) of each type of behavior. m, Average traces (mean ± SEM) showing the responses of neurons activated only during allogrooming, only during pup grooming, or during both types of behaviors. Time 0 indicates behavior onset. **h, i**, Performance of models trained to decode allogrooming versus baseline in predicting pup grooming (**h**) and models trained to decode pup grooming versus baseline in predicting allogrooming (**i**). **j, k**, Performance of models trained to decode allogrooming versus baseline in predicting self-grooming (**j**) and models trained to decode self-grooming versus baseline in predicting allogrooming (**k**). In (h-k), decoders in the control groups (grey boxes or lines) are constructed using temporally permutated calcium traces. (h-k), two-sided Wilcoxon signed-rank test. (d), repeat measure one-way ANOVA with post hoc Sidak's multiple comparisons test.
n = 23 mice in each group in (d), and 18 mice in (h-k).

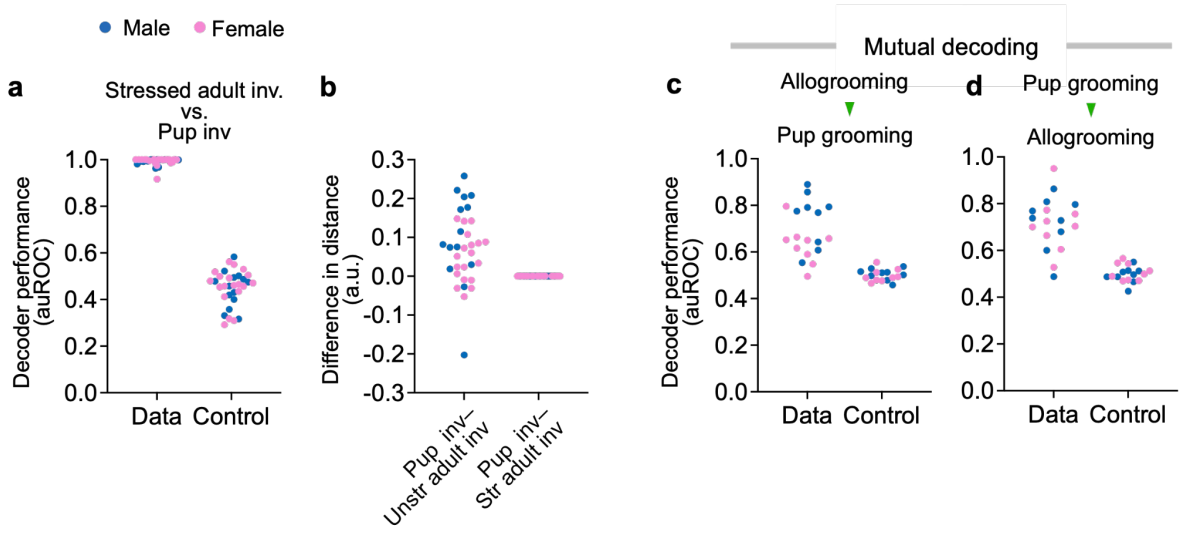

Figure 3-8. Allogrooming and pup grooming elicit partially shared neural representations in the MPOA in males and females. a, Performance of decoders in differentiating between investigation events toward stressed adults versus pups in males (blue dots) and females (pink dots). Data correspond to those presented in Fig. 3-7d. **b,** Average Mahalanobis distances between investigation events toward pups and unstressed adults ("Pup inv–Unstr adult inv") and between investigation events toward pups and stressed adults ("Pup inv–Str adult inv") in males (blue dots) and females (pink dots). Data correspond to those presented in Fig. 3-7f. **c, d,** Performance of models trained to decode allogrooming versus baseline in predicting pup grooming (c) and models trained to decode pup grooming versus baseline in predicting allogrooming (d) in males (blue dots) and females (pink dots). The data correspond to those shown in Fig. 3-7h,i.

MATERIALS AND METHODS

Animals

Wild-type animals used in experiments were male and female C57BL/6J mice purchased at 8–10 weeks old from Jackson Laboratories Laboratory (strain #: 000664). The Cre driver lines VgatCre/+ and Vglut2Cre/+ were first purchased from Jackson Laboratory (strain #: 016962 and 016963) and backcrossed to C57BL/6J to generate a breeding colony. Fostm2.1(icre/ERT2)Luo/J mice were purchased Jackson Laboratory (strain #: 030323). Pups (P2-P10) used for behavior experiments were produced from our breeding colony. Animals were housed in a 12-h light/dark cycle (21:00–9:00 light) at a temperature of 21–23°C with 30–70% humidity, with food and water ad libitum. All behavior experiments were performed

during the dark cycle of the animals in a dark room illuminated by infrared or red light. All experimental procedures were carried out in compliance with the NIH Guide for Care and Use of Laboratory Animals and approved by the UCLA institutional animal care and use committee (IACUC).

Surgical Procedures

Mice at 8-14 weeks of age were anesthetized with isoflurane and mounted on a stereotactic alignment system (Kopf instruments).

For microendoscopic imaging experiments, 400 nL AAV1-Syn-jGCaMP7f (Addgene) was injected in the MPOA (AP: +0.10 mm, ML: +0.45 mm, DV: -5.10 mm). A GRIN lens (Inscopix) was implanted 0.20 mm above the virus injection site. The GRIN lens was protected with a silicon adhesive (Kwik-cast, WPI) after implantation. A baseplate was fixed above the GRIN lens 2-3 weeks after the surgery.

Histology

Animals were euthanized and perfused with phosphate-buffered saline (PBS) followed by 4% paraformaldehyde (PFA). The brains were dissected out, post-fixed in 4% PFA overnight, rinsed with PBS and bathed in 20% sucrose overnight. Brains were sectioned at 60-μm thickness with a Leica CM1950 cryostat and imaged with a Leica DM6 B microscope.

Behavior Assays

Prosocial interaction assay

Prosocial interaction assays in Fig. 3-1, 3-2, 3-3, and 3-4 were performed as previously described [26,138]. We previously demonstrated that subject animals display similar prosocial allogrooming behavior toward partner animals that experienced various acute stressors, including foot shock, forced swim, and physical restraint [26]. Same-sex animals were paired-housed for at least 5 weeks before behavioral testing. Animals were extensively habituated to

handling procedures for at least 3 days prior to the behavioral test. One animal was randomly assigned as the “subject” and the other as the “partner”. For the baseline control session, the partner was removed from the home cage and placed into a separate cage with home cage bedding for 15 min. For the stress session, the partner was removed from the home cage and subjected to forced swim in 20-22ºC water for 5 minutes. After either separation only or stress, the partner was returned to the home cage to reunite with the subject, and behavior was recorded for 15 min. The separation-only control sessions were performed at least 4 hours before the separation-with-stress sessions.

For the assay in mothers and fathers, male and female animals were mated and pair-housed for at least 3 weeks. Behavioral testing was conducted after the birth of the litter. Most (13 of 16) pairs were tested with their first litter, and we found no differences between pairs tested following their first litter and pairs tested after their second litter. The prosocial interaction assay was performed on the mothers and fathers as described above, with their mating partners exposed to stress. The pups were removed from the home cage during the experiments.

All experiments were performed during the dark cycle of the animals in a sound-attenuating chamber (Med Associates) illuminated by infrared or red light. Behaviors were manually annotated frame-by-frame using a custom-written Python software (https://github.com/hongw-lab/Behavior_Annotator). Investigation was defined as the subject mouse orienting its snout toward the partner and positioning itself within half a head length of the partner. Allogrooming was defined as visible licking and/or mouth contact accompanied by head bobbing movements directed at the body trunk, shoulders, and head of the partner mouse. Self-grooming was defined as visible licking of paws and grooming face and/or body by the subject mouse. In Fig. 3-2a, e, 3-3e, and 3-4a, d, g, the increase in the duration of allogrooming was calculated as the difference in the duration of allogrooming toward stressed

adults compared to unstressed adults. Baseline investigation and self-grooming are defined as the social investigation and self-grooming displayed during interactions with unstressed adults.

Pup interaction assay

Subject animals that underwent the prosocial interaction assay were subsequently tested in the pup interaction assay, with an interval of ~2 hours between the two assays. The subject animals were tested alone in their home cages. 3-4 P6-9 pups were introduced simultaneously at the beginning of the assay and behavior was recorded for 13 min. Pup investigation was defined as sniffing within half a head length of any part of the pup. Pup grooming was defined as visible licking or mouth contact directed at the pup. Pup crouching was defined as quiescent, slightly arched, posturing over the pups. Pup retrieval was defined as carrying the pup to the nest. Given that both male and female animals predominantly engage in pup grooming, with <2% of time engaged in pup retrieval, we focused on the pup grooming component of the parenting behavioral repertoire in our microendoscopic imaging and functional manipulation experiments.

Miniscope calcium imaging

Behavior assays

Subject animals were habituated to human handling procedures, the microendoscope, and the experimental setups for at least 3 days before the behavior test (at least 1 hour/day). The calcium fluorescence signals were recorded using UCLA Miniscope V4 equipped with a data acquisition board (Open Ephys) and the behaviors were recorded using a web camera simultaneously. The miniscope and the behavior camera were controlled by a miniscope DAQ software (https://github.com/Aharoni-Lab/Miniscope-DAQ-QT-Software). Calcium

fluorescence signals were recorded at 15 Hz, and behaviors were recorded at 30 Hz. Behaviors were manually annotated frame by frame using a custom Python software (https://github.com/hongw-lab/Behavior_Annotator) to identify onset and offset times of individual behaviors exhibited by the subject animals, including close investigation, allogrooming, pup grooming, and self-grooming.

During the imaging experiment, each subject animal was presented with 2-6 familiar, same-sex adult animals and 4-8 pups in total on the same day, with a ~5-min interval between two successive presentations. Each adult animal was presented twice—firstly in an unstressed state and subsequently in a stressed state (induced by physical restraint, forced swim, or electric foot-shocks, as described previously [26]. During each presentation, the subject animal was allowed to freely interact with the adult animal or pups for ~5-10 min. Following presentations of the adults and pups, the subject animal was subjected to 3-6 rounds of physical restraint (15-30 s each with an interval of 30-60 s). The adult animals used in these imaging experiments included cage mates and familiar non-cage mates. We familiarized the subject animals with non-cage mate adults by allowing them to freely interact for 30 minutes per day for at least 3 consecutive days before conducting the imaging experiments.

Extraction of calcium signals

Raw videos from each imaging session were processed using an integrated Miniscope Analysis package (https://github.com/etterguillaume/MiniscopeAnalysis). Briefly, raw videos were first processed using the NormCorre algorithm (https://github.com/flatironinstitute/NoRMCorre)[222] for motion correction. Motion-corrected videos were then processed using Constrained Non-Negative Matrix Factorization (CNMF-E, https://github.com/zhoupc/CNMF_E)[223] to isolate cellular signals and associated regions of interest (ROI). $\Delta F/F$ calcium traces of individual cells were z-scored and presented throughout in units of standard deviation (s.d.) prior to downstream analysis. As CNMF-E can identify

fluorescence changes from non-neuronal sources, such as motion artefacts or neuropil signals, we manually inspected extracted ROIs and traces using a custom Python software (https://github.com/hongw-lab/CScreener) to remove ROIs that lacked a soma-like shape and/or showed signs of motion artefacts in their traces.

Analysis of single-cell responses

Identification of responsive cells. We used an ROC (receiver operating characteristic) analysis[26,224] to identify individual cells that were significantly responsive during various behaviors or events. A binary threshold was applied to the $\Delta F/F$ signal to classify each time point as showing or not showing a particular event. The true positive rate and false positive rate of detection were calculated over a range of binary thresholds spanning the minimum and maximum values of the neural signal and used to construct an ROC curve that describes how well the neural signal detects each event at different thresholds. The area under the ROC curve (auROC) was then calculated as a measure of how strongly neural activity was modulated by each event. The observed auROC was compared to a null distribution generated by circularly permuting the calcium signals by a random time shift 200 times. A neuron was considered significantly responsive ($\alpha < 0.05$) if its observed auROC value was above the 97.5th percentile (activated) or below the 2.5th percentile (suppressed) of the null distribution. Only time points annotated as the event of interest and times points annotated as baseline (not exhibiting any of the annotated events) were included in this analysis, so that the identification of cells responsive to a particular event was not influenced by their activity during other types of events.

Quantification of average activity change in response to behavior. To quantify average cell responses during different types of behavior, the activity of individual cells during each behavior bout was aligned to behavior onset (time 0) and averaged across all behavior bouts within each imaging session. The values of activity change were derived by subtracting the

baseline activity, which was defined as averaged activity over a 3-s time window between 5 s and 2 s before behavior onset.

Analysis of population dynamics

Binary decoding between different types of events. Support Vector Machine (SVM) models were used to identify hyperplanes that best separate population vectors associated with different types of events. A complete recording process for each subject animal, involving multiple sessions of interactions with different types of social targets or self-stress experiences on the same day, was considered one experiment. For each experiment, the mean population activity associated with an event was considered as a sample, and samples were taken for all instances of each of the two types of events. The mean activity of each cell during a behavior event was calculated by averaging the activity within a 10-s period following behavior onset (if the duration of the event was > 10 s) or during the entire bout (if the duration of the event was 10 s). For the decoding between stimulation epochs and baseline periods, mean activity was calculated by averaging the activity within the 5-s stimulation period.

Decoder performance was computed independently for each experiment using a leave-one-out cross-validation (LOOCV) procedure. We used a hold-out sample for testing in each validation fold, while the remaining samples were used for training. To equalize representation of training samples for each group in each fold, we randomly downsampled the group with more samples. In each fold, we first performed partial-least-square (PLS) regression on the training set with behavior type as the response variable. Next, we utilized the first n PLS components in the training data that explain at least 50% of the total variance to construct an SVM model. We then computed the first n components for the held-out sample using the loadings determined from the training set and generated a prediction score for the hold-out sample based on these components. Finally, we compared all prediction scores from all validation folds with ground truth sample labels using an ROC curve, and we used the area

under this curve (auROC) as the final performance metric. The number of test samples for each group was equalized by randomly downsampling the group with more samples. The LOOCV procedure was repeated 10 times to account for the randomness during the downsampling of training and test samples. The averaged auROC was then computed across the 10 rounds. We measured the chance performance for each experiment by performing the same procedure but first circularly permuting the activity trace for each neuron. This process was repeated 20 times and the average auROC was calculated.

To perform the population analysis with sufficient training examples, we included experiments during which the animals displayed at least 3 bouts of either of the two types of events in the decoding analyses. In addition, in the LOOCV procedures, we included folds in which the number of training samples for any group was at least 3 for the calculation of decoding performance. These criteria led to variations in the number of mice included in each analysis, depending on the types of events being decoded.

Mutual decoding between allogrooming, pup grooming, and self-grooming. To investigate whether the population activity pattern during allogrooming has similarities to that during pup grooming or self-grooming, we examined whether classification models trained to decode allogrooming epochs from baseline periods could also predict pup grooming or self-grooming, and vice versa (Fig. 3-7h-k). We first calculated the mean activity of each cell during each event of allogrooming, pup grooming, or baseline period (defined as a period during which the subject animal did not exhibit social investigation, allogrooming, pup grooming, or self-grooming). Mean activity was calculated by averaging the activity over a 10-s period following behavior onset (if bout duration was > 10 s) or over the entire duration of the bout (if bout duration was 10 s). For baseline periods, we excluded the first and last 1 s of each bout from the calculation of mean activity to avoid influence from neighboring behavior bouts. All instances of pup grooming and baseline periods during pup interaction were taken as the test

set, and all instances of allogrooming events and baseline periods during interaction with stressed adults were used to construct the training set. The number of training samples for each group was equalized by randomly downsampling the group with more samples. We performed PLS regression on the training set with event type as the response variable, and utilized the first n PLS components that explain at least 50% of the total variance to construct an SVM model. We then computed the first n components for the test samples using the loadings determined from the training set and generated a prediction score for the test sample based on these components. We subsequently compared prediction scores for all test samples with ground truth labels using an ROC curve, and we used the area under this curve (auROC) as the final performance metric. The number of test samples for each group was equalized by randomly downsampling the group with more samples. This procedure was repeated 10 times to account for the randomness during the downsampling of training and test samples, and the averaged auROC across the 10 rounds was computed. To calculate chance performance, we utilized the same procedure, but with the additional step of circularly permuting the activity trace for each neuron. This permutation process was repeated 20 times, and the averaged auROC was computed.

Principal component analysis. To analyze the separation of population vectors associated with different types of behaviors, we performed principal component analyses based on mean population activity during different behavior events for each experiment. The mean activity of each cell during each event was calculated by averaging the activity over a 5-s period following behavior onset (if bout duration was > 5 s) or over the entire duration of the bout (if bout duration was 5 s). To examine the relationship between population activity patterns during investigations toward unstressed adults, stressed adults, and pups (FIg. 3-6e,f), we used the top 3 PC projections of each experiment to compute the Mahalanobis distances between all pairs of investigation events toward unstressed adults and pups and

between all pairs of investigations events toward stressed adults and pups. We then calculated the average distance for all unstressed adult-pup pairs and compared it to the average distance for all stressed adult-pup pairs within each animal.

CHAPTER FOUR

MPOA→VTA circuit controls prosocial allogrooming and parenting behavior

INTRODUCTION

The medial preoptic area (MPOA) is a highly heterogeneous brain region that plays a central role in coordinating a wide range of social and motivational behaviors. Recent transcriptomic and functional studies have revealed a rich diversity of molecularly defined cell types within the MPOA, many of which exhibit distinct projection patterns and behavioral roles[225–227]. If MPOA neurons encode caregiving behavior towards both stressed conspecifics and pups, does that mean they are also functionally significant? Results in Chapter 3 showed that MPOA neurons encode prosocial allogrooming and that a subset of neurons is recruited during both allogrooming and pup grooming. These findings suggest a potential shared circuit mechanism for caregiving responses across social contexts. Although the MPOA is well-known to control parenting behavior, its role in regulating prosocial allogrooming toward stressed adult conspecifics remain unclear. In this chapter, we investigate the functional role of MPOA GABAergic neurons in regulating prosocial allogrooming behavior. Using cell-type-specific manipulations, we test whether these neurons are necessary and sufficient for initiating comforting behavior toward stressed conspecifics, and which downstream circuits mediate this effect. Finally, to assess whether these behaviors share a common neural substrate, we ask whether the same MPOA neurons involved in pup-directed caregiving are also recruited during allogrooming.

RESULTS

MPOA^{Vgat+} neurons bidirectionally regulate allogrooming behavior

Given that MPOA glutamatergic neurons have been shown to promote anxiety-like behavior and inhibit parenting behavior[228], we focused on the GABAergic (Vgat+) population in the MPOA in investigating whether MPOA neurons play a causal role in regulating allogrooming behavior. To first determine if the activity of MPOA GABAergic neurons are

required for naturally occurring allogrooming, we performed chemogenetic inhibition by injecting an AAV expressing a Cre-dependent inhibitory DREADD (hM4Di)[229] into the MPOA of Vgat-Cre animals (Fig. 4-1a,). While I performed pilot experiments not presented in this chapter, the chemogenetic data included here are from experiments conducted by FS. Following CNO injection, animals displayed significantly reduced allogrooming behavior during interaction with stressed adult conspecifics, compared with the same animals following saline injection (Fig. 4-1d1). By contrast, control animals expressing only mCherry exhibited no alteration in allogrooming following CNO injection (Fig. 4-1e1). Furthermore, the duration of investigation toward stressed conspecifics or self-grooming was unchanged following chemogenetic inhibition (Fig. 4-1d2, d3, e2, e3), and the locomotion and anxiety level of the animals appeared unaffected in the open-field test (Fig. 4-1f-i). This suggests that the effect on allogrooming was not due to non-specific changes in general social investigation or motility.

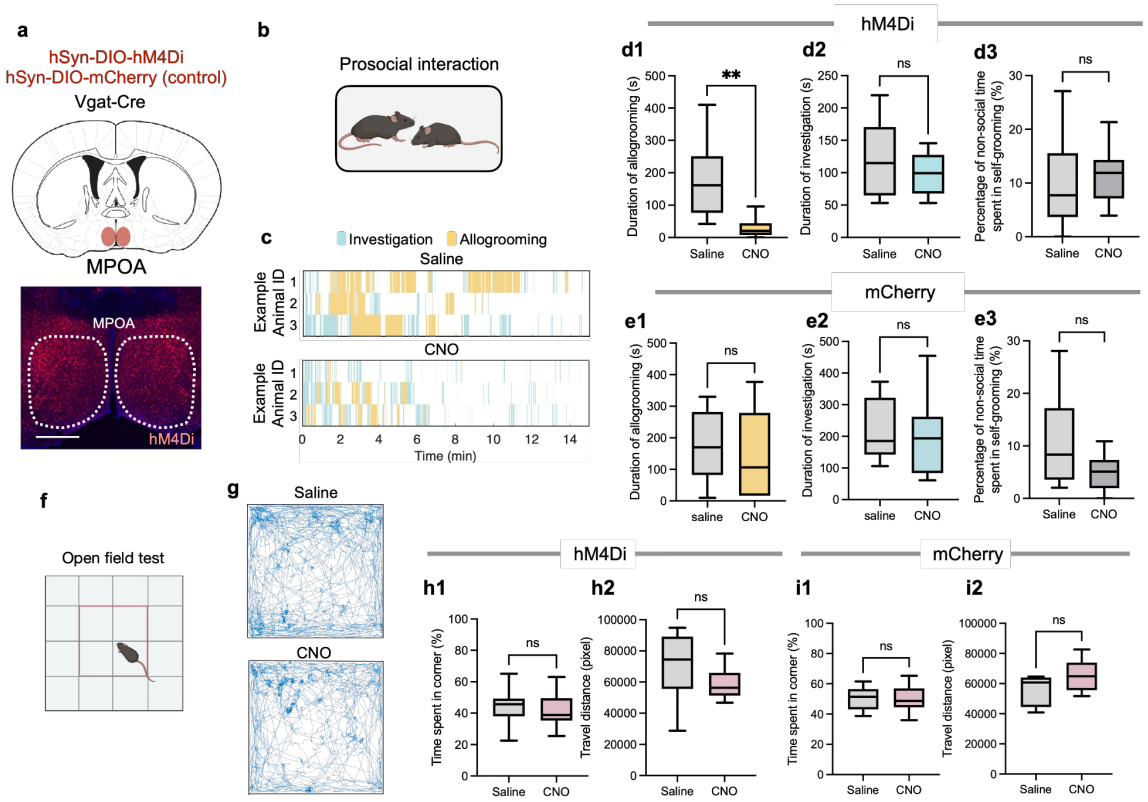

Figure 4-1: Chemogenetic inhibition of MPOA^{Vgat+} neurons. a, Schematic of chemogenetic inhibition of MPOAVgat+ neurons (top) and example micrograph of hM4Di expression in the MPOA (bottom). Scale bar, 500 μm. **b**, Schematics of the prosocial interaction and the open field test paradigms. The red square in the open field indicates the center zone. **c**, Example raster plots showing behaviors exhibited by hM4Di-expressing animals injected with either saline (control) or CNO during interactions with stressed adults. **d, e,** Duration of allogrooming (**d1, e1**) and investigation (**d2, e2**) toward stressed adults and selfgrooming (**d3, e3**) following saline or CNO injection in hM4Di-expressing animals (**d**) or mCherry-expressing control animals (**e**). **f**, Schematic of open field test. **g,** Example locomotion trajectories in the open field test following saline or CNO injection in hM4Di-expressing animals. **h, i,** Time spent in the corners (**h1, i1**) and travel distance (**h2, i2**) in the open field test following saline injection or CNO injection in hM4Di-expressing animals (**h**) or mCherry-expressing control animals (**i**). (d, e, h, i), two-sided Wilcoxon signed-rank test.
n = 10 mice (5 male, 5 females) in (d, h), 6 mice (2 male, 4 females) in (e, i).

To further examine whether acute inhibition of MPOA^{Vgat+} neurons leads to an acute suppression of allogrooming, I injected an AAV expressing the Cre-dependent silencing opsin stGtACR2[230] (or mCherry as a control) into the MPOA of Vgat-Cre animals and acutely suppressed the activity of MPOA^{Vgat+} neurons as the animals displayed allogrooming toward stressed adult partners (Fig. 4-2a, b). Photo-inhibition of MPOA^{Vgat+} neurons in stGtACR animals led to an acute suppression of naturally occurring allogrooming compared with sham stimulations (light off) or mCherry-expressing control animals (Fig. 4-2c-f). The observed reduction in allogrooming did not appear to be due to general suppression of social investigation, as photo-inhibition produced no significant effect on the duration of social investigation compared with the sham stimulation (Fig. 4-2g, h). These results suggest that MPOA^{Vgat+} neurons are essential for promoting natural allogrooming behavior.

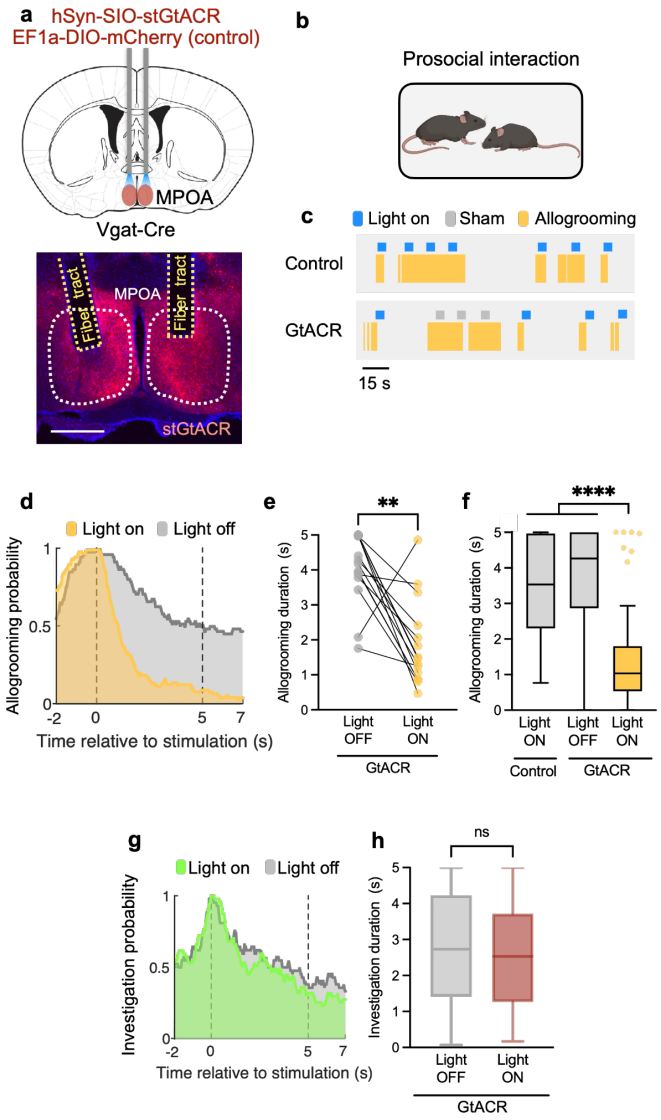

Figure 4-2: Photo-inhibition of MPOA^{Vgat+} neurons. a, Schematic of optogenetic inhibition of MPOAVgat+ neurons (top) and example micrograph showing GtACR expression and optic fiber placement in the MPOA (bottom). Scale bar, 500 μm. **b**, Schematic showing optogenetic inhibition during prosocial interactions with stressed adults. **c**, Example raster plots showing allogrooming behavior during 5-s real (light on) and sham (light off) photo-inhibition in GtACR-expressing animals or during light delivery in mCherry-expressing control animals. **d, e, f**, The probability of showing allogrooming at various time points (**d**), average allogrooming duration across all trials within individual mice (**e**), and allogrooming duration in individual trials (**f**) during the 5-s real (light on) and sham (light off) photo-inhibition in GtACR-expressing mice and during light delivery in mCherry-expressing control mice. **g, h**, The probability of showing investigation toward stressed adults at various time points (**g**) and investigation duration in individual trials (**h**) during the 5-s real (light on) and sham (light off) photo-inhibition in GtACR-expressing mice. (e), two-sided Wilcoxon signed-rank test. (f), Kruskal-Wallis test with post hoc Dunn's multiple comparisons test. (h), two-sided Wilcoxon rank-sum test.

n = 15 mice (7 male, 8 female) in (e), 90-118 trials from 15 mice (7 male, 8 female) for GtACR and 62 trials from 10 mice (5 male, 5 female) for control in in (f), 84-96 trials from 11 mice (5 male, 6 female) in (h).

To determine whether MPOA^{Vgat+} neurons are also sufficient to drive allogrooming, I expressed the Cre-dependent excitatory opsin ChR2 (or mCherry as a control) in the MPOA of Vgat-Cre animals and optogenetically activated these neurons during baseline periods in which animals were not spontaneously engaging in allogrooming (Fig. 4-3a). I found that photoactivation of MPOA^{Vgat+} neurons elicited an acute increase of allogrooming, with a longer duration and a shorter onset latency during photostimulation compared to sham stimulations or mCherry-expressing control animals (Fig. 4-3b-f). Together, these results demonstrate a critical role of MPOA^{Vgat+} neurons in driving allogrooming behavior.

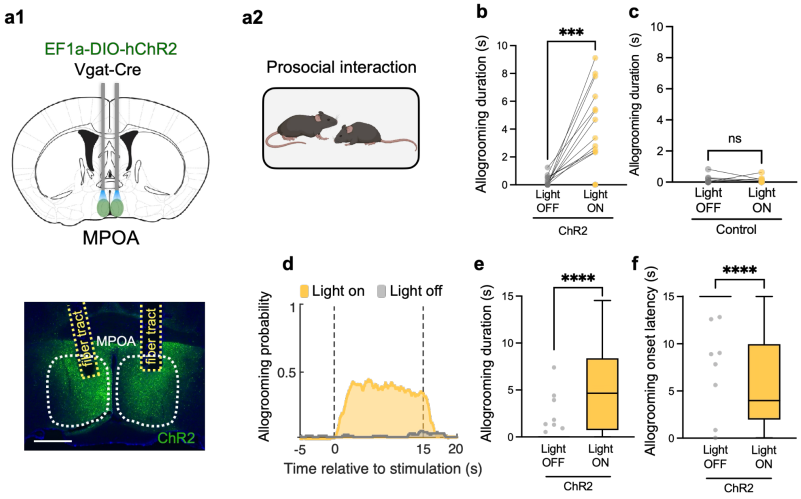

Figure 4-3: Photo-activation of MPOA^{Vgat+} neurons. a, Schematics of optogenetic activation of MPOAVgat+ neurons (a1, top), example micrograph showing ChR2 expression and optic fiber placement in the MPOA (a1, bottom), and the prosocial interaction paradigm (a2). Scale bar, 500 µm. **b, c**, Average allogrooming duration across all trials during the 15-s real (light on) and sham (light off) photo-activation in individual mice expressing ChR2 (**c**) or EYFP (**c**). **d-f**, Allogrooming probability (**d**), allogrooming duration in individual trials (**e**), and allogrooming onset latency in individual trials (**f**) during the 15-s real (light on) and sham (light off) photo-activation in ChR2-expressing mice that showed any allogrooming during stimulations. (b, c), two-sided Wilcoxon signed-rank test. (e), two-sided unpaired t-test. (f), two-sided Wilcoxon rank-sum test.
n = 32 mice (18 female, 14 male) in (d), 10 mice (5 female, 5 male) in (e), and 76-166 trials from 12 mice (9 female, 3 male) in (e, f).

In accordance with the role of MPOA^{Vgat+} neurons in pup-directed behaviors[228,231], we confirmed that both chemogenetic and optogenetic inhibition of these neurons also led to the suppression of naturally occurring pup grooming behavior (Fig. 4-4a-f, g-j), with no obvious effect on pup investigation (Fig. 4-4c2, f2). Additionally, activation of MPOA Vgat+ neurons during interaction with pups induced pup grooming behavior (Fog. 4-4 k-o). Together, our results indicate that the MPOA Vgat+ neurons not only regulate parenting behavior but also promote allogrooming behavior.

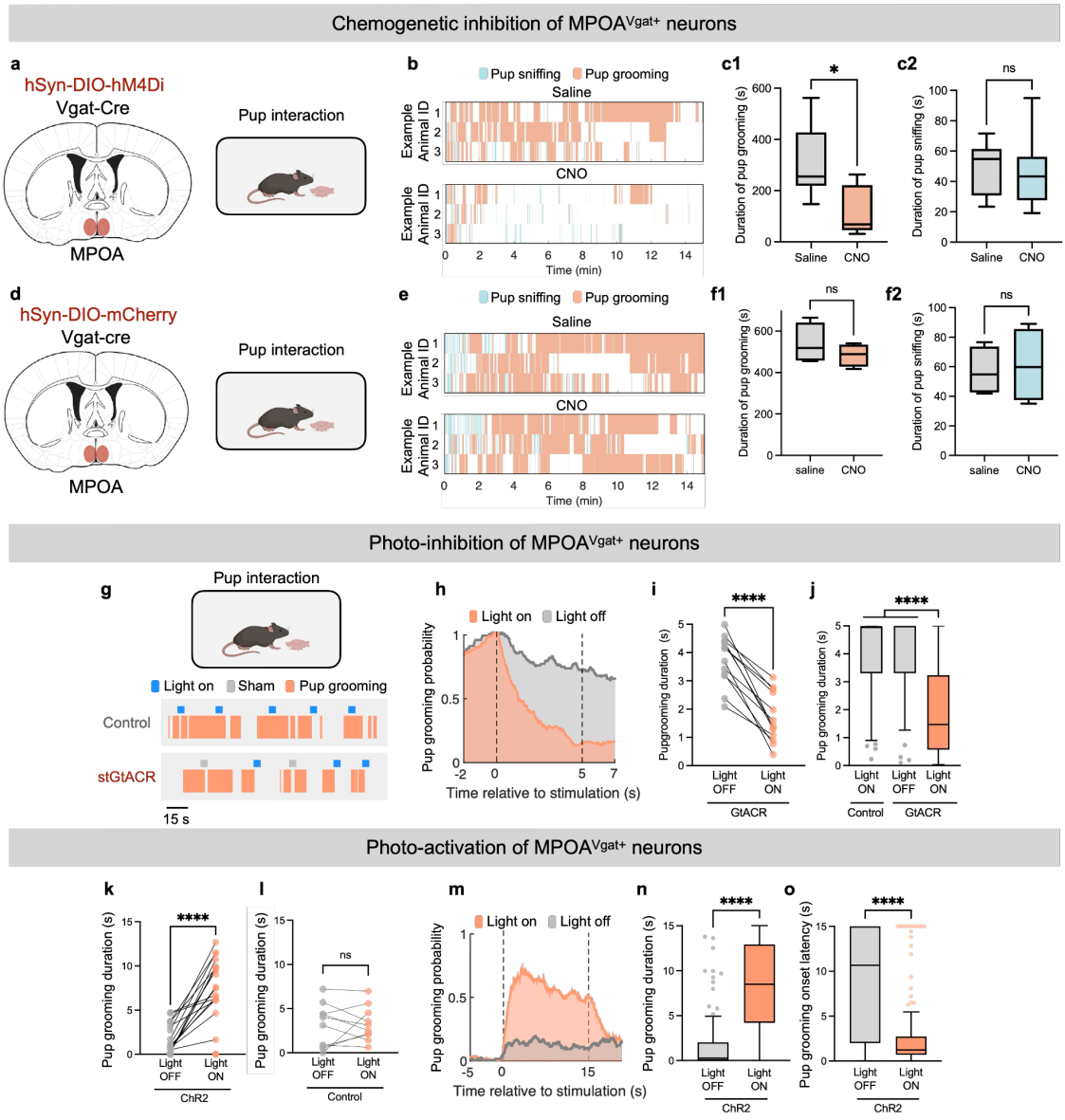

Figure 4-4. Functional manipulations of the MPOA in pup grooming. a, d, Schematics of chemogenetic inhibition of MPOAVgat+ neurons during pup interactions (**a**) and control experiments in mCherry-expressing animals (**d**). **b, e**, Example raster plots showing pup-directed behaviors exhibited by hM4Di-expressing (**b**) or mCherry-expressing (**e**) animals injected with either saline or CNO. **c, f,** Duration of pup grooming (**c1, f1**) and pup sniffing (**c2, f2**) following saline or CNO injection in hM4Di-expressing (**c**) or mCherry-expressing (**f**) animals. **g,** Schematic of optogenetic inhibition of MPOA^{Vgat+} neurons during pup interactions (top) and example raster plots showing pup grooming during 5-s real (light on) and sham (light off) photo-inhibition in GtACR-expressing animals or during light delivery in mCherry-expressing control animals. **h-j**, The probability of showing pup grooming at various time points (**h**), average pup grooming duration across all trials within individual mice (**i**), and pup grooming duration in individual trials (**j**) during the 5-s real (light on) and sham (light off) photo-inhibition in GtACR-expressing mice and during light delivery in mCherry-expressing control mice. **k, l**, Average pup grooming duration during the 15-s real (light on) and sham (light off) photo-activation in individual mice expressing ChR2 (**k**) or EYFP (**l**). **m-o**, Pup grooming probability (**m**), pup grooming duration in individual trials (**n**), and pup grooming onset latency in individual

trials (**o**) during the 15-s real (light on) and sham (light off) photo-activation in ChR2-expressing mice that showed any pup grooming during stimulations. (c, f, k), two-sided Wilcoxon signed-rank test. (i, l), two-sided paired t-test. (j), Kruskal-Wallis test with post hoc Dunn's multiple comparisons test. (n), two-sided unpaired t-test. (o), two-sided Wilcoxon rank-sum test. n = 7 mice (2 males, 5 females) in (c), 6 mice (2 males, 4 females) in (f), 12 mice (3 males, 9 females) in (i), 90-115 trials in 13 mice (5 males, 8 females) for GtACR and 89 trials from 10 mice (5 males, 5 females) for control in (j), 31 mice (14 males, 17 females) in (k), 10 mice (5 males, 5 females) in (l), and 107-171 trials from 17 mice (9 males, 8 females) in (n,o).

Manipulation of other molecularly-defined MPOA cell types did not produce consistent effects

Given that Vgat+ neurons comprise approximately 80% of the MPOA neuronal population[211], and that previous studies have identified molecularly defined MPOA subtypes involved in specific social behaviors (such as Esr1+ neurons in both parenting and mating), I explored whether other genetically defined subpopulations within the MPOA might similarly regulate allogrooming behavior. These included Esr1, Oxtr, Tac1, Tac1/Vgat, Tacr1, Cck, and Sst. In the medial amygdala, Tac1∩Vgat neurons promote allogrooming behavior[26], prompting the question of whether their MPOA counterparts play a comparable role. Oxtr-expressing neurons in the MPOA have also been linked to parenting, primarily through loss-of-function studies[232,233]. Tac1 and Cck have been associated with sleep and arousal modulation, while the behavioral roles of Sst-expressing neurons in the MPOA remain less well-defined. While Gal, Calcr, and Prlr are also promising targets given their established involvement in parenting[209,214,234–237], they were not tested here due to the unavailability of Cre-driver lines in our colony.

To test whether each of these populations of neurons are also sufficient to drive allogrooming, I expressed the Cre-dependent excitatory opsin ChR2 in the MPOA of Esr1-, Oxtr-, Tac1-, Tac1∩Vgat, Tacr1-, Cck, and Sst-cre animals and optogenetically activated these neurons while subjects interacted with adult conspecifics, during baseline periods in which animals were not spontaneously engaging in allogrooming (Fig. 4-5a, left and middle).

None of these manipulations produced consistent or robust changes in allogrooming (Fig. 4-5b) across animals. These findings are broadly consistent with prior reports – for instance, activation of Esr1+ MPOA promotes mounting behavior[211,238]. However, some of my results (such as the limited effects observed in Tacr1-Cre animals) contrast with previous reports linking this population to sexual behavior in male mice[239], likely due to methodological differences such as laser power. I also performed similar photoactivation experiments during interactions with pups (Fig. 4-5a,b, right), and found that Esr1- and Oxtr-expressing neurons produced modest effects on pup grooming, consistent with earlier findings. Interestingly, I also identified new evidence that Tac1∩Vgat+ MPOA neurons modestly increased pup grooming,. While these pilot experiments were limited in scope and not sufficiently powered to support strong conclusions, the lack of clear behavioral effects suggest that the activity of these subtypes may not be sufficient to independently drive prosocial grooming.

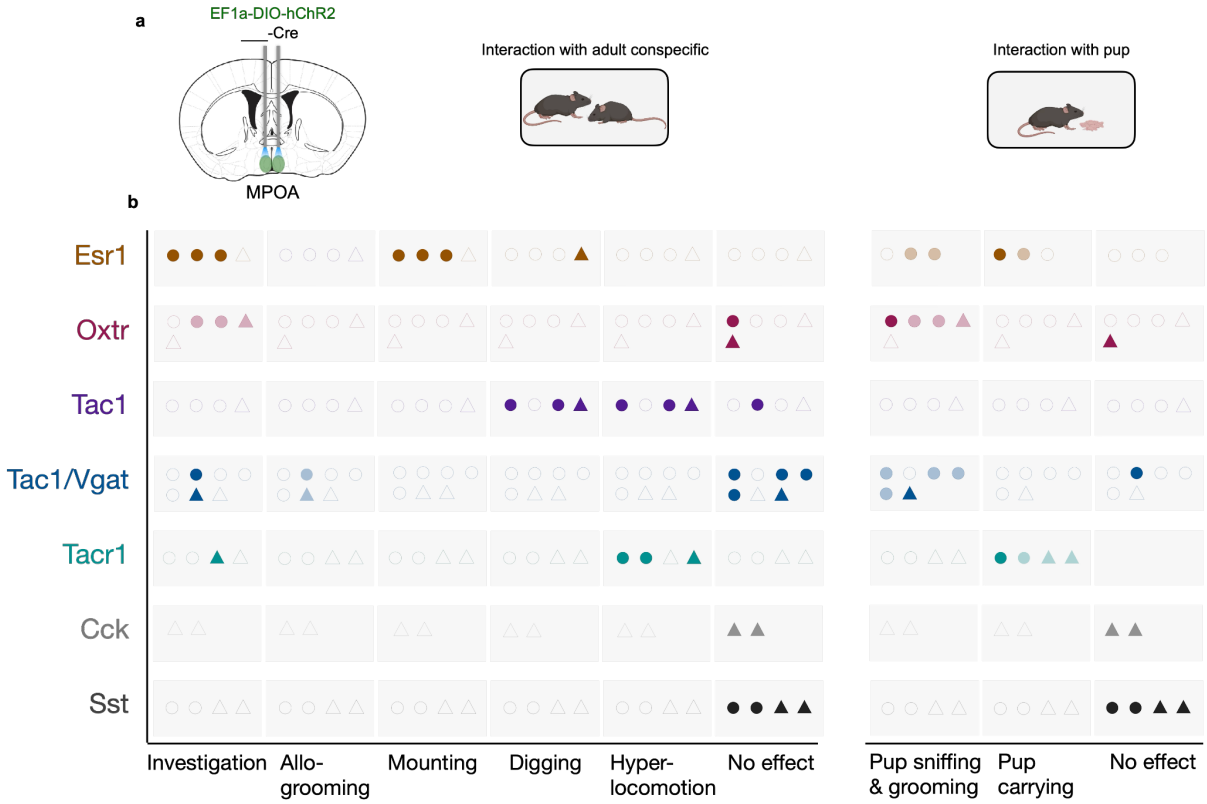

Figure 4-5. Summary of photo-stimulation of additional molecularly defined MPOA cell types. a, Schematics of optogenetic activation of MPOA neurons in a variety of cre-driver lines during interaction with adult conspecific or with pups. **b**, Behavioral responses of individual animals across different cell types during interaction with adults (left) or pups (right). Each row indicates genetically targeted cell populations. Each symbol represents a single animal, circle for females and triangles for males. Color intensity of the symbol indicates the presence and strength of behavioral phenotypes – dark filled symbols represent animals that showed the behavior in >50% of stimulation trials, light filled symbols indicate the behavior occurred in <25% of trials, and empty symbols denote no observed phenotype for that behavior.

The molecularly diverse neuronal subtypes in the MPOA are each defined by a combination of multiple marker genes[225]. Although some individual marker genes have been used to label neuronal populations with functional roles in parenting behavior, each of these markers is expressed across multiple neuronal subtypes[208,209,225,225,234] and may label either a subset of a functional population or a mixture of different functional populations. In these experiments, I activated Cre-line defined single-marker cell populations, some including GABAergic and glutamatergic populations within them. Given our finding that Vgat+ neurons

are both necessary and sufficient for allogrooming (Fig. 4-1 to 4-4), it is likely that the relevant population lies within a specific subset of $MPOA^{Vgat+}$ neurons defined by additional, as-yet-unidentified molecular features.

Allogrooming, pup grooming, and $MPOA^{Vgat+}$ activity are associated with NAc dopamine release

Another approach to defining functionally relevant neuronal subtypes is by their projection targets. My findings that $MPOA^{Vgat+}$ neurons promote allogrooming raise the question of how this population exerts its effects through downstream circuits. Additionally, the partially shared neural representation of allogrooming and pup grooming behaviors in the MPOA prompts the hypothesis that these behaviors may also engage common downstream circuits. One such candidate is the mesolimbic dopamine system, which has been implicated in the motivational and self-rewarding aspects of prosocial behavior[240–244]. Given previous findings that a subset of MPOA neurons project to the ventral tegmental area (VTA) and mediate social reward[221], we hypothesized that a shared mechanism for prosocial and parenting behaviors may involve the generation of self-reward through the connection between the MPOA and the reward circuitry.

To determine whether allogrooming is indeed linked to a rewarding experience, I collaborated with co-author FS to examine dopamine release in the NAc during this behavior. FS virally expressed a genetically encoded dopamine sensor $GRAB_{DA2m}$[245] in the NAc core and recorded dopamine dynamics during social interactions with stressed adults (Fig. 4-6a,b). She showed a significant increase in dopamine signals during allogrooming toward stressed conspecifics (Fig. 4-6c,d), suggesting a rewarding nature of this behavior. There was also a substantial increase in dopamine signals increased during pup grooming (Fig. 4-6e,f), consistent with previous findings that close contact with pups leads to dopamine release[246].

In contrast, a negative experience (restraint stress) led to a significant reduction in dopamine signal (Fig. 4-6g,h). To examine whether direct activation of $MPOA^{Vgat+}$ neurons evokes NAc dopamine release, FS virally expressed ChrimsonR (or mCherry as a control) in $MPOA^{Vgat+}$ neurons and $GRAB_{DA2m}$ in NAc and recorded NAc dopamine dynamics during optogenetic stimulation of MPOA neurons (Fig. 4-6i). Consistent with previous studies[247], activating $MPOA^{Vgat+}$ neurons in ChrimsonR-expressing animals led to a robust, time-locked increase in dopamine signal, but in not mCherry-expressing control animals (Fig. 4-6k,l). By contrast, activation of ChrimsonR-expressing $MPOA^{Vglut2+}$ neurons evoked a substantially weaker dopamine response, followed by a modest rebound at the offset of the stimulation (Fig. 4-6m,n). In line with these findings, I show that activation of $MPOA^{Vgat+}$ neurons led to a positive preference in a real-time place preference test (Fig. 4-7), suggesting that activity of $MPOA^{Vgat+}$ neurons are associated with a rewarding experience. Taken together, our results indicate that both allogrooming and pup grooming are associated with dopamine release, possibly facilitated by a connection between $MPOA^{Vgat+}$ neurons and the mesolimbic dopamine pathway.

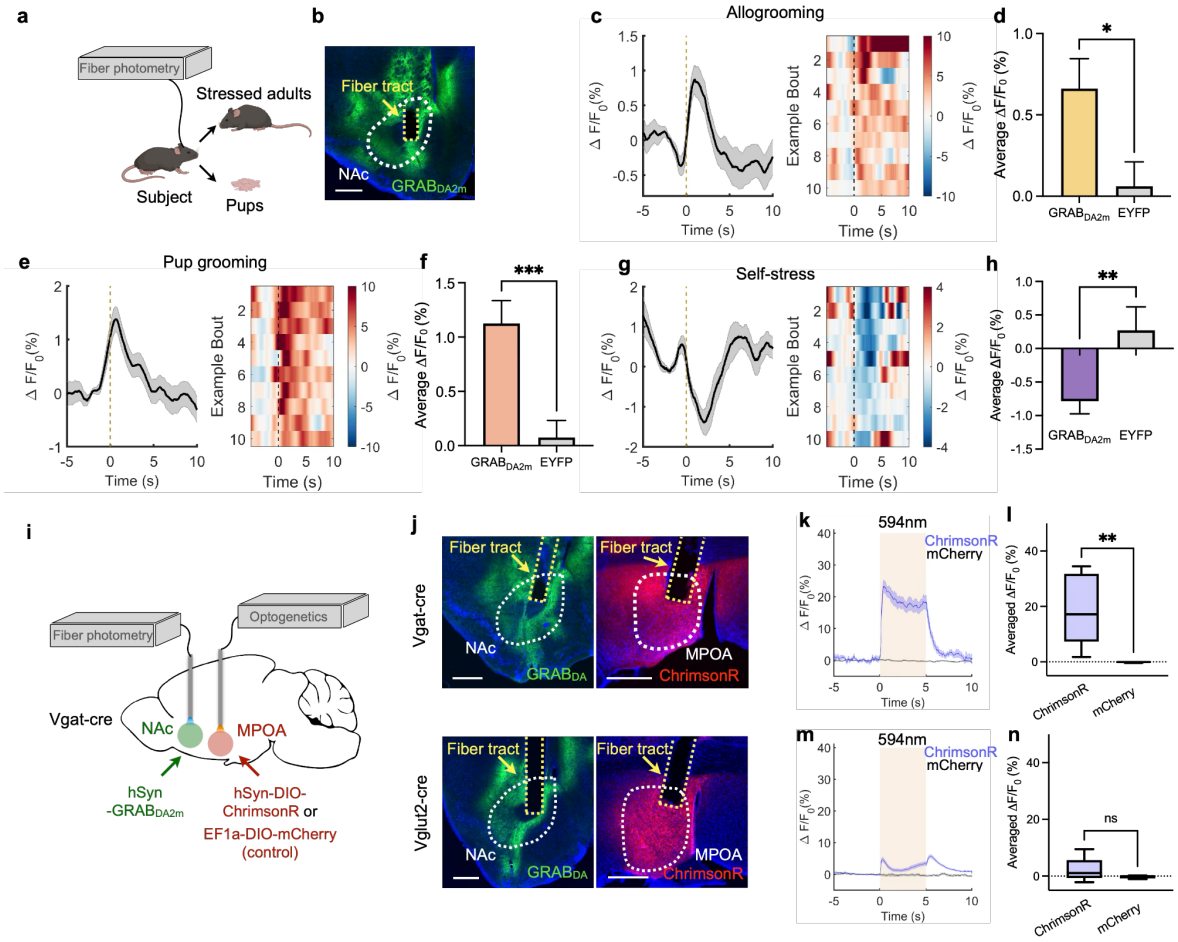

Figure 4-6. Dopamine release during allogrooming and pup grooming. a, Schematic of fiber photometry recording in the NAc during prosocial interaction and pup interaction. **b**, Example micrograph of $GRAB_{DA}$ expression and optic fiber placement in the NAc. Scale bar, 500 μm. **c, e, g**, Average NAc dopamine signal changes (left; mean ± SEM) and heatmaps of example trials (right) during allogrooming (**c**), pup grooming (**e**), or self-stress experience (**g**). Time 0 indicates behavior onset. **d, f, h**, Average ΔF/F0 during 0-2s following the onset of allogrooming (**d**), pup grooming (**f**), or self-stress (**h**) in GRABDA-expressing mice and EYFP-expressing control mice. **i**, Schematic of fiber photometry recording in the NAc combined with optogenetic activation of MPOAVgat+ neurons. **j**, Example micrographs showing $GRAB_{DA}$ expression and optic fiber placement in the NAc as well as ChrimsonR expression and optic fiber placement in the MPOA in VgatCre/+ and VglutCre/+ animals. Scale bar, 500 μm. **k-n**, Average responses of NAc dopamine signals (**k, m**) and mean ΔF/F0 (**l, n**) during 5-s photo-activation of $MPOA^{Vgat+}$ neurons (**k, l**) or $MPOA^{Vglut2+}$ neurons (**m, n**) in ChrimsonR-expressing mice and mCherry-expressing control mice. (d, f, h, l, n), two-sided Wilcoxon rank-sum test. n = 109 bouts from 13 mice for the $GRAB_{DA}$ group and 24 bouts from 4 mice for the EYFP group in (d), 174 bouts from 13 mice for the $GRAB_{DA}$ group and 54 bouts from 4 mice for the EYFP group in (f), 18 bouts from 6 mice for the $GRAB_{DA}$ group and 15 bouts from 5 mice for the EYFP group in (h), and 7 mice for the ChrimsonR group and 4 mice for the mCherry group in (l, n).

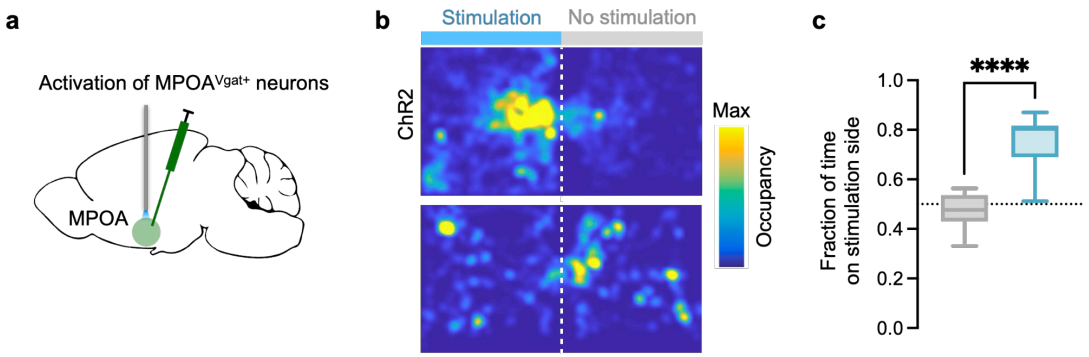

Figure 4-7. Activation of MPOA^{Vgat+} is associated with positive valence. a-c, Schematic of stimulation strategy (**a**), example heatmaps (**b**), and the fraction of time spent on the stimulation side (**c**) in ChR2-expressing mice and EYFP-expressing control mice in the real-time place preference test (RTPP) during photo-activation of MPOA^{Vgat+} neurons.
n = 13 mice in the ChR2 group and 6 mice in the control group in (c).

VTA-projecting MPOA neurons bidirectionally control allogrooming behavior

Given the observed engagement of the mesolimbic dopamine system during allogrooming and MPOA^{Vgat+} activation, we next asked whether the MPOA-to-VTA projection plays a causal role in mediating prosocial and parenting behaviors. To address this, I collaborated with co-author FS, who performed the retrograde inhibition experiment by injecting a retrograde AAV expressing Cre-dependent stGtACR in the VTA of Vgat-Cre animals and implanting fibers in the MPOA to illuminate the VTA-projecting MPOA^{Vgat+} neurons (Fig. 4-8a). Photo-inhibition of these neurons suppressed naturally occurring allogrooming and pup grooming in both males and females (Fig. 4-8b-e), supporting that the VTA-projecting MPOA^{Vgat+} neurons are not only required for pup grooming, but also essential for allogrooming. Moreover, we asked whether photo-activation of the MPOA^{Vgat+}-VTA pathway is sufficient to promote allogrooming and pup grooming. I first manipulated the axonal projections of the MPOA^{Vgat+} neurons in the VTA by virally expressing Cre-dependent ChR2 in the MPOA and implanting optic fibers in the VTA (Fig. 4-8f,g). Photo-activation of this projection indeed induced both allogrooming toward stressed animals (Fig. 4-8h-k) and pup

grooming (Fig. 4-8l-o). In addition, I activated the somas of the VTA-projecting MPOA^{Vgat+} neurons by injecting a retrograde AAV expressing Cre-dependent ChR2 in the VTA and implanting optic fibers in MPOA (Fig. 4-8p). This also led to an acute increase in both prosocial allogrooming (Fig. 4-8q, r) and pup grooming (Fig. 4-8s, t) in both males and females.

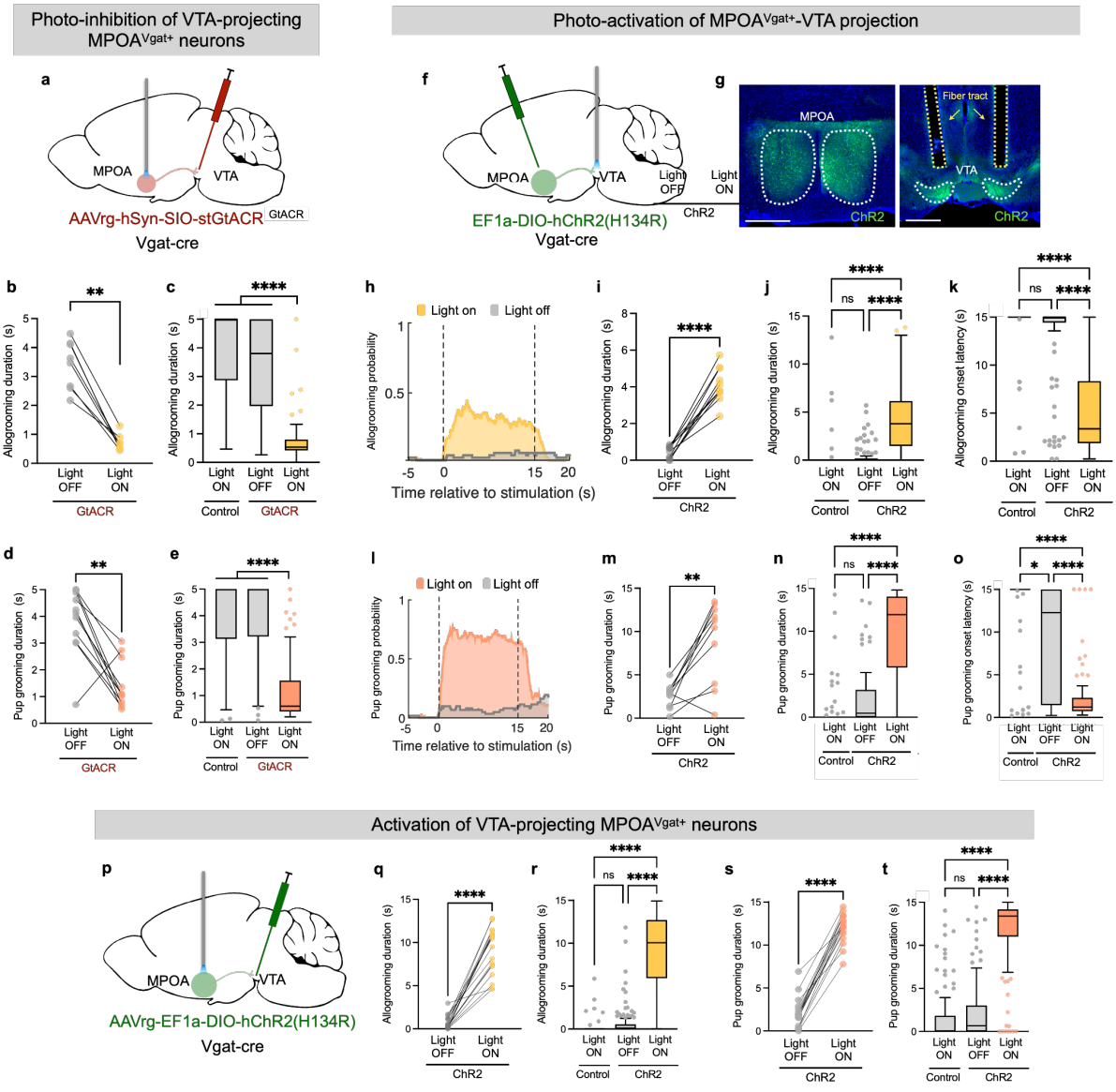

Figure 4-8. An MPOA^{Vgat+}-VTA pathway controls both allogrooming and parenting behaviors. a, Schematic of optogenetic inhibition of VTA-projecting MPOA^{Vgat+} neurons. **b, c**, Average duration of allogrooming across all trials within individual mice (**b**) and the duration of allogrooming in individual trials (**c**) during the 5-s real (light on) and sham (light off) photo-

inhibition in GtACR-expressing mice and during light delivery in EYFP-expressing control mice. **d, e,** Average duration of pup grooming across all trials within individual mice (**d**) and the duration of pup grooming in individual trials (**e**) during the 5-s real (light on) and sham (light off) photo-inhibition in GtACR-expressing mice and during light delivery in EYFP-expressing control mice. **f**, Schematic of optogenetic activation of the MPOA^{Vgat+}-VTA projection. **g**, Example micrographs showing ChR2 expression in the MPOA and the axonal projections of MPOAVgat+ neurons and optic fiber placement in the VTA. Scale bar, 500 μm. **h-i,** The probability of showing allogrooming at various time points (**h**), average allogrooming duration across all trials within individual mice (**i**), duration of allogrooming in individual trials (**j**), and onset latency of allogrooming (**k**) in individual trials during the 15-s real (light on) and sham (light off) photo-activation in ChR2-expressing mice and during light delivery in EYFP-expressing control mice. **l-o**, The probability of showing pup grooming at various time points (**l**), average pup grooming duration across all trials within individual mice (**m**), duration of allogrooming pup grooming in individual trials (**n**), and onset latency of pup grooming in individual trials (**o**) during the 15-s real (light on) and sham (light off) photo-activation in ChR2-expressing mice and during light delivery in EYFP-expressing control mice. **p**, Schematic of optogenetic activation of VTA-projecting MPOA^{Vgat+} neurons. **q-t**, Average allogrooming or pup grooming duration across all trials within individual mice and duration of allogrooming (**q, r**) or pup grooming (**s, t**) in individual trials during the 15-s real (light on) and sham (light off) photo-activation in ChR2-expressing mice and during light delivery in EYFP-expressing control mice. (b, d, q, s), two-sided Wilcoxon signed-rank test. (c, e, j, k, n, o, r, t), Kruskal-Wallis test with post hoc Dunn's multiple comparisons test. (i, m), two-sided paired t-test.
n = 8 mice in (b), 65-68 trials from 6-8 mice in each group in (c), 11 mice in (d), 64-91 trials from 7-11 mice in each group in (e), 10 mice in (i), and 58-162 trials from 6-10 mice in each group in (j, k), 10 mice in (m), 44-82 trials from 6-10 mice in each group in (n, o), 18 mice in (q), 93-202 trials from 10-18 mice in each group in (r), 17 mice in (s), 96-160 trials from 10-17 mice in each group in (t).

Interestingly, compared to activation of the general Vgat+ population, selective activation of the VTA-projecting Vgat+ subpopulation produced more pronounced behavioral effects, with significantly higher percentages of animals exhibiting allogrooming or pup grooming in response to stimulation (Fig. 4-9a,b). This suggests a more select role of this subpopulation in driving these behaviors compared to the general Vgat+ population. To further confirm that the observed behavioral effects of activating the MPOA^{Vgat+}-VTA projection were not due to activation of collateral projections to other brain areas, I optogenetically activated the VTA projection while concurrently infusing lidocaine in the MPOA to prevent antidromic activation of cell bodies in the MPOA (Fig. 4-9c). I observed comparable increases in allogrooming in animals infused with lidocaine and those infused with saline (Fig. 4-9d,e), suggesting that the MPOAVgat+-VTA projection is indeed involved in promoting allogrooming.

Together, these findings indicate that the MPOA Vgat+ neurons that project to the VTA represent a select subpopulation of neurons that regulate both allogrooming and pup grooming. Similar to MPOA^{Vgat+} neurons, activation of the projections of these neurons in the VTA and activation of VTA-projecting Vgat+ subpopulation also led to a positive preference in a real-time place preference test (Fig. 4-10, suggesting that the same MPOA^{Vgat+}-VTA connection facilitates a rewarding experience.

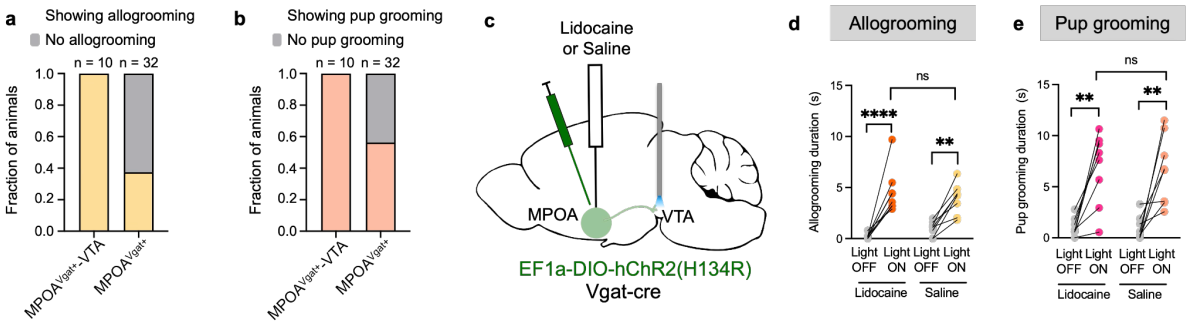

Figure 4-9. Selective activation of VTA-projecting MPOA^{Vgat+} neurons drives allogrooming and pupgrooming. a, b, Fraction of animals showing optogenetically induced allogrooming (**a**) or pup grooming (**b**) during stimulation of the general MPOA^{Vgat+} population or selective activation of the VTA-projecting subpopulation of MPOA^{Vgat+} neurons. Subject mice are virgin males or females. **c**, Schematic of optogenetic activation of the MPOA^{Vgat+}-VTA projection with concurrent lidocaine infusion in the MPOA. **d, e**, Average allogrooming (**d**) or pup grooming (**e**) duration across all trials within individual mice during the 15-s real (light on) and sham (light off) photo-activation of the MPOA^{Vgat+}-VTA projection with the infusion of lidocaine or saline in the MPOA. (a, b) Fisher's exact test; allogrooming, $p < 0.0001$; pup grooming, $p = 0.017$. (d, e), two-way ANOVA with post hoc Fisher's LSD test.
n = 8 mice in each group in (d, e).

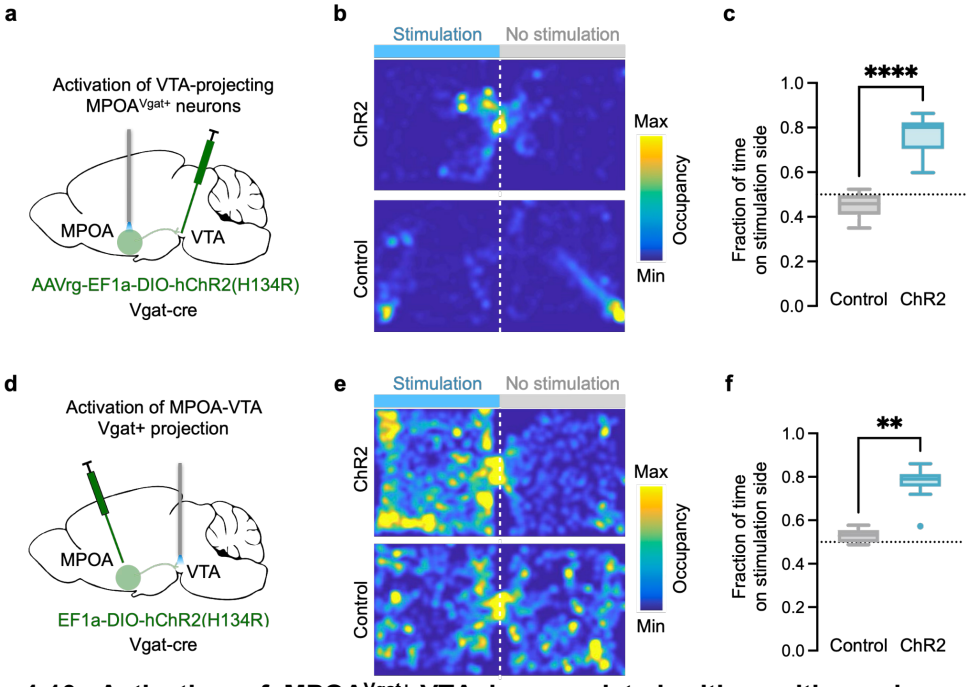

Figure 4-10. Activation of MPOA^{Vgat+}-VTA is associated with positive valence. a-c, Schematic of stimulation strategy (**a**), example heatmaps (**b**), and the fraction of time spent on the stimulation side (**c**) in ChR2-expressing mice and EYFP-expressing control mice in the RTPP test during photo-activation of VTA-projecting MPOA^{Vgat+} neurons. **d-f**, Schematic of stimulation strategy (**d**), example heatmaps (**e**), and the fraction of time spent on the stimulation side (**f**) in ChR2-expressing mice and EYFP-expressing control mice in the RTPP test during photo-activation of the VTA projections of MPOA^{Vgat+} neurons. (c, f), two-sided Wilcoxon rank-sum test.
n = 18 mice in the ChR2 group and 9 mice in the control group in (c), and 10 mice in the ChR2 group and 5 mice in the control group in (f).

To investigate whether allogrooming may also be modulated by other MPOA projections, we examined another major downstream target of MPOA neurons, the periaqueductal gray (PAG)[214,247]. FS first performed retrograde labeling of VTA-projecting and PAG-projecting MPOA Vgat$^+$ neurons and found that these two populations were largely separable (Fig. 4-11 a-c). To assess the role of the MPOA^{Vgat+}-PAG connection, I optogenetically stimulated the projections of MPOA^{Vgat+} neurons in the PAG (Fig. 4-11d). I found that while this manipulation led to a modest increase in parenting behavior (Fig. 4-11h,i, consistent with previous reports[228]) it did not lead to a significant increase in allogrooming behavior (Fig. 4-11f,g). This finding further highlights that the MPOA Vgat$^+$ neurons that

project to the VTA represent an anatomically and functionally distinct subpopulation of neurons that regulate both allogrooming and pup grooming.

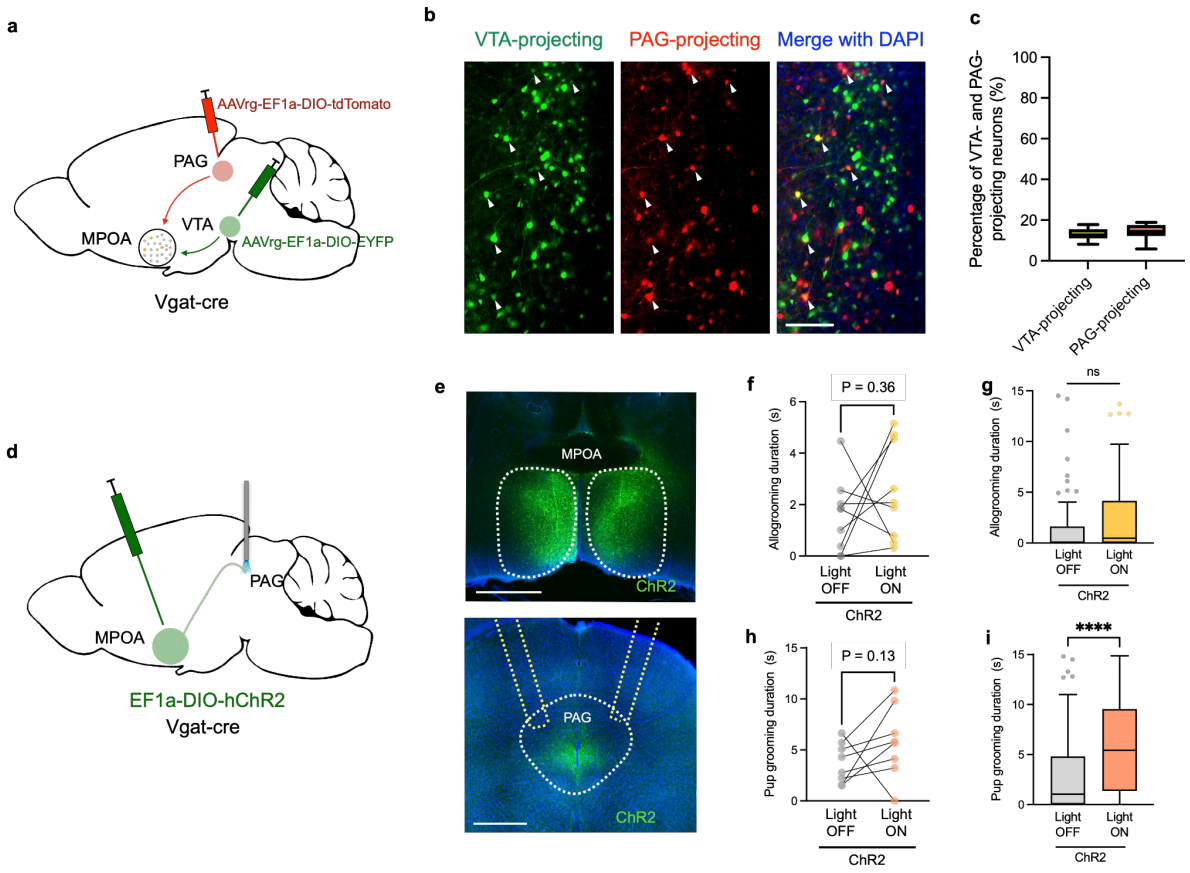

Figure 4-11. Activation of MPOA-PAG pathway promotes pup grooming, but not allogrooming. **a**, Schematic of retrograde labeling of VTA- and PAG-projecting MPOA neurons. **b**, Example micrographs showing VTA-projecting neurons (green), PAG-projecting neurons (red), and neurons projecting to both regions (arrowheads) in the MPOA. Scale bar, 150 µm. **c**, Percentages of neurons projecting to both the VTA and PAG within the VTA-projecting and PAG-projecting populations. **d**, Schematic of optogenetic activation of the $MPOA^{Vgat+}$-PAG projection. **e**, Example micrographs showing ChR2 expression in the MPOA as well as the axonal projections of $MPOA^{Vgat+}$ neurons and optic fiber placement in the PAG. Scale bar, 500 µm. **f,g**, Average allogrooming duration across all trials within individual mice (f) and duration of allogrooming in individual trials (**g**) during the 15-s real (light on) and sham (light off) photo-activation of the $MPOA^{Vgat+}$-PAG projection. **h,i**, Average pup grooming duration across all trials within individual mice (**h**) and duration of allogrooming in individual trials (**i**) during the 15-s real (light on) and sham (light off) photo-activation of the $MPOA^{Vgat+}$-PAG projection. (f,h) two-sided paired t -test, (g,i) two-sided Mann-Whitney test.
n = 10 independently injected hemispheres (c), 10 mice (5 females, 5 males) in (f,h), 67-133 trials from 10 mice (5 females, 5 males) (g), 69-114 trials from 10 mice (5 females, 5 males) (i).

Lastly, all optogenetic experiments presented thus far tested the effects of circuit manipulation during interactions with stressed conspecifics. To assess whether the elicited behavioral response depends on the affective state of the social partner, I also photo-activated the MPOA^{Vgat+}-to-VTA projection (axonal projections and somas) while interacting with an unstressed partner and found that MPOA^{Vgat+}-to-VTA stimulation produces a marginally weaker increase in grooming when the partner is non-stressed (Fig 4-11), suggesting that stress-related cues may enhance the behavioral effect of circuit activation. This supports the idea that the MPOA^{Vgat+}-to-VTA projection is more strongly engaged in contexts of conspecific need.

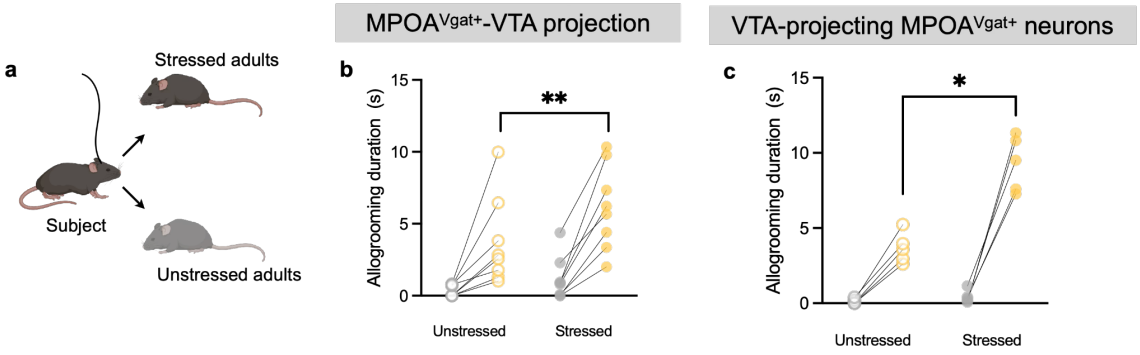

Figure 4-12. MPOA^{Vgat+}-VTA induced allogrooming is modulated by partner stress state. **a,** Schematic of stimulation experiment, with each subject being tested separately with a stressed partner and an unstressed partner. **b, c,** Average allogrooming duration across all trials within individual mice towards unstressed partners versus stressed partners, during the 15-s real (light on) and sham (light off) photo-activation of the MPOA^{Vgat+}-VTA projection (b) and photo-activation of the VTA projections of MPOA^{Vgat+} neurons (c), (b, c) Two-way repeated measures ANOVA, with uncorrected fisher's LSD posthoc (b) and Sídák's multiple comparisons test (c).
n = 8 mice (4 females, 4 males) in (b), 5 mice (3 females, 2 males) in (c).

MPOA neurons recruited during pup interactions are required for allogrooming

Given that (1) allogrooming and pup grooming are associated with partially overlapping neural representations in the MPOA and (2) both allogrooming and pup grooming are controlled by a select subpopulation of MPOA Vgat+ neurons that project to the VTA, we further sought to directly determine whether the subset of MPOA neurons recruited during pup interactions are causally involved in promoting allogrooming behavior toward stressed adults.

To gain access to a select neuronal subpopulation engaged during pup interaction without relying on a single genetic marker, we performed activity-dependent genetic labeling using the TRAP2 mouse line, which expresses a tamoxifen-inducible Cre recombinase in cells that express the immediate early gene Fos[248]. While I performed some pilot experiments not presented in this chapter, the TRAP data included here are from experiments conducted by FS. FS injected an AAV expressing a Cre-dependent hM4Di into the MPOA for chemogenetic inhibition of the labeled cells. Following free interaction with pups in their home cages, animals were injected 4-hydroxytamoxifen (4-OHT) to enable the expression of hM4Di in neurons that were activated during pup interaction ("pup-TRAP") (Fig 4-12a,b). Histological examination revealed robust labeling of MPOA neurons in animals using this strategy (Fig 4-12c).

To evaluate the functional role of the pup-TRAP+ cells, she inhibited these cells by injecting CNO (or saline as control) into the pup-TRAP animals and examined their behaviors during pup interaction (Fig 4-13b,d,e). Compared to saline-injected controls, CNO-injected animals displayed significantly reduced pup grooming behavior (Fig 4-12e,j,k). In contrast, the control-TRAP animals showed no significant changes in pup-directed behaviors following CNO injection (Fig 4-12p,q). This confirms that pup-TRAP+ cells were indeed required for pup grooming behavior. She next examined whether inhibition of pup-TRAP+ cells could also suppress allogrooming behavior. Remarkably, following CNO injection, the pup-TRAP

animals exhibited significantly reduced allogrooming toward stressed adults (Fig 4-12g,l,m), whereas the control-TRAP animals showed no change (Fig 4-12r,s). This demonstrates that TRAP+ cells induced by pup interaction are also required for allogrooming behavior. Importantly, chemogenetic inhibition of these pup-TRAP+ cells had no impact on self-grooming behavior, locomotor activity or anxiety-related behavior in the open-field test or social investigation behavior (Fig 4-12h,i,n,o,t,u), suggesting a direct role of the pup-TRAP+ cells in allogrooming behavior. Therefore, these observations, together with (1) the positive correlation between naturally occurring allogrooming and parenting behaviors, (2) the partial overlap between their neural representations, and (3) their co-regulation by the MPOA-VTA pathway, suggest that adult-directed prosocial behavior and offspring-directed parenting behavior could be mediated by shared neural mechanisms.

While these findings provide causal evidence that neurons recruited during pup interactions are necessary for both parenting and prosocial allogrooming, further experiments will help to more rigorously define the specificity of these TRAPed populations. Future to complement this loss-of-function approach with gain-of-function manipulations and employing additional control-TRAP strategies (such as experimental conditions like self-stress that activate similar numbers of neurons in the MPOA as pup-TRAP) to better isolate the functional relevance of pup-activated circuits in the MPOA.

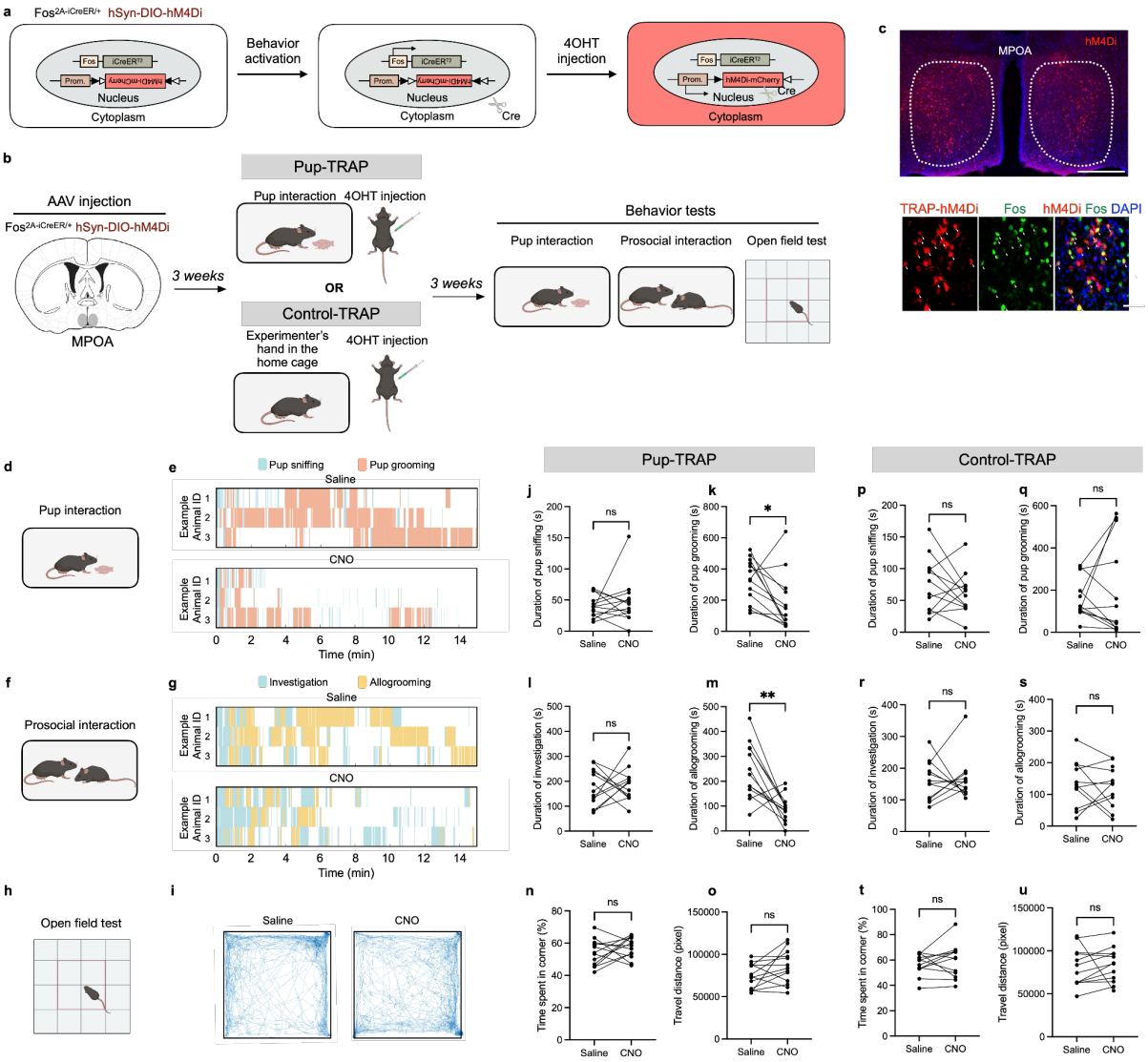

Figure 4-13. Pup-activated MPOA neurons are required for allogrooming. a, Schematic of the strategy for expressing hM4Di in pup-activated MPOA neurons using the TRAP2 mouse line. **b**, Schematic of the experimental timeline, including virus injection, labeling of pup-activated cells or control labeling, and behavioral testing. **c**, Example micrographs showing hM4Di-mCherry expression in pup-TRAP+ cells in the MPOA (top, Scale bar, 500 μm) and showing pup-TRAP+ cells expressing hM4Di-mCherry (red), cells expressing FOS (green) following subsequent pup interactions, and the overlap between the two populations in the MPOA. (bottom, Scale bar, 50 μm). **d, f, h**, Schematics of the behavioral paradigms used, including interaction with pups (**d**), prosocial interaction with stressed adults (**f**), and the open field test (**h**). The red square in the open field indicates the center zone. **e, g**, Example raster plots showing behaviors exhibited by pup-TRAP animals injected with either saline (control) or CNO during interactions with pups (**e**) or stressed adults (**g**). **j, k,** The duration of pup investigation (**j**) and pup grooming (**k**) exhibited by pup-TRAP animals injected with either saline (control) or CNO during pup interactions. **l, m**, The duration of social investigation (**l**) and allogrooming (**m**) exhibited by pup-TRAP animals injected with either saline (control) or CNO during interactions with stressed animals. **i**, Example locomotion trajectories of pup-TRAP animals in the open field test following saline (control) or CNO injection. **n, o,** Time spent in the

corners (**n**) and travel distance (**o**) of pup-TRAP animals in the open field test following saline (control) or CNO injection. **p, q**, The duration of pup investigation (**p**) and pup grooming (**q**) exhibited by control-TRAP animals injected with either saline (control) or CNO during pup interactions. **r, s**, The duration of social investigation (**r**) and allogrooming (**s**) exhibited by pup-TRAP animals injected with either saline (control) or CNO during interactions with stressed animals. **t, u**, Time spent in the corners (**t**) and travel distance (**u**) of control-TRAP animals in the open field test following saline (control) or CNO injection. (j, k, l, m, n, o), two-sided Wilcoxon signed-rank test.
n = 8 independently injected hemispheres (2-4 brain sections per hemisphere) in the pup-TRAP group and 6 independently injected hemispheres in the control-TRAP group in (c), 13 mice (7 females, 6 males) in (j, k, l, m, n, o), 12 mice (6 females, 6 males) in (p, q, r, s, t, u).

MATERIALS AND METHODS

Animals

Wild-type animals used in experiments were male and female C57BL/6J mice purchased at 8–10 weeks old from Jackson Laboratory Laboratory (strain #: 000664). The following Cre and Flp driver lines were used: Vgat-Cre/+, Vglut2-Cre/+, Esr1-Cre/+, Oxtr-Cre/+, Sst-cre/+, Cck-Cre/+, Tac1-Cre/+, Tacr1-Cre/+, and Vgat-Flp/+. All genotypes were first purchased from Jackson Laboratory (strain #: 016962, 016963, 017913, 031303, 013044, 012706, 021877, 035046, 029591) and backcrossed to C57BL/6J to generate a breeding colony. $Vgat^{flp/+}$ and $Tac1^{cre/cre}$ mice were crossed to generate $Vgat^{flp/+}$; $Tac1^{cre/+}$ mice. $Fos^{tm2.1(icre/ERT2)Luo/J}$ mice were purchased Jackson Laboratory (strain #: 030323). Pups (P2-P10) used for behavior experiments were produced from our breeding colony. Animals were housed in a 12-h light/dark cycle (21:00–9:00 light) at a temperature of 21–23°C with 30–70% humidity, with food and water ad libitum. All behavior experiments were performed during the dark cycle of the animals in a dark room illuminated by infrared or red light. All experimental procedures were carried out in compliance with the NIH Guide for Care and Use of Laboratory Animals and approved by the UCLA institutional animal care and use committee (IACUC).

Surgical Procedures

Mice at 8-14 weeks of age were anesthetized with isoflurane and mounted on a stereotactic alignment system (Kopf instruments).

For chemogenetic inhibition of $MPOA^{Vgat+}$ neurons, 300 nL AAV5-hSyn-DIO-hM4D(Gi)-mCherry (Addgene) (or AAV2-EF1α-DIO-mCherry (UNC Vector Core) as the control)) was injected bilaterally in the MPOA (AP: +0.10 mm, ML: ± 0.45mm, DV: -5.10 mm) from bregma.

For photo-inhibition or photo-activation of $MPOA^{Vgat+}$ neurons, 400 nL AAV1-hSyn1-SIO-stGtACR2-FusionRed (Addgene) (or AAV2-EF1α-DIO-mCherry as the control (UNC Vectore Core) or 350–450 nL AAV2-EF1a-DIO-hChR2(H134R)-EYFP (UNC Vector Core) (or AAV2-EF1α-DIO-mCherry as the control) (Addgene) was injected bilaterally in the MPOA (AP: +0.10 mm, ML: ± 0.45mm, DV: -5.10 mm) from bregma. Ferrule fiber-optic cannulas (200 μm core diameter; Inper) were implanted 0.50 mm above the virus injection sites.

For photo-inhibition or photo-activation of VTA-projecting $MPOA^{Vgat+}$ neurons, 300 nL AAVrg-hSyn1-SIO-stGtACR2-FusionRed (or AAVrg-EF1α-DIO-EYFP as the control) (Addgene) or 300 nL AAVrg-EF1a-DIO-hChR2(H134R)-EYFP (or AAVrg- EF1α-DIO-EYFP as the control) (Addgene) was injected bilaterally in the VTA (AP: -3.20 mm, ML: ± 0.50 mm, DV: -4.35 mm). Ferrule fiber-optic cannulas were implanted 0.50 mm above the MPOA using the coordinates (AP: +0.10 mm, ML: -0.45 mm, DV: -4.65 mm) and (AP: +0.10 mm, ML: +0.45 mm, DV: -4.60 mm, angled 6 degrees from the midline DV axis).

For photo-activation of MPOA-VTA projections, 350–400 nL AAV2-EF1a-DIO-hChR2(H134R)-EYFP (UNC Vector Core) was injected bilaterally in the MPOA (AP: +0.10 mm, ML: ± 0.45 mm, DV: -5.10 mm). Ferrule fiber-optic cannulas were implanted 0.50 mm above the VTA using the coordinates (AP: -3.20 mm, ML: -0.55 mm, DV: -4.00 mm) and (AP: -3.20 mm, ML: +1.0 mm, DV: -3.95 mm, angled 6 degrees from the midline DV axis). For

photo-activation of MPOA-VTA projections with lidocaine infusion in the MPOA, a 26-gague bilateral guide cannula was additionally implanted above the MPOA (AP: +0.10 mm, ML: ± 0.45 mm, DV: -5.10 mm).

For activity-dependent labeling of MPOA neurons, 400 nL AAV5-hSyn-DIO-hM4D(Gi)-mCherry (Addgene) was injected bilaterally in the MPOA (AP: +0.10 mm, ML: ± 0.45 mm, DV: -5.10 mm) of Fos2A-iCreER (TRAP2) mice.

For fiber photometry recording of dopamine signals in the NAc, 350 nL AAV9-hSyn-$GRAB_{DA2m}$ (Vigene Biosciences) (or AAV2-Syn-EYFP as the control) (Addgene) was injected in the NAc (AP: +1.40 mm, ML: -1.20 mm, DV: -4.30 mm). Ferrule fiber-optic cannulas were implanted 0.20 mm above the virus injection sites.

For fiber photometry recording of dopamine signals in the NAc during activation of $MPOA^{Vgat+}$ neurons, 400 nL AAV5-Syn-FLEX-rc[ChrimsonR-tdTomato] (Addgene) (or AAV2-EF1α-DIO-mCherry as the control) (UNC Vector Core) was injected in the MPOA (AP: +0.10 mm, ML: +0.45 mm, DV: -5.10 mm) of VgatCre/+ or VglutCre/+ mice and a ferrule fiber-optic cannula was implanted 0.40 mm above the virus injection site. 350 nL AAV9-hSyn-$GRAB_{DA2m}$ (Vigene Biosciences) was injected in the ipsilateral NAc (AP: +1.40 mm, ML: +1.20 mm, DV: -4.30 mm) and a ferrule fiber-optic cannula was implanted 0.20 mm above the virus injection site.

For retrograde labeling of VTA-projecting $MPOA^{Vgat+}$ neurons and PAG-projecting $MPOA^{Vgat+}$ neurons in the same animals, 200 nL AAVrg-EF1α-DIO-EYFP was injected bilaterally in the VTA (AP: -3.20 mm, ML: ± 0.50 mm, DV: -4.35 mm), and 200 nL AAVrg-FLEX-tdTomato was injected bilaterally in the PAG (AP: -3.40 mm, ML: ± 0.20 mm, DV: -2.70 mm) in VgatCre/+ mice.

Ferrule fiber-optic cannulas with a 0.37 numerical aperture (NA) were used in optogenetic experiments. Ferrule fiber-optic cannulas with a 0.50 NA were used in fiber photometry experiments.

Histology

Animals were euthanized and perfused with phosphate-buffered saline (PBS) followed by 4% paraformaldehyde (PFA). The brains were dissected out, post-fixed in 4% PFA overnight, rinsed with PBS and bathed in 20% sucrose overnight. Brains were sectioned at 60-μm thickness with a Leica CM1950 cryostat and imaged with a Leica DM6 B microscope.

Fiber photometry

Fluorescence signals were acquired using a fiber photometry system (Doric lenses) and recorded by a Micro 1401 digitizer (CED, Cambridge, UK) using the Spike2 software (v10.09a). 460-490 nm light was used for excitation and 500-550 nm emission light was collected. The LED power was adjusted at the tip of the optical fiber to ~3-10 μW. Behaviors were recorded by a Point Grey Camera (FLIR) with a 15-Hz sampling rate. Behaviors are manually annotated frame by frame using custom-written Python software (https://github.com/hongw-lab/Behavior_Annotator) and aligned to the photometry signal.

For fiber photometry experiments, animals were habituated for at least three days (30 min/day) before the behavioral test. During both habituation and imaging experiments, a ferrule patch cord was connected to the ferrule fiber implanted in the subject animals using a zirconia split sleeve (Doric Lenses). Animals were tested in the prosocial interaction assay (using forced swim or physical restraint as the stressor, as described previously[26] and pup interaction assay. Both assays contain a 3–5-min baseline period during which the animals were allowed to move freely in their home cages with no social partner present. The animals

were then allowed to interact with stressed adult partners for 10–15 min during the prosocial interaction assay and with pups (P2–P10) for ~5 min during the pup interaction assay.

For fiber photometry recording of NAc dopamine signal coupled with optogenetic activation of the MPOA, animals were habituated as described above and were allowed to move freely in their home cages in the absence of social partners. For the photo-activation of $MPOA^{Vgat}$ or $MPOA^{Vglut2}$ neurons during photometry recording, yellow (594 nm) light was delivered in 20 ms pulses at 20 Hz for 5 s, at an irradiance of ~3.7 mW mm^{-2} in the target region. 10 trials of stimulation were delivered to each animal with a 1–2-min interval.

For the calculation of the correlation between the fluorescence signals in the two different brain areas, we first corrected for systematic drifts in the raw fluorescence signals over long time scales to minimize the correlation caused by these overall shifts. To this end, we first smoothed the signal over the entire session using a 1000-s moving window and then normalized the smoothed signal by its maximum value, generating drift values between 0 and 1. Drift-corrected signal was then calculated as $F_{corrected}$ = F/normalized drift. For peri-event time histograms, time 0 was defined as the onset of a behavior or stimulation event. The average fluorescence between 3 s and 1s prior to the behavior onset was defined as F0 and the relative fluorescence change was calculated as $\Delta F/F_0 = (F-F_0) / F_0$.

Optogenetic experiments

Before the experiment, a ferrule patch cord was coupled to the ferrule fiber implanted in the subject mouse using a zirconia split sleeve (Doric Lenses). Optic fibers were connected using an FC/PC adaptor (Doric Lenses) to a 473-nm blue laser (CNI Laser). An Arduino micro-controller board and a customized MATLAB program were used to control light pulses. Animals were habituated to the handling procedures and optic fibers for 3 days before the behavioral test. Animals were tested in the prosocial interaction assay (using forced swim or

physical restraint as the stressor, as previously described[26] and pup interaction assay as described above. Behaviors were manually annotated frame-by-frame using a custom-written Python software (https://github.com/hongw-lab/Behavior_Annotator).

For photo-inhibition of MPOA cell bodies, light was delivered continuously for 5 s at an irradiance of ~4-6 mW mm^{-2} in the target region while the animals displayed spontaneous allogrooming toward the stressed adult partners or spontaneous pup grooming toward the pups. Real stimulation (light on) and sham stimulation (light off) were delivered manually in an interleaved manner.

For photo-activation of MPOA cell bodies, light was delivered in 20 ms pulses at 20 Hz for 15 s at an irradiance of ~4-6 mW mm^{-2} in the target region while the animals were in the vicinity of and oriented toward stressed partners or pups. Real stimulation (light on) and sham stimulation (light off) were delivered in a manually interleaved manner. Photo-activation of $MPOA^{Vgat+}$ neurons triggered allogrooming and/or pup grooming in a subset of tested animals. The quantifications in Fig. 4-3b and 4-4k show all tested animals. The quantifications in Fig. 4-3e,f and 4-4n,o show animals that exhibited any allogrooming or pup grooming behavior during stimulations.

For photo-activation of the MPOA-VTA pathway, light was delivered in 10 ms pulses at 40 Hz for 15 s for VTA terminal stimulation and 20 ms pulses at 20 Hz for 15 s for MPOA cell body stimulation at an irradiance of ~3-5 mW mm^{-2} in the target region while the animals were in the vicinity of and oriented toward the stressed partners or pups. Real stimulation (light on) and sham stimulation (light off) were delivered manually in an interleaved manner. Light stimulation triggered allogrooming in all tested animals.

For photo-activation of MPOA-VTA projections with lidocaine infusion in the MPOA, stylets were first removed from the guide cannulas and 10 μg lidocaine (20 mg mL^{-1} in saline, injection volume 500 nL) was infused at 0.2 uL min^{-1} into the MPOA 7 minutes before the

behavior assay. Injection needles remained in place for an additional 2 min before being removed and replaced immediately with stylets. Light was delivered in 10 ms pulses at 40 Hz for 15 s for terminal stimulation at an irradiance of ~3-5 mW mm^{-2} in the target region while the animals were in the vicinity of and oriented toward the stressed partners or pups. Real stimulation (light on) and sham stimulation (light off) were delivered manually in an interleaved manner. Saline or lidocaine sessions for each subject were performed on separate days.

For photo-activation of MPOA-PAG projections, light was delivered in 10 ms pulses at 40 Hz for 15 s for terminal stimulation at an irradiance of ~3-5 mW mm^{-2} in the target region while the animals were in the vicinity of and oriented toward the stressed partners or pups. Real stimulation (light on) and sham stimulation (light off) were delivered manually in an interleaved manner.

For photo-activation during real-time place preference (RTPP) test, animals were attached to the ferrule patch cord and placed in a two-chamber apparatus (60 cm × 60 cm × 30cm for each chamber) and allowed to move freely between the two chambers. Animals were habituated in the apparatus for 15 min before the test. Each test contains two 15-minute sessions. Light stimulation was firstly paired with the left chamber in the first session and then paired with the right chamber in the second session after a 15-min interval. Entering the light-paired chamber triggered a light stimulation delivered in 5 ms pulses at 20 Hz at an irradiance of ~5-6 mW mm^{-2} in the target region and exiting the light-paired chamber terminated the light stimulation. To prevent overheating of brain tissues, the stimulation was terminated automatically if the animals stayed in the light-paired chamber for over 20 s. The percentage of time spent in the light-paired chamber was averaged across the two sessions. An Arduino board with a custom-written MATLAB program was used to pair the real-time animal location with the initiation and termination of light stimulation.

Chemogenetic experiments

Animals were habituated to human handling and intraperitoneal injection by receiving an injection of 0.2 mL saline daily for at least 3 days before the behavioral test. During the test, animals were intraperitoneally injected with 1% DMSO in saline (as control) or CNO[229] (5 mg/kg body weight; Enzo, Catalog # BML-NS105) diluted in saline with 1% DMSO 30-40 min before the behavioral assays. Animals were then subjected to the prosocial interaction assay (using forced swim as the stressor, as described previously[26]) and the pup interaction assay sequentially as described above. The order of CNO and saline administration was counterbalanced across animals. Behaviors are manually annotated frame-by-frame using custom-written Python software (https://github.com/hongw-lab/Behavior_Annotator).

Activity-dependent labeling and manipulation experiments

For pup-TRAP, animals that were injected with pAAV-hSyn-DIO-hM4D(Gi)-mCherry 3 (Addgene) weeks prior were allowed to interact sequentially with 6 groups of pups (3 pups/group) for a total duration of 1 h (10 min/group). For control-TRAP, the animals were exposed to the experimenter's hand in the home cage in the absence of pups. The animals were intraperitoneally injected with 4-Hydroxytamoxifen (4OHT, Sigma-Aldrich, Catalog # H6278, 50 mg/kg body weight) 1 h after the interaction. To enhance labeling efficiency, the same procedures were repeated after 48 h. Behavioral tests were performed 3 weeks later. Animals were intraperitoneally injected with 1% DMSO in saline (as control) or CNO (5 mg/kg body weight) and subjected to the prosocial interaction assay, the pup interaction assay, and the open field test as described above.

To evaluate the specificity of this labeling strategy, we followed a previously established method[248,249] in which we first performed activity-dependent labeling as described above and subsequently subjected the animals to another pup exposure 6-8 weeks later. We

then performed immunohistochemistry to examine the overlap between acutely induced FOS+ cells and the initially labeled pup-TRAP+ or control-TRAP+ cells. Mice were perfused with 4% PFA 1 h after the pup interaction. Brains were sectioned at 60-μm thickness. The sections were first incubated with rabbit anti-c-Fos antibody (SYSY, Catalog #226 008) at 1:500, and then incubated with donkey anti-rabbit secondary antibody (Alexa FluorTM 488; Invitrogen, Catalog # A-21206) at 1:500 in the following day. Images were acquired using a confocal microscope (Zeiss LSM 780). The overlap between the Fos+ cells and the pup-TRAP+ or control-TRAP+ cells was quantified using ImageJ. We found that the Fos+ cells showed an overlap of 50.0% with the pup-TRAP+ cells, substantially higher than their overlap with the control-TRAP+ cells (18.6%). These results are comparable to observations in previous studies using activity-dependent labeling[248–250] and confirm that our strategy indeed preferentially labels populations of cells that are activated during pup interactions.

CHAPTER FIVE

Extending comforting towards other distressed states

INTRODUCTION

Social responses to aversive states

Animals experience a variety of aversive states, including pain, sickness, nausea, and distress, each of which alters behavior and physiology in ways that can shape social interactions[251–253]. Sickness, typically induced by immune activation (e.g. liposaccharide-injection), and nausea, often triggered by toxins or gastrointestinal distress, both engage inflammatory pathways and can lead to self-isolation and decreased activity[253,254]. Similarly, stress, particularly chronic or acute social stress, activates the hypothalamic-pituitary-adrenal (HPA) axis and can reduce motivation for social engagement, promoting social withdrawal and altered threat assessment. While these negative states share overlapping features, such as disengagement from social partners and changes in olfactory cues, the extent to which observers distinguish between them, and whether their social responses are shaped by the underlying cause of conspecific distress, remains poorly understood.

While recent studies have examined how animals respond to distressed conspecifics experiencing stress, pain or even sedation[138,255,256], relatively little is known about how animals behave toward peers experiencing physiological illness. Given that sickness behaviors often involve self-isolation and lethargy[257], it is unclear whether conspecifics interpret these as similar signals warranting comfort or as cues to avoid potential contagion. The goal of these next experiments is to understand whether and how animals provide social support to sick or nauseous conspecifics, offering insights into the conditions under which prosocial comforting persists despite potential risks associated with pathogen exposure or physiological discomfort.

Approach or avoid?

When confronted with sick individuals, animals must navigate competing pressures: maintaining social bonds versus minimizing risks associated with infection or instability. Many species across the animal kingdom exhibit outright avoidance of sick conspecifics, as seen in bullfrog tadpoles[258] and juvenile Caribbean spiny lobsters[259]. However, other species, particularly those with highly social structures, show more variable responses. Banded mongooses[260] and rhesus monkeys[261] do not reliably avoid sick group members but instead continue social interactions with sick group members, potentially because the benefits of maintaining social ties outweigh the risks of contagion, particularly in species where indirect transmission is common[262]. Vampire bats, another highly social species, demonstrate a different pattern: immune-challenged bats receive less grooming, indicating that social disengagement may arise from the sick individuals themselves rather than active avoidance by group members[263].

Avoidance of sick conspecifics has been well documented in rodents, particularly in experimental paradigms that limit social interaction. In two-choice assays, mice and rats actively avoid sick conspecifics and their odors[264], and when presented with anesthetized individuals, they preferentially sniff healthy animals over those displaying sickness cues[265]. Similar avoidance patterns have been observed in response to parasitic infections, with rodents reducing interaction with infected conspecifics[266]. However, not all studies indicate strict avoidance. In cross-sex interactions, sickness suppresses mating behaviors but does not eliminate investigation or other social behaviors[267], suggesting that avoidance is context-dependent. Some studies also report increased investigation of sick individuals, potentially as a form of risk assessment[266].

Despite these findings, much of the research on sickness-related social behaviors has relied on constrained behavioral assays or cross-sex interactions, leaving key questions

unanswered. Do rodents engage in prosocial behaviors toward sick group members when allowed naturalistic social interactions? If rodents exhibit comforting behaviors toward sick or nauseous partners, it suggests that social support extends beyond acute distress and may be guided by a more general sensitivity to conspecific well-being. Addressing these gaps will clarify how rodents balance infection avoidance and prosocial comforting in different contexts.

RESULTS

Sickness and malaise states elicit prosocial behavioral responses in mice

Before testing if mice display prosocial behavioral responses toward sick and nauseous social partners, I first validated the sickness states induced by immune challenge and nausea-inducing drug delivery in stimulus animals. To determine the time course of LPS-induced sickness behavior, I injected animals with liposaccharide (LPS, from E. coli *O55:B5*) and assessed their behavior at multiple timepoints using a standardized scoring system that included scores for appearance, mobility, and respiration (Table 1, Fig 5-1a). In addition to behavioral scoring, I used an infrared camera to measure changes in surface temperature as a proxy for fever response[268,269], which has been documented following LPS administration in mice[257,270]. Mice consistently showed mild weight loss from acute inflammation and lack of food intake (Fig. 5-1d). Sickness scores peaked approximately 2 hours post-injection (Fig. 5-1e-g), consistent with prior reports[257,271].

Next, to determine the time course of a LiCl-induced visceral malaise state, I injected animals with 200 mg/kg LiCl and assessed their behavior post-injection (Fig. 5-1h). Prior work in rats and mice has identified a range of LiCl-induced unconditioned nausea-related behaviors, including pica (consuming non-nutritive substances e.g. kaolin), lying-on-belly posture (LOB), hypolocomotion, and hypophagia[272–275]. Given that C57BL/6J mice do not reliably exhibit pica[276], I focused on food intake and locomotor changes as primary readouts.

LiCl-injected mice exhibited reduced food consumption and fewer food approaches (Fig. 5-1i,j) as well as reduced locomotion in the home cage (Fig 5-1k) relative to saline controls. These effects typically resolved within 2 hours.

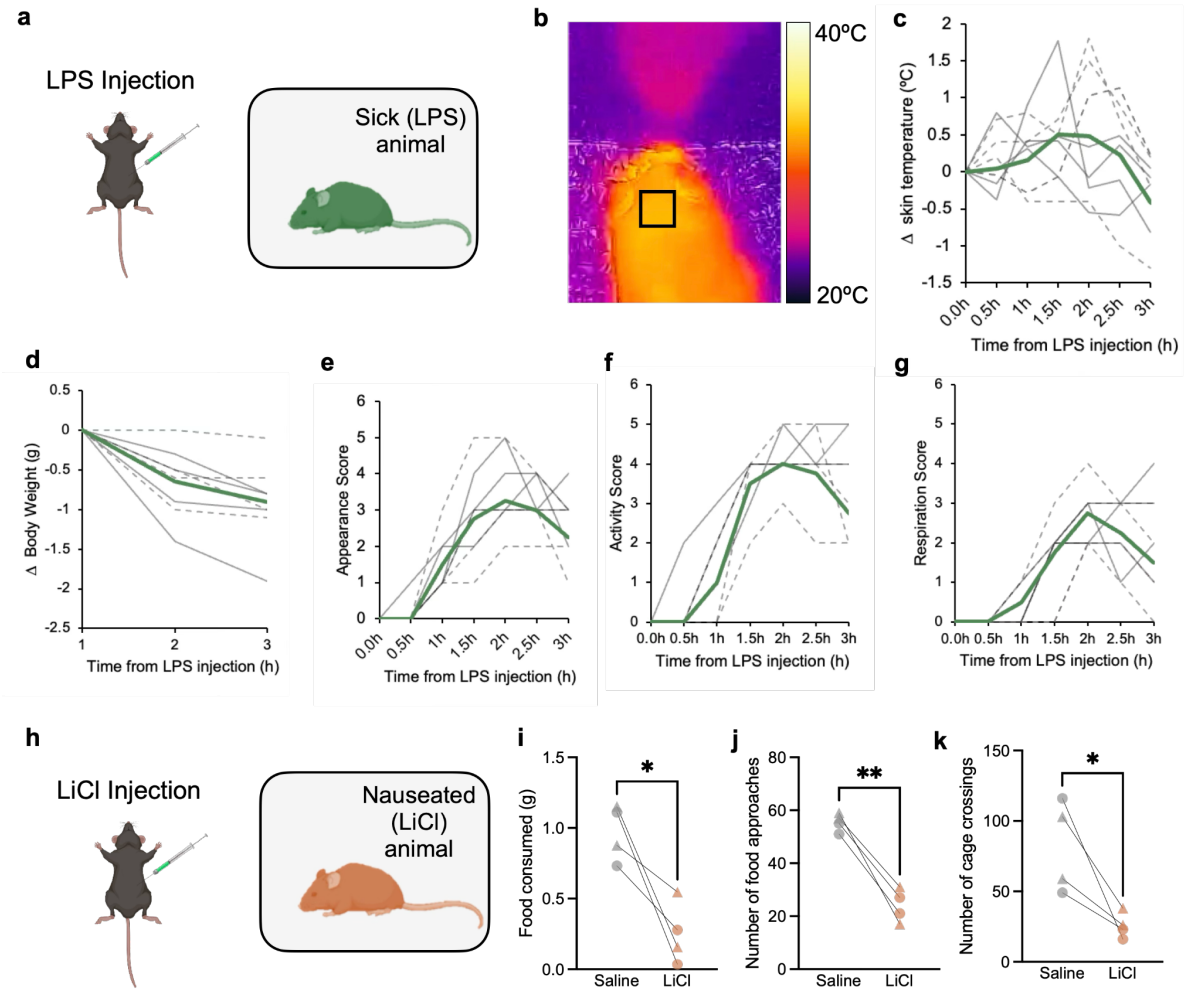

Figure 5-1. Validation of LPS-induced sickness and LiCl-induced malaise in mice. a, Schematic of LPS injection and post-injection monitoring. **b**, Example pseudocolored image from FLIR Thermography infrared camera showing top-down view of surface skin temperature. **c-g**, Following LPS injection, change in max skin temperature from baseline at 0h (**c**), change in body weight (**d**), change in appearance score (**e**), change in activity score (**f**), change in respiration score (**g**). Grey dashed lines represent individual females and solid grey lines represent individual males, and the green line indicates the mean. **h**, Schematic of LiCl injection and post-injection monitoring. **i-k**, Food consumption (**i**), number of food approaches (**j**), and number of cage crossings (**k**) in LiCl-injected animals compared to saline-injected controls. (i,j,k), two-sided paired t-test.
n = 8 mice (4 females, 4 males) in (c-g), 4 mice (2 females, 2 males) in (i-k).

As described above in the introduction, there is not a clear understanding of how mice respond to sick or nauseated (forms of aversive states) same-sex conspecifics in a freely moving context. To test whether mice display prosocial comforting responses towards these states, I characterized behavioral interactions with sick or nauseous mice (Fig. 5-2a). In these experiments, behavioral annotations of allogrooming were further separated by specific body regions that subjects targeted allogrooming towards (e.g. head, body, underbelly) to explore whether the target of grooming might reflect sensitivity to specific somatic cues (Fig. 5-2b,c). This was motivated by the observation that LiCl induces abdominal discomfort and has been associated with abdominal spasms[277], raising the possibility that subject animals could differentially tailor their comforting responses based on the partner's physical state.

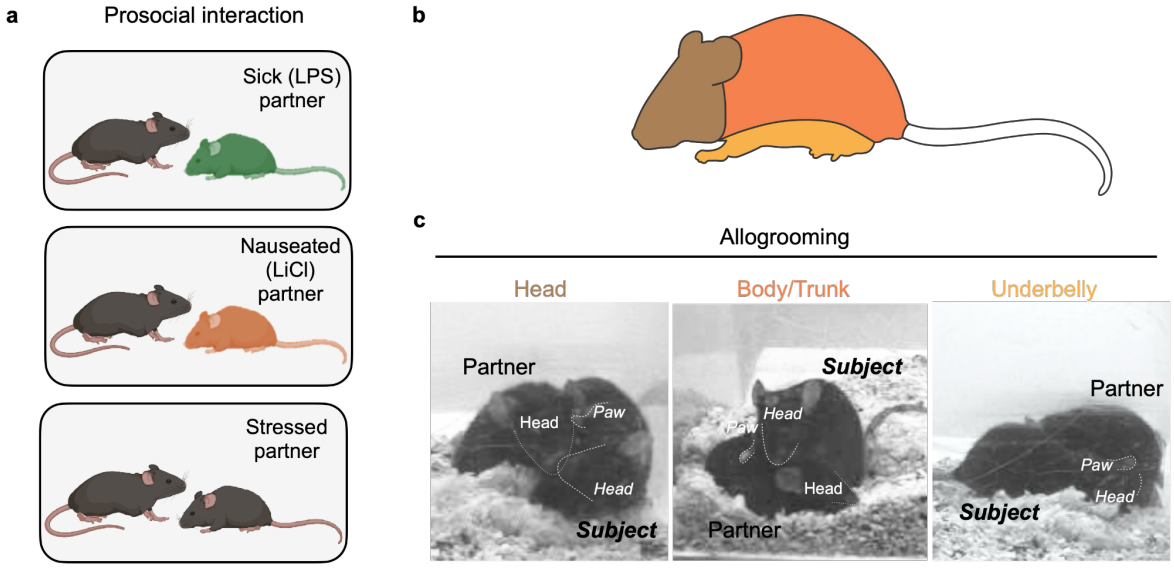

Figure 5-2. Behavioral paradigms and body targets of allogrooming. a, Schematics of the behavioral paradigms used, including prosocial interaction with sick adults (top), nauseated adults (middle), and stressed adults (bottom). **b**, Schematic of different body parts of the partner that received allogrooming. **c**, Representative photographs of different allogrooming interactions (Head, Body/trunk, Underbelly), where the subject (including its body parts) is labelled in italics.

During interactions with LPS-treated conspecifics, subject mice exhibited a significant increase in allogrooming directed toward the sick partner, compared to interactions with saline-injected controls (Fig. 5-3a). A similar pattern was observed when subject mice interacted with LiCl-injected partners (Fig. 5-3b). While mice showed greater head allogrooming toward LPS- compared to LiCl-treated partners (Fig. 5-3c,d), they displayed more underbelly allogrooming toward LiCl-treated partners (Fig. 5-3e), potentially reflecting sensitivity to the somatic localization of abdominal malaise. These results suggest that mice may be able to distinguish among different forms of distress in their social partners and may adapt their affiliative behaviors accordingly. These findings support the idea that prosocial allogrooming behavior is part of a generalized comforting repertoire, yet may also be modulated by the specific nature or perceived source of the partner's distress.

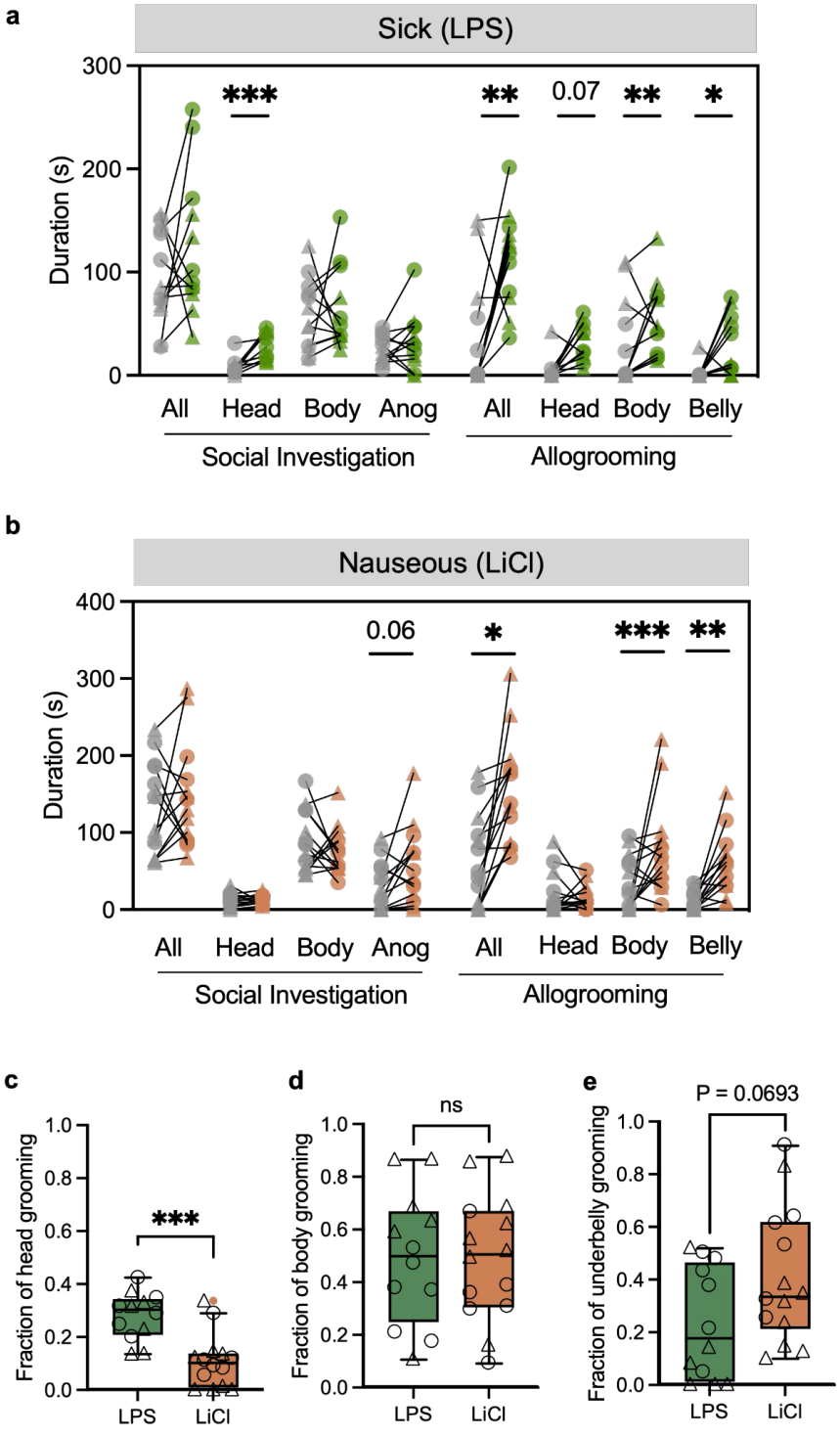

Figure 5-3. Mice display prosocial allogrooming towards sick (LPS) and nauseous (LiCl) partners. a,b The total duration of various behaviors displayed by individual subject animals during interactions with saline or LPS partners (**a**) and saline or LiCl partners (**b**). **c-e**, Differential allogrooming responses toward sick versus nauseous versus stressed partners in

head grooming (**c**), body grooming (**d**), and underbelly grooming (**e**). (a,b) Two sided paired t-tests, (c,d,e) Two sided unpaired t-tests.
n = 12 mice (6 females, 6 males) in (a), 14 mice (6 females, 8 males) in (b). Mice from a and b are presented in (c,d,e).

Huddling behavior increases in response to conspecific distress

Huddling – prolonged physical proximity and body contact – may also offer comfort and strengthen social bonding[4,84,104,105] and was only recently implicated in a prosocial consolation context[74]. In addition to allogrooming, I examined whether mice increase affiliative body contact in response to distressed conspecifics by quantifying various forms of physical proximity during interactions with sick, nauseous, or stressed partners (Fig. 5-2a). Huddling was defined and categorized into several contact states, including active side-by-side huddling (one or both animals may be engaging in allogrooming, sniffing, or self-grooming) and quiescent side-by-side huddling (Fig. 5-4a, Methods).

Across all three conditions, mice spent significantly more time huddling with sick, nauseous, or stressed partners compared to their controls (Fig. 5-4b-d). Interestingly, the average amount of total huddling was similar across all three conditions (39-41% of total interaction time), and the majority of huddling occurred during active states (e.g. concurrent allogrooming or other behaviors) (Fig. 5-4e-g). Mice also displayed a higher average proportion of quiescent side-by-side huddling specifically when interacting with sick or nauseated partners compared to stressed partners (Fig. 5-4e-g). While proximity is a prerequisite for behaviors like allogrooming, the observed differences in quality and distribution of sustained body contact state suggest that mice may adjust their patterns of sustained body contact based on the perceived internal state of their social partner. Moreover, the duration of huddling was substantially longer than allogrooming across all three conditions (Fig. 5-4h-j), suggesting that huddling may also offer additional comforting or affiliative functions beyond those provided by allogrooming.

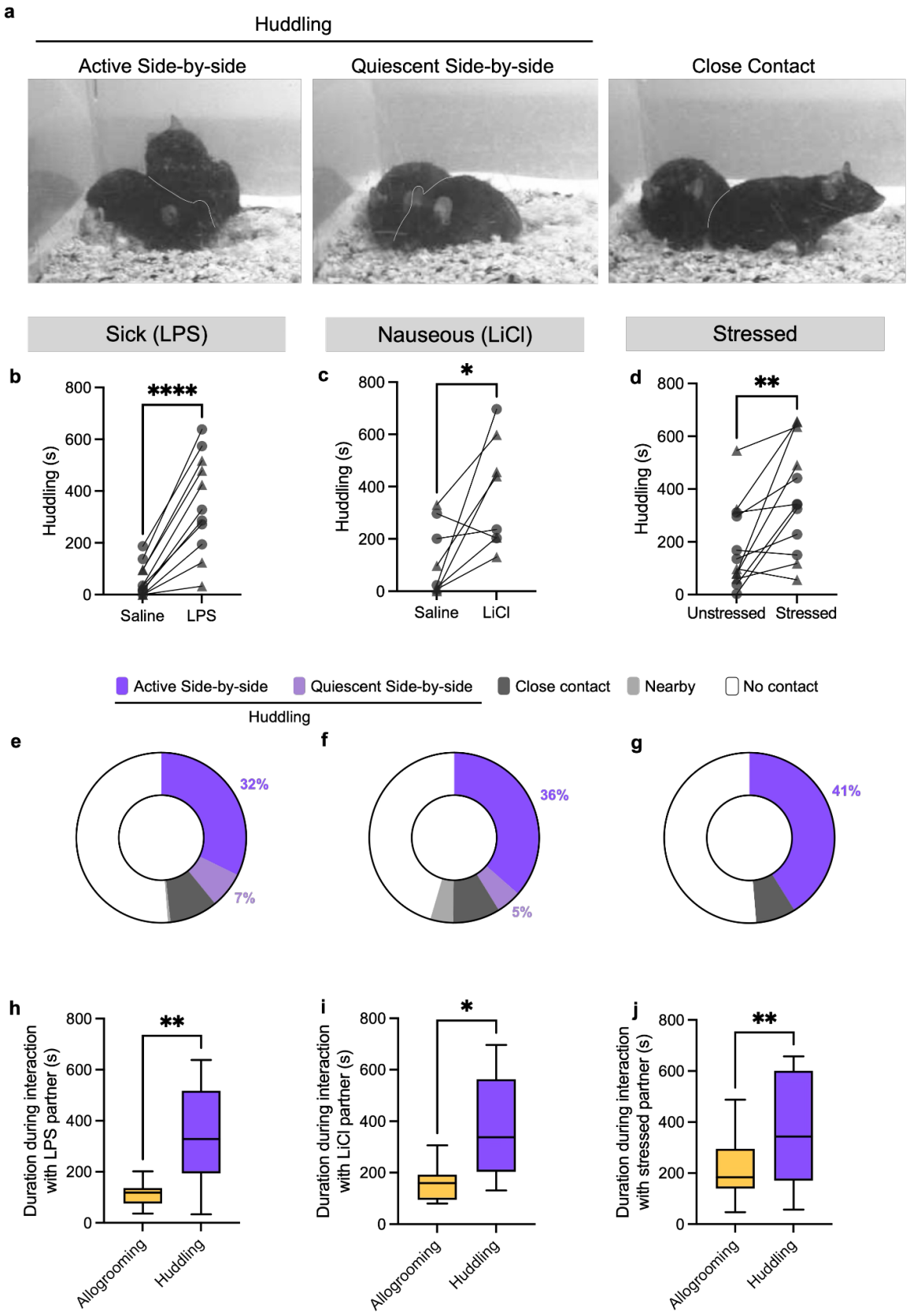
a
Huddling
Active Side-by-side
Quiescent Side-by-side
Close Contact
Sick (LPS)
Nauseous (LiCl)
Stressed
b
c
d
Huddling (s)
****
*
**
Saline
LPS
LiCl
Unstressed
Stressed
Active Side-by-side
Quiescent Side-by-side
Close contact
Nearby
No contact
Huddling
e
f
g
32%
7%
36%
5%
41%
h
i
j
Duration during interaction with LPS partner (s)
Duration during interaction with LiCl partner (s)
Duration during interaction with stressed partner (s)
Allogrooming
Huddling

Figure 5-4. Mice show increased huddling during interaction with sick, nauseous, and stressed conspecifics. **a**, Representative photographs of different huddling states, line indicating the boundary of body contact. **b-d**, Comparison of the percentage of time that pairs of mice spent huddling during interactions with saline controls and sick partners (**b**), nauseous partners (**c**), and stressed partners (**d**). Circles represent females, triangles represent males. **e-g**, Pie charts showing the average percentage of time mice spent in each huddle, close contact, or no contact state during interactions with sick partners (**d**), nauseous partners (**e**), and stressed partners (**f**). **h-j**, Duration of allogrooming compared to huddling during interaction with sick (**h**), nauseous (**i**), or stressed (**j**) partner. (b-d, h-j), two-sided paired t-test.
n = 11 mice (6 females, 5 males) in (b,e), 8 mice (3 females, 5 males) in (c,f), 12 mice (6 females, 6 males) in (d,g).

MATERIALS AND METHODS

Animals

Wild-type animals used in experiments were male and female C57BL/6J mice purchased at 8–10 weeks old from Jackson Laboratory (strain #: 000664). Pups (P2-P10) used for behavior experiments were produced from our breeding colony. Animals were housed in a 12-h light/dark cycle (21:00–9:00 light) at a temperature of 21–23°C with 30–70% humidity, with food and water *ad libitum*. All behavior experiments were performed during the dark cycle of the animals in a dark room illuminated by infrared or red light. All experimental procedures were carried out in compliance with the NIH Guide for Care and Use of Laboratory Animals and approved by the UCLA institutional animal care and use committee (IACUC).

Behavior assays

LPS and LiCl Validation

Mice were injected intraperitoneally (IP) with 0.5mg/kg Lipopolysaccharide (LPS, from E. coli O55:B5) dissolved in saline (10uL/g body weight), and were introduced to a clean cage and left alone for observation for 3 hours. Mice were weighed at the 1, 2, and 3 hour mark

after LPS injection. Thermography images were captured every 15 minutes, and scores for appearance, mobility, and respiration (Table 1) were assessed every 30 minutes.

12h food-deprived mice received an IP injection of 200 mg/kg LiCl solution (10uL/g body weight), remained alone in a temporary cage for 5 minutes, then introduced to a clean cage with a 3.6g food pellet. Each mouse was tested alone, and observed for postural changes, piloerection, general locomotor activity, and food intake.

Prosocial interaction assay

Prosocial interaction assays in this chapter were performed as previously described in Chapter 3. For the baseline control session, the partner was removed from the home cage and placed into a separate cage with home cage bedding for 15-105 min before being reunited with the subject for 15 minutes of recorded interaction. The separation-only control sessions were performed at least 4 hours before the experimental condition sessions.

In the **forced swim stress** condition, the partner was placed in 20-22ºC water for 5 minutes before reuniting with the subject. In the **LPS-induced sickness** condition, the partner was injected IP with 0.5mg/kg Lipopolysaccharide (LPS, from *E. coli* O55:B5) dissolved in saline (10uL/g body weight) and left undisturbed in a separate cage for 105 minutes prior to reunion. Validation experiments indicated that observable sickness behavior and disease scores peaked at approximately 2 hours post-injection and largely resolved within 24 hours. The chosen delay ensured robust expression of sickness behavior during social interaction testing. In the **LiCl-induced malaise** condition, the partner received an intraperitoneal (IP) injection of 200 mg/kg LiCl solution (10uL/g body weight), remained alone in a temporary cage for 10 minutes, and was then reunited with the subject. Pilot experiments confirmed that this dose elicited a stereotyped posture (lying-on-belly), piloerection, and hypolocomotion that

typically resolved within 2 hours. The protocol was established based on initial validation data confirming behavioral effects and recovery time.

All experiments were conducted during the animals' dark cycle illuminated with infrared or red light. Animals were continually monitored for signs of distress or adverse effects, including posture changes, locomotion, and general appearance. Body temperature and food/water intake were also tracked following all procedures to ensure full recovery. Behaviors were manually annotated frame-by-frame using a custom-written Python software (https://github.com/hongw-lab/Behavior_Annotator). Behavior definitions in this chapter diverge from earlier chapters, where investigation and allogrooming is now divided into subcategories by body part. Investigation was defined as the subject mouse orienting its snout toward the partner and positioning itself within half a head length of the partner. Head, body, and underbelly allogrooming was defined as visible licking and/or mouth contact accompanied by head bobbing movements localized on the head (face, mouth, and ear), body (trunk, shoulders, limbs), and under the belly of the partner mouse (Fig 5-2b,c). Self-grooming was defined as visible licking of paws and grooming face and/or body by the subject mouse. Baseline investigation and self-grooming are defined as the social investigation and self-grooming displayed during interactions with unstressed adults.

In addition to these core behaviors, we annotated a broader range of affiliative and proximity-based behavioral states to capture variations in close contact. These proximity-based behavioral states may be comprised of the previously described behaviors above. Active side-by-side huddling was defined as animals sitting side-by-side with ≥50% body contact while one or both engage in grooming, sniffing, or selfgrooming. Quiescent side-by-side huddling was defined as side-by-side contact without any active behavior. Subject under was defined as when the subject crawls under the partner and remains there. Partner under was defined as when partner crawls under the subject. Close contact was defined as 30–50%

body contact, typically during locomotion or brief interactions. Nearby was defined as close proximity without direct physical contact.

Table 1. Murine Sickness Score Assessment

Adapted from [278], used for assessing LPS in [279]

Assessment		**Score**
Appearance	Smooth coat	0
	Ruffled flur (patches of piloerected hair)	1
	Spiky flur (majority of hair is pilorected)	2
	Presence piloerection of may be there or absent, mouse looks puffy	3
	Presence piloerection of may be there or absent, mouse appears very thin	4
Activity	Normal activity (any is present: eating, drinking, climbing, running, fighting)	0
	Activity slightly suppressed. Moving of the mouse on the bottom of the cage	1
	Activity is suppressed. Stationary mouse with occasional movements	2
	No activity, stationary mouse, no movements	3
	No activity, mouse with tremors particularly of the back hinds	4
Level of consciousness	Active mouse	0
	Active mouse without standing upright	1
	Active mouse that appears slowed.	2
	Impaired activity. Moves only after provocation	3
	Severely impaired activity. Stationary mouse even after provocation	4
Eyes	Open	0
	Not full open, possibly with secretion	1
	Half-closed eyes, secretion possible	2
	At least half-closed eyes, secretion possible	3
	Closed or milky eyes	4
Respiration rate	Normal respiration (rapid mouse respiration, not visible by eye)	0
	Respiration slightly decreased (Respiration rate visible but not quantifiable by eye)	1
	Respiration moderately reduced (can be just quantified by eye)	2
	Respiration severely reduced (easily countable, 0.5 s between breaths)	3
	Respiration extremely reduced (> 1s between breaths)	4
Respiration quality	Normal	0
	Mouse with short periods of difficult breaths	1
	Difficult breaths, no gasping	2
	Mouse with intermittent gasps	3
	Mouse gasping	4

CHAPTER SIX

Conclusions and Future Directions

In this dissertation, I examined the behavioral and neural mechanisms of comforting behavior in mice, focusing on its relationship to parental care and its specificity to different forms of conspecific distress. I first demonstrated that parenting and allogrooming are positively correlated across individual animals. The MPOA, a brain region well established in the regulation of parenting, was found to contain neurons that encode the perception of distressed adults, and MPOA Vgat+ neurons bidirectionally regulate prosocial allogrooming. Moreover, prosocial comforting is associated with dopamine release in the nucleus accumbens and is specifically causally regulated by a subpopulation of MPOA Vgat+ neurons projecting to the VTA, which also promote pup grooming. Furthermore, MPOA neurons activated during pup interactions are required for prosocial allogrooming toward stressed adult conspecifics. Together, these findings identify new circuit elements underlying allogrooming behavior and provide neurobiological insights into its potential evolutionary relationship with parenting behavior. In a separate set of experiments, I found that mice also display prosocial comforting toward conspecifics experiencing sickness or malaise, extending the behavioral profile of comforting beyond stress. This work contrasts with prior paradigms that primarily reported avoidance behavior using non-naturalistic setups such as anesthetized or enclosed conspecifics, and instead employs freely moving, unrestrained dyads. Together, these results offer converging evidence that comforting behavior in mice is shaped by ethologically relevant social cues, engages neural systems traditionally associated with caregiving, and is sustained in part by self-rewarding mechanisms. They support the view that evolutionarily conserved circuits for parental care may scaffold broader forms of prosocial support.

Functional convergence between parenting and comforting

In many social species, offering comfort through physical contact is a powerful form of social support. This type of prosocial behavior resembles parenting behavior in that both

require the ability to recognize the needs or negative states of others and the motivation to address them. These parallels have led to the hypothesis that the biological systems supporting parenting behavior may serve as a foundation for adult-directed prosocial behavior[1,205]. However, these behaviors are manifested in distinct social contexts and involve markedly different adult- and pup-specific sensory cues. This raises important questions regarding how the neural substrates of these two behaviors may be related, both at the level of neural circuits and individual neurons.

Our findings indicate that the MPOA regulates both parenting and comforting behaviors, and that these behaviors are supported by partially overlapping neuronal populations. While adult and pup stimuli elicit distinct neural representations in the MPOA (likely reflecting the unique sensory cues associated with these two types of social targets), the representation of pups more closely resembles that of stressed adults than of unstressed adults. This is consistent with the idea that both behaviors recruit caregiving-related circuits that respond to social vulnerability. The observed behavioral and neural overlap between allogrooming and parenting supports the idea that caregiving-related circuits may be recruited to support adult-directed prosocial behavior.

Causal manipulations further supported this convergence: the same MPOA^{Vgat+}-VTA projection that supports parenting also drives comforting behavior. The connection between the two behaviors is further supported by our activity-dependent labeling experiments that confirmed that neurons activated during pup interactions are required for adult-directed comforting behavior, highlighting how caregiving circuits may be flexibly engaged beyond the specific context of parenting. The MPOA is a heterogeneous structure consisting of diverse cell types, each characterized by distinct combinations of genetic markers[225]. While several neuronal subpopulations defined by single genes have been reported to regulate specific types of behaviors, including parenting behavior (e.g., Gal, Nts, Esr1, Calcr)[208,209,221,225,234],

these markers label multiple molecular cell types that may encompass different functional populations. Precise dissection of specific molecular cell types in regulating parenting and prosocial behaviors will require sophisticated intersectional genetic tools and remains an open question for future investigation. Nevertheless, our activity-dependent labeling approach allowed us to target a functionally defined subset of neurons engaged during pup interactions without relying on a single genetic marker. Our findings provided functional evidence that MPOA neurons involved in pup interactions are also required for allogrooming behavior. Importantly, our projection-defined subpopulation of MPOA Vgat+ cells (VTA-projecting MPOA neurons constitute a small population of MPOA cells, ~10%[247]), emerged as a key circuit node for both comforting and parenting behavior, underscoring their specific role in mediating affiliative responses.

Other-benefitting prosocial behavior is also self-rewarding

A fundamental principle underlying human and non-human animal behavior is the motivation to seek rewarding experiences. Although prosocial and parenting behaviors occur in different social contexts and serve distinct ethological functions, they both require positive reinforcement to be sustained. Here we show that allogrooming behavior toward a stressed conspecific is associated with a significant increase in dopamine release in the nucleus accumbens. This suggests that while prosocial allogrooming behavior serves to benefit the well-being of other individuals, it is also associated with the actor's own reward. This echoes previous findings of the "warm glow" effect of prosocial behavior in humans, where heightened positive emotions are commonly reported after engaging in acts of kindness and are thought to contribute to the reinforcement of such behavior[240,243]. Indeed, we found that the MPOA^{Vgat+}-to-VTA pathway, which enhances midbrain dopaminergic activity, bidirectionally controls allogrooming behavior. These findings suggest that the actor's own reward may be an

important factor in driving prosocial allogrooming and identify a neural circuit mediating this process. Interestingly, in humans, it has been shown that a brain-wide increase in dopamine levels can enhance certain aspects of prosocial tendencies[244]. This MPOA-social reward mechanism appears to play a similar role in regulating parenting; parenting behavior is also linked to accumbal dopamine release, consistent with its rewarding nature, and is also bidirectionally influenced by the MPOA-VTA connection[208,246]. These findings suggest that the MPOA-to-VTA pathway may serve as a convergent neural mechanism mediating the motivational drive and reward that support both prosocial and parenting behaviors.

Context-dependent stimulation

Although MPOA activation can drive allogrooming, the magnitude and likelihood of this behavior are shaped by social context. Stimulation-induced allogrooming was heightened in the presence of a distressed partner compared to with an unstressed partner, indicating that contextual factors modulate the expression of experimentally-induced comforting. One possibility is that distressed animals are more receptive to receiving allogrooming, thereby facilitating the interaction. Alternatively, social context may modulate the activation of downstream or parallel circuits that may dynamically gate the behavioral output of MPOA stimulation. Understanding how these contextual factors dynamically shape affiliative behaviors remains an important avenue for future work.

Prosocial comforting behavior extends toward diverse negative states

While prosocial comforting is often considered a generalized response to distress, findings from Chapter 5 reveal that mice display comforting behavior across a broader range of negative states than previously demonstrated. Specifically, mice exhibited allogrooming and increased huddling toward partners experiencing sickness and nausea-like conditions.

This stands in contrast to prior studies that largely report avoidance of sick conspecifics, particularly in paradigms involving anesthetized or restrained animals presented in confined spaces (e.g., pencil cups). Additionally, much of the freely moving literature has focused on mating or reproductive contexts, where behavioral priorities differ substantially.

In same-sex, non-reproductive dyads, we found that mice do not avoid sick partners and instead display prosocial allogrooming. When confronted with sick individuals, animals must navigate competing pressures: maintaining social bonds versus minimizing risks associated with infection or instability. Our findings suggest that, at least under naturalistic, same-sex, non-reproductive conditions, mice do not default to avoidance and are mice are capable of prosocial behaviors toward physically ill partners. This challenges the prevailing assumption that illness uniformly drives avoidance in service of avoiding contagion. Social disengagement and raises new questions about the cues and computations that govern such decisions. Our findings highlight that in non-reproductive, same-sex interactions, mice are capable of affiliative responses to physically ill conspecifics. Moreover, enhanced huddling alongside allogrooming may reflect a form of tactile social buffering across these aversive states, though future work is needed to determine whether these behaviors reduce distress or benefit the recipient in measurable ways.

Methodological Considerations

Although all animals used in our experiments were genetically identical, individuals exhibited variations in the level of allogrooming behavior, as observed in other prosocial behaviors[242]. These may stem from individual differences in developmental and social experiences, environmental or situational factors, internal physiological states, or neuromodulatory tone; the exact mechanisms remain largely unknown. Similarly, it is still largely unclear how individual differences in parenting behavior are regulated. Interestingly,

we found that animals exhibiting a higher level of allogrooming behavior also had a higher proportion of allogrooming-activated cells and allogrooming/pup-grooming shared cells in the MPOA, suggesting that individual behavioral tendencies may be reflected in the extent of circuit engagement. In addition, MPOA neurons express receptors for several neuromodulators that influence parenting behavior, including oxytocin, prolactin, estrogen, and progesterone[280]. Of note, oxytocin signaling has also been shown to regulate prosocial behavior[31,111]. It is therefore plausible that hormonal signaling contributes to individual variability and the co-regulation of parenting and comforting behaviors. Future studies that combine endocrine profiling with cell-type–specific activity mapping may help clarify these mechanisms.

Additionally, while I used causal manipulations to probe the function of MPOA neurons and their projections, finer resolution at the molecular or cell-type–specific level would be needed to determine how genetically distinct populations contribute to comforting versus parenting. Future studies combining intersectional genetic tools, single-cell transcriptomics, or whole-brain circuit mapping could help delineate these pathways more precisely.

Broader Implications for Social Neuroscience

This work contributes to a growing body of research at the intersection of social behavior and affective neuroscience, advancing our understanding of how animals detect and respond to the needs of others. The findings presented here provide evidence for the hypothesis that both prosocial and parenting behaviors rely on the ability to perceive and respond with caring behavior to others' salient distress or negative states, and that the neural architecture underlying parenting behavior may also contribute to the biological drive to detect and address the needs of adult conspecifics. While our study does not directly address evolutionary mechanisms, the identification of shared neural pathways for parenting and

adult-directed allogrooming aligns with the hypothesis that caregiving systems may have provided a scaffold for the emergence of a broader suite of social support behaviors.

Future directions

Next, I discuss several open questions and promising avenues and experimental approaches:

Circuit specificity: Do parenting and comforting rely on distinct MPOA-VTA subpopulations, are they supported by shared ensembles that are differentially modulated by social context? Leveraging tools such as intersectional genetic strategies or molecular profiling of activated (TRAPed or imaged) cell populations could address this question.

Cellular identity and signaling: What are the molecular markers and signaling properties of neurons engaged during comforting? What neuropeptides or transmitters do they use?

Sensory integration: How are affective cues (e.g. stress vs sickness vs nausea) detected and represented upstream of the MPOA? How do different sensory modalities gate the expression of comforting behavior? Dissecting how different sensory modalities – including olfactory, tactile, or auditory inputs – are integrated and mapped onto behavioral outputs may provide insight into conspecific state-specific prosocial comforting strategies.

Parental experience: Although comforting and parenting behaviors are correlated across both virgin and parental mice, suggesting that parental status does not critically alter their co-regulation, it remains unknown whether parental experience alters circuit sensitivity or thresholds for comforting behavior. Previous studies have shown that both virgin and parental mice can display a substantial amount of parenting behavior, especially in the form

of pup grooming[214,281,282]. Despite extensive research on parenting behavior, the neural mechanisms of how this behavior is modulated by parental status remain largely unclear. While we have investigated the potential link between prosocial and parenting behaviors, additional research is needed to understand how this relationship may be shaped by parental status. Does parental status modulate sensitivity to adult distress or alter the MPOA's encoding of conspecific distress? Longitudinal imaging or manipulation studies across reproductive states could offer insight into how experience reshapes social circuits.

Individual variability: Substantial variation in comforting behavior was observed across genetically identical animals. These individual differences may reflect variation in developmental history, prior social experience, or internal physiological state. The precise factors contributing to this variability remain unclear but represent an important direction for future research. How do early-life environments or social exposure shape the propensity to comfort others? Do neuroendocrine profiles such as oxytocin or stress hormone signaling predict individual differences in prosocial behavior? Future work might also examine how internal state, social history, or neuromodulatory signaling shape the expression and neural representation of comforting behavior. Similarly, individual variability in parenting behavior remains incompletely understood and could offer a useful point of comparison.

Testing the evolutionary hypothesis directly: While this dissertation provides evidence consistent with the idea that prosocial comforting may have co-opted neural circuits originally shaped for parental caregiving, directly testing this evolutionary hypothesis remains an exciting frontier. Do species that exhibit limited or no parenting behaviors also lack adult-directed comforting behavior? Comparative studies across species with varying levels of parental care (e.g. biparental, maternal care, minimal parental care) could reveal whether the capacity to comfort depends on evolutionarily conserved caregiving circuits. Are species with more extensive parental care more likely to display adult-directed prosocial behaviors, and do

these species show similar recruitment of homologous brain regions in caregiving and comforting contexts?

Importantly, the expression of prosocial behaviors, including comforting, may not only depend on ancestral caregiving mechanisms but also on the ecological and social organization of the species. As others have noted, the reach of empathy and the extent of affiliative behavior varies with species-typical social structure – not necessarily because the underlying mechanisms differ, but because different environments place distinct demands on social functioning[1,283,284]. Collaboration with evolutionary biologists could enable phylogenetic signal analyses[285] to assess whether traits like parental care and prosocial behavior co-evolved across species, and under what ecological conditions these behaviors emerge or are suppressed.

Ethologically relevant behavioral paradigms: All experiments were conducted in the home cage environment. However, future studies could further enhance ecological validity by testing comforting behavior in more naturalistic or decision-based paradigms. Would mice voluntarily approach and comfort a distressed partner when doing so incurs risk or effort, such as crossing a mildly anxiogenic or risky environment? Would they show a preference for interacting with a distressed partner over a neutral one when given the choice? These paradigms could clarify the motivational strength and flexibility of comforting behavior, and whether such decisions reflect active prosocial intent under competing behavioral demands.

Bidirectional dynamics between helper and recipient: Much of the existing literature, including this dissertation, has focused on the behavioral and neural correlates of the helper. We highlight the importance of examining helper and recipient as a dynamic system where distress precipitates comforting that then reduces distress[213,286]. Future work using simultaneous long-term physiological measurements or neuronal recordings of stress

signals across animal dyads could capture how distress signals are transmitted, perceived, and resolved. Such work is essential for providing a more comprehensive understanding of the neurobiology and dynamics of comforting touch.

In sum, this dissertation presents evidence that comforting behavior in mice engages neural circuits that overlap with those for parental care, suggesting a shared biological foundation for responding to others' distress. While comforting and parenting are behaviorally distinct, these data support a functional model in which neural systems involved in responding to offspring need may be flexibly engaged to support broader forms of social care. At the same time, comforting behavior is state-specific and dynamically modulated, pointing to the complexity of prosocial motivation even in rodents. These findings underscore the utility of mouse models for understanding the building blocks of social behavior and open new pathways for exploring how caregiving and empathy emerge in the brain.

APPENDIX: STATISTICAL METHODS

All statistical analyses were conducted using Prism (v9 or v10, GraphPad) or MATLAB (R2019b or R2021b, MathWorks). All statistical tests, corresponding p-values, and sample sizes are provided within the figures or in the figure legends. P-value labels denote *P < 0.05. **P < 0.01. ***P < 0.001 ****P < 0.0001. ns, not significant, unless otherwise indicated. In all figures with boxplots, the center line in the boxplots indicates the median, the box limits indicate the upper and lower quartiles, and the whiskers indicate data within 1.5× interquartile range. Data normality was examined using D'Agostino & Pearson test and Kolmogorov-Smirnov test when parametric tests were conducted. P values were corrected for multiple comparisons when necessary.

All experiments were conducted using two to five cohorts of animals. The results were reproducible across cohorts and combined for the final analysis. When possible, males and females were combined in subsequent analyses if there was no significant main effect of sex in an initial two-way ANOVA, with the treatment (e.g. Photoactivation) as other factor. Animals were randomly assigned to control and treatment groups. Example micrographs show representative results based on at least three independent animals. Sample sizes were not predetermined using statistical methods. Experiments were randomized whenever possible. Experimenters were not blind to group allocation during experimental procedures due to the experimental design, but were partially blind during behavioral scoring that was performed from video recordings using predefined criteria.

REFERENCES

1. de Waal, F. B. M. & Preston, S. D. Mammalian empathy: behavioural manifestations and neural basis. *Nat Rev Neurosci* **18**, 498–509 (2017).

2. Dunfield, K. A. A construct divided: prosocial behavior as helping, sharing, and comforting subtypes. *Front Psychol* **5**, (2014).

3. Mussen, P. & Eisenberg-Berg, N. *Roots of Caring, Sharing, and Helping: The Development of pro-Social Behavior in Children*. ix, 212 (W. H. Freeman, Oxford, England, 1977).

4. Rault, J.-L. Be kind to others: Prosocial behaviours and their implications for animal welfare. *Applied Animal Behaviour Science* **210**, 113–123 (2019).

5. Wu, Y. E. & Hong, W. Neural basis of prosocial behavior. *Trends in Neurosciences* **45**, (2022).

6. Almeida, D. M. *et al.* Charting adult development through (historically changing) daily stress processes. *American Psychologist* **75**, 511–524 (2020).

7. Eckstein, M., Mamaev, I., Ditzen, B. & Sailer, U. Calming Effects of Touch in Human, Animal, and Robotic Interaction—Scientific State-of-the-Art and Technical Advances. *Frontiers in Psychiatry* **11**, (2020).

8. Korisky, A., Eisenberger, N. I., Nevat, M., Weissman-Fogel, I. & Shamay-Tsoory, S. G. A dual-brain approach for understanding the neuralmechanisms that underlie the comforting effects of social touch. *Cortex* **127**, 333–346 (2020).

9. Suvilehto, J. T., Glerean, E., Dunbar, R. I. M., Hari, R. & Nummenmaa, L. Topography of social touching depends on emotional bonds between humans. *Proceedings of the National Academy of Sciences* **112**, 13811–13816 (2015).

10. Dunfield, K. A. & Kuhlmeier, V. A. Classifying Prosocial Behavior: Children's Responses to Instrumental Need, Emotional Distress, and Material Desire. *Child Dev* **84**, 1766–1776 (2013).

11. Fujisawa, K. K., Kutsukake, N. & Hasegawa, T. Peacemaking and consolation in Japanese preschoolers witnessing peer aggression. *J Comp Psychol* **120**, 48–57 (2006).

12. Zahn-Waxler, C., Radke-Yarrow, M., Wagner, E. & Chapman, M. Development of concern for others. *Developmental Psychology* **28**, 126–136 (1992).

13. Eisenberg, N. Prosocial behavior, empathy, and sympathy. in *Well-being: Positive development across the life course* 253–265 (Lawrence Erlbaum Associates Publishers, Mahwah, NJ, US, 2003). doi:10.4324/9781410607171.

14. Zahn-Waxler, C., Hollenbeck, B. & Radke-Yarrow, M. The Origins of Empathy and Altruism. in *Advances in Animal Welfare Science 1984* (eds. Fox, M. W. & Mickley, L.

D.) 21–41 (Springer Netherlands, Dordrecht, 1985). doi:10.1007/978-94-009-4998-0_2.

15. Jakubiak, B. K. & Feeney, B. C. Affectionate Touch to Promote Relational, Psychological, and Physical Well-Being in Adulthood: A Theoretical Model and Review of the Research. *Pers Soc Psychol Rev* **21**, 228–252 (2017).

16. Ferretti, V. & Papaleo, F. Understanding others: Emotion recognition in humans and other animals. *Genes, Brain and Behavior* **18**, e12544 (2019).

17. Meyza, K. Z., Bartal, I. B.-A., Monfils, M. H., Panksepp, J. B. & Knapska, E. The roots of empathy: Through the lens of rodent models. *Neuroscience & Biobehavioral Reviews* **76**, 216–234 (2017).

18. Panksepp, J. B. & Lahvis, G. P. Rodent Empathy and Affective Neuroscience. *Neurosci Biobehav Rev* **35**, 1864–1875 (2011).

19. Paradiso, E., Gazzola, V. & Keysers, C. Neural mechanisms necessary for empathy-related phenomena across species. *Curr Opin Neurobiol* **68**, 107–115 (2021).

20. Sivaselvachandran, S., Acland, E. L., Abdallah, S. & Martin, L. J. Behavioral and mechanistic insight into rodent empathy. *Neuroscience & Biobehavioral Reviews* **91**, 130–137 (2018).

21. Atrooz, F., Alkadhi, K. A. & Salim, S. Understanding stress: Insights from rodent models. *Current Research in Neurobiology* **2**, 100013 (2021).

22. Brechbühl, J. *et al.* Mouse alarm pheromone shares structural similarity with predator scents. *Proc Natl Acad Sci U S A* **110**, 4762–4767 (2013).

23. Inagaki, H. *et al.* The volatility of an alarm pheromone in male rats. *Physiology & Behavior* **96**, 749–752 (2009).

24. Kiyokawa, Y., Kikusui, T., Takeuchi, Y. & Mori, Y. Alarm Pheromones with Different Functions are Released from Different Regions of the Body Surface of Male Rats. *Chemical Senses* **29**, 35–40 (2004).

25. Novotny, M. V. Pheromones, binding proteins and receptor responses in rodents. *Biochemical Society Transactions* **31**, 117–122 (2003).

26. Wu, Y. E. *et al.* Neural control of affiliative touch in prosocial interaction. *Nature* **599**, 262–267 (2021).

27. Geng, K.-W. *et al.* Image-Forming Visual Basis of Empathy for Pain in Mice. *Neurosci. Bull.* **36**, 1563–1569 (2020).

28. Marsh, A. A. & Ambady, N. The influence of the fear facial expression on prosocial responding. *Cognition and Emotion* **21**, 225–247 (2007).

29. Peled-Avron, L., Goldstein, P., Yellinek, S., Weissman-Fogel, I. & Shamay-Tsoory, S. G. Empathy during consoling touch is modulated by mu-rhythm: An EEG study.

Neuropsychologia **116**, 68–74 (2018).

30. Pérez-Manrique, A. & Gomila, A. The comparative study of empathy: sympathetic concern and empathic perspective-taking in non-human animals. *Biological Reviews* **93**, 248–269 (2018).

31. Burkett, J. P. *et al.* Oxytocin-dependent consolation behavior in rodents. *Science* **351**, 375–378 (2016).

32. Carneiro de Oliveira, P. E. *et al.* Mice Cohabiting With Familiar Conspecific in Chronic Stress Condition Exhibit Methamphetamine-Induced Locomotor Sensitization and Augmented Consolation Behavior. *Frontiers in Behavioral Neuroscience* **16**, (2022).

33. Li, L.-F. *et al.* Involvement of oxytocin and GABA in consolation behavior elicited by socially defeated individuals in mandarin voles. *Psychoneuroendocrinology* **103**, 14–24 (2019).

34. Zeng, Q., Shan, W., Zhang, H., Yang, J. & Zuo, Z. Paraventricular thalamic nucleus plays a critical role in consolation and anxious behaviors of familiar observers exposed to surgery mice. *Theranostics* **11**, 3813–3829 (2021).

35. Aureli, F., Preston, S. D. & de Waal, F. B. M. Heart rate responses to social interactions in free-moving rhesus macaques (Macaca mulatta): A pilot study. *Journal of Comparative Psychology* **113**, 59–65 (1999).

36. Boccia, M. L., Reite, M. & Laudenslager, M. On the physiology of grooming in a pigtail macaque. *Physiology & Behavior* **45**, 667–670 (1989).

37. Normando, S., Haverbeke, A., Meers, L., Ödberg, F. & TALLEGON, M. Heart rate reduction by grooming in horses (Equus caballus). in (2002).

38. Sato, S. & Tarumizu, K. Heart rates before, during and after allo-grooming in cattle (Bos taurus). *J. Ethol.* **11**, 149–150 (1993).

39. Fraser, O. N., Stahl, D. & Aureli, F. Stress reduction through consolation in chimpanzees. *PNAS Proceedings of the National Academy of Sciences of the United States of America* **105**, 8557–8562 (2008).

40. Kaada, B. & Torsteinbø, O. Increase of plasma beta-endorphins in connective tissue massage. *Gen Pharmacol* **20**, 487–489 (1989).

41. Keverne, E. B., Martensz, N. D. & Tuite, B. Beta-endorphin concentrations in cerebrospinal fluid of monkeys are influenced by grooming relationships. *Psychoneuroendocrinology* **14**, 155–161 (1989).

42. Russell, Y. I. & Phelps, S. How Do You Measure Pleasure? A Discussion About Intrinsic Costs and Benefits in Primate Allogrooming. *Biology and Philosophy* **28**, 1005–1020 (2013).

43. Feh, C. & de Mazières, J. Grooming at a preferred site reduces heart rate in horses.

Animal Behaviour **46**, 1191–1194 (1993).

44. Coulon, M. *et al.* Do Lambs Perceive Regular Human Stroking as Pleasant? Behavior and Heart Rate Variability Analyses. *PLOS ONE* **10**, e0118617 (2015).

45. Tinbergen, N. *The Study of Instinct*. xii, 237 (Clarendon Press/Oxford University Press, New York, NY, US, 1951).

46. Bateson, P. & Laland, K. N. Tinbergen's four questions: an appreciation and an update. *Trends in Ecology & Evolution* **28**, 712–718 (2013).

47. Mayr, E. Cause and Effect in Biology. *Science* **134**, 1501–1506 (1961).

48. Laland, K. N., Sterelny, K., Odling-Smee, J., Hoppitt, W. & Uller, T. Cause and effect in biology revisited: is Mayr's proximate-ultimate dichotomy still useful? *Science* **334**, 1512–1516 (2011).

49. Dunbar, R. I. M. The social role of touch in humans and primates: Behavioural function and neurobiological mechanisms. *Neuroscience & Biobehavioral Reviews* **34**, 260–268 (2010).

50. Pellis, S. M. & Pellis, V. C. Social play, social grooming, and the regulation of social relationships. in *Neurobiology of grooming behavior* 66–87 (Cambridge University Press, New York, NY, US, 2010). doi:10.1017/CBO9780511676109.005.

51. Spruijt, B. M., van Hooff, J. A. & Gispen, W. H. Ethology and neurobiology of grooming behavior. *Physiological Reviews* **72**, 825–852 (1992).

52. Morrison, I. Keep Calm and Cuddle on: Social Touch as a Stress Buffer. *Adaptive Human Behavior and Physiology* **2**, 344–362 (2016).

53. Clay, Z. & de Waal, F. B. M. Bonobos respond to distress in others: consolation across the age spectrum. *PLoS One* **8**, e55206 (2013).

54. de Waal, F. B. M. & van Roosmalen, A. Reconciliation and consolation among chimpanzees. *Behav Ecol Sociobiol* **5**, 55–66 (1979).

55. Jablonski, N. G. Social and affective touch in primates and its role in the evolution of social cohesion. *Neuroscience* **464**, 117–125 (2021).

56. Newton-Fisher, N. E. & Kaburu, S. S. K. Grooming decisions under structural despotism: the impact of social rank and bystanders among wild male chimpanzees. *Animal Behaviour* **128**, 153–164 (2017).

57. Schino, G. & Aureli, F. The relative roles of kinship and reciprocity in explaining primate altruism. *Ecology Letters* **13**, 45–50 (2010).

58. Plotnik, J. M. & Waal, F. B. M. de. Asian elephants (Elephas maximus) reassure others in distress. *PeerJ* **2**, e278 (2014).

59. de Freslon, I., Peralta, J. M., Strappini, A. C. & Monti, G. Understanding Allogrooming Through a Dynamic Social Network Approach: An Example in a Group of Dairy Cows. *Frontiers in Veterinary Science* **7**, (2020).

60. Wood, M. T. Social grooming patterns of dairy cattle. *Proceedings of the New Zealand Society of Animal Production* **35**, 219–220 (1975).

61. Shimada, M. & Suzuki, N. The Contribution of Mutual Grooming to Affiliative Relationships in a Feral Misaki Horse Herd. *Animals* **10**, 1564 (2020).

62. VanDierendonck, M. C. & Spruijt, B. M. Coping in groups of domestic horses – Review from a social and neurobiological perspective. *Applied Animal Behaviour Science* **138**, 194–202 (2012).

63. Narizano, H. & Carter, G. G. Do vampire bats groom others based on need? *Behavioral Ecology* **31**, 107–113 (2020).

64. Bradshaw, J. W. S. Sociality in cats: A comparative review. *Journal of Veterinary Behavior* **11**, 113–124 (2016).

65. Matoba, T., Kutsukake, N. & Hasegawa, T. Head Rubbing and Licking Reinforce Social Bonds in a Group of Captive African Lions, Panthera leo. *PLOS ONE* **8**, e73044 (2013).

66. van den Bos, R. The function of allogrooming in domestic cats (Felis silvestris catus); a study in a group of cats living in confinement. *J. Ethol.* **16**, 1–13 (1998).

67. Fraser, O. N. & Bugnyar, T. Do Ravens Show Consolation? Responses to Distressed Others. *PLOS ONE* **5**, e10605 (2010).

68. Kenny, E., Birkhead, T. R. & Green, J. P. Allopreening in birds is associated with parental cooperation over offspring care and stable pair bonds across years. *Behavioral Ecology* **28**, 1142–1148 (2017).

69. Lewis, S., Roberts, G., Harris, M. P., Prigmore, C. & Wanless, S. Fitness increases with partner and neighbour allopreening. *Biology Letters* **3**, 386–389 (2007).

70. Radford, A. N. & Du Plessis, M. A. Dual function of allopreening in the cooperatively breeding green woodhoopoe, Phoeniculus purpureus. *Behav Ecol Sociobiol* **61**, 221–230 (2006).

71. Seed, A. M., Clayton, N. S. & Emery, N. J. Postconflict Third-Party Affiliation in Rooks, Corvus frugilegus. *Current Biology* **17**, 152–158 (2007).

72. Simpson, J. A. & Beckes, L. Evolutionary perspectives on prosocial behavior. in *Prosocial motives, emotions, and behavior: The better angels of our nature.* (eds. Mikulincer, M. & Shaver, P. R.) 35–53 (American Psychological Association, Washington, 2010). doi:10.1037/12061-002.

73. Gilbert, P. The Evolution of Pro-social Behavior: From Caring to Compassion. in *The*

Cambridge Handbook of Evolutionary Perspectives on Human Behavior (eds. Workman, L., Reader, W. & Barkow, J. H.) 419–435 (Cambridge University Press, 2020). doi:10.1017/9781108131797.035.

74. Phillips, H. L. *et al.* Dorsomedial prefrontal hypoexcitability underlies lost empathy in frontotemporal dementia. *Neuron* (2023) doi:10.1016/j.neuron.2022.12.027.

75. Lu, Y.-F. *et al.* Social interaction with a cagemate in pain increases allogrooming and induces pain hypersensitivity in the observer rats. *Neurosci Lett* **662**, 385–388 (2018).

76. Dolensek, N., Gehrlach, D. A., Klein, A. S. & Gogolla, N. Facial expressions of emotion states and their neuronal correlates in mice. *Science* **368**, 89–94 (2020).

77. Whittaker, A. L., Liu, Y. & Barker, T. H. Methods Used and Application of the Mouse Grimace Scale in Biomedical Research 10 Years on: A Scoping Review. *Animals (Basel)* **11**, 673 (2021).

78. Langford, D. J. *et al.* Coding of facial expressions of pain in the laboratory mouse. *Nat Methods* **7**, 447–449 (2010).

79. Ebbesen, C. L. & Froemke, R. C. Body language signals for rodent social communication. *Current Opinion in Neurobiology* **68**, 91–106 (2021).

80. Lee, I.-C., Yu, T.-H., Liu, W.-H. & Hsu, K.-S. Social Transmission and Buffering of Hippocampal Metaplasticity after Stress in Mice. *J. Neurosci.* **41**, 1317–1330 (2021).

81. Keysers, C., Knapska, E., Moita, M. A. & Gazzola, V. Emotional contagion and prosocial behavior in rodents. *Trends in Cognitive Sciences* **26**, 688–706 (2022).

82. Sterley, T.-L. *et al.* Social transmission and buffering of synaptic changes after stress. *Nat Neurosci* **21**, 393–403 (2018).

83. Kiyokawa, Y., Kikusui, T., Takeuchi, Y. & Mori, Y. Partner's stress status influences social buffering effects in rats. *Behav Neurosci* **118**, 798–804 (2004).

84. Arakawa, H., Blanchard, D. C. & Blanchard, R. J. Colony formation of C57BL/6J mice in visible burrow system: identification of eusocial behaviors in a background strain for genetic animal models of autism. *Behav Brain Res* **176**, 27–39 (2007).

85. Kalueff, A. V., Minasyan, A., Keisala, T., Shah, Z. H. & Tuohimaa, P. Hair barbering in mice: Implications for neurobehavioural research. *Behavioural Processes* **71**, 8–15 (2006).

86. Barnett, S. A. *The Rat: A Study in Behavior*. (University of Chicago Press, 1963).

87. Geyer, L. A. & Kornet, C. Effects of tastants on caching, gnawing, grooming and taste aversions in Pine Voles (Microtus pinetorum) and Meadow Voles (M. pennsylvanicus).

88. Happold, M. Social Behavior of the Conilurine Rodents (Muridae) of Australia. *Zeitschrift für Tierpsychologie* **40**, 113–182 (1976).

89. Mondragón, R., Mayagoitia, L., López-Luján, A. & Díaz, J. L. Social structure features in three inbred strains of mice, C57Bl/6J, Balb/cj, and NIH: a comparative study. *Behav Neural Biol* **47**, 384–391 (1987).

90. Schweinfurth, M. K., Stieger, B. & Taborsky, M. Experimental evidence for reciprocity in allogrooming among wild-type Norway rats. *Sci Rep* **7**, 4010 (2017).

91. Schweinfurth, M. K. *et al.* Do female Norway rats form social bonds? *Behav Ecol Sociobiol* **71**, 98 (2017).

92. Schweinfurth, M. K. & Taborsky, M. Reciprocal Trading of Different Commodities in Norway Rats. *Current Biology* **28**, 594-599.e3 (2018).

93. So, N., Franks, B., Lim, S. & Curley, J. P. A Social Network Approach Reveals Associations between Mouse Social Dominance and Brain Gene Expression. *PLOS ONE* **10**, e0134509 (2015).

94. Hart, B. L. Behavioral adaptations to pathogens and parasites: Five strategies. *Neuroscience & Biobehavioral Reviews* **14**, 273–294 (1990).

95. Murray, M. D. Effects of host grooming on louse populations. *Parasitology Today* **3**, 276–278 (1987).

96. Schweinfurth, M. K. The social life of Norway rats (Rattus norvegicus). *eLife* **9**, e54020 (2020).

97. Weisbroth, S. H., Friedman, S., Powell, M. & Scher, S. The parasitic ecology of the rodent mite Myobia musculi. I. Grooming factors. *Lab Anim Sci* **24**, 510–516 (1974).

98. Lee, W., Fu, J., Bouwman, N., Farago, P. & Curley, J. P. Temporal microstructure of dyadic social behavior during relationship formation in mice. *PLoS One* **14**, e0220596 (2019).

99. Barabas, A. J., Lucas, J. R., Erasmus, M. A., Cheng, H.-W. & Gaskill, B. N. Who's the Boss? Assessing Convergent Validity of Aggression Based Dominance Measures in Male Laboratory Mice, Mus Musculus. *Frontiers in Veterinary Science* **8**, (2021).

100. Fernández-Vargas, M., Tang-Martínez, Z. & Phelps, S. M. Singing, allogrooming, and allomarking behaviour during inter- and intra-sexual encounters in the Neotropical short-tailed singing mouse (Scotinomys teguina). *Behaviour* **148**, 945–965 (2011).

101. Polechová, J. & Stopka, P. Geometry of social relationships in the Old World wood mouse, *Apodemus sylvaticus*. *Can. J. Zool.* **80**, 1383–1388 (2002).

102. Stopka, P. & Graciasová, R. Conditional allogrooming in the herb-field mouse. *Behavioral Ecology* **12**, 584–589 (2001).

103. Stopka, P. & Macdonald, D. W. The Market Effect in the Wood Mouse, Apodemus sylvaticus:Selling Information on Reproductive Status. *Ethology* **105**, 969–982 (1999).

104. Wilson, S. P. Modelling the emergence of rodent filial huddling from physiological huddling. *R Soc Open Sci* **4**, 170885 (2017).

105. Groó, Z., Szenczi, P., Bánszegi, O., Nagy, Z. & Altbäcker, V. The influence of familiarity and temperature on the huddling behavior of two mouse species with contrasting social systems. *Behav Processes* **151**, 67–72 (2018).

106. Alberts, J. R. Huddling by rat pups: Group behavioral mechanisms of temperature regulation and energy conservation. *Journal of Comparative and Physiological Psychology* **92**, 231–245 (1978).

107. Gilbert, C. *et al.* One for all and all for one: the energetic benefits of huddling in endotherms. *Biological Reviews* **85**, 545–569 (2010).

108. Sánchez, E. R., Solís, R., Torres-Contreras, H. & Canals, M. Self-organization in the dynamics of huddling behavior in Octodon degus in two contrasting seasons. *Behav Ecol Sociobiol* **69**, 787–794 (2015).

109. Glancy, J. P., Gross, R., Stone, J. V. & Wilson, S. P. A Self-Organising Model of Thermoregulatory Huddling. *PLOS Computational Biology* **11**, (2015).

110. Sukhchuluun, G., Zhang, X.-Y., Chi, Q.-S. & Wang, D.-H. Huddling Conserves Energy, Decreases Core Body Temperature, but Increases Activity in Brandt's Voles (Lasiopodomys brandtii). *Front. Physiol.* **9**, (2018).

111. Matsumoto, M. *et al.* Indispensable role of the oxytocin receptor for allogrooming toward socially distressed cage mates in female mice. *J Neuroendocrinol* **33**, e12980 (2021).

112. Muroy, S. E., Long, K. L. P., Kaufer, D. & Kirby, E. D. Moderate Stress-Induced Social Bonding and Oxytocin Signaling are Disrupted by Predator Odor in Male Rats. *Neuropsychopharmacology* **41**, 2160–2170 (2016).

113. Fukumitsu, K. *et al.* Amylin-Calcitonin receptor signaling in the medial preoptic area mediates affiliative social behaviors in female mice. *Nat Commun* **13**, 709 (2022).

114. Brudzynski, S. M. Biological Functions of Rat Ultrasonic Vocalizations, Arousal Mechanisms, and Call Initiation. *Brain Sciences* **11**, 605 (2021).

115. Blumberg, M. S., Efimova, I. V. & Alberts, J. R. Ultrasonic vocalizations by rat pups: The primary importance of ambient temperature and the thermal significance of contact comfort. *Developmental Psychobiology* **25**, 229–250 (1992).

116. Bowen, M. T. *et al.* Defensive Aggregation (Huddling) in Rattus Norvegicus toward Predator Odor: Individual Differences, Social Buffering Effects and Neural Correlates. *PLoS One* **8**, e68483 (2013).

117. Kim, J. *et al.* A bird's-eye view of brain activity in socially interacting mice through mobile edge computing (MEC). *Sci Adv* **6**, eabb9841 (2020).

118. Kim, S.-W., Kim, M. & Shin, H.-S. Affective empathy and prosocial behavior in rodents. *Current Opinion in Neurobiology* **68**, 181–189 (2021).

119. Allsop, S. A. *et al.* Corticoamygdala Transfer of Socially Derived Information Gates Observational Learning. *Cell* **173**, 1329-1342.e18 (2018).

120. Andraka, K. *et al.* Distinct circuits in rat central amygdala for defensive behaviors evoked by socially signaled imminent versus remote danger. *Curr Biol* **31**, 2347-2358.e6 (2021).

121. Jeon, D. *et al.* Observational fear learning involves affective pain system and Ca v 1.2 Ca 2+ channels in ACC. *Nat Neurosci* **13**, 482–488 (2010).

122. Rogers-Carter, M. M. *et al.* Insular cortex mediates approach and avoidance responses to social affective stimuli. *Nature Neuroscience* **21**, 404–414 (2018).

123. Ryan, B. C., Young, N. B., Moy, S. S. & Crawley, J. N. Olfactory cues are sufficient to elicit social approach behaviors but not social transmission of food preference in C57BL/6J mice. *Behavioural Brain Research* **193**, 235–242 (2008).

124. Sterley, T.-L. & Bains, J. S. Social communication of affective states. *Current Opinion in Neurobiology* **68**, 44–51 (2021).

125. Barabas, A. J., Aryal, U. K. & Gaskill, B. N. Protein profiles from used nesting material, saliva, and urine correspond with social behavior in group housed male mice, Mus musculus. *Journal of Proteomics* **266**, 104685 (2022).

126. Barabas, A. J. *et al.* Compounds from plantar foot sweat, nesting material, and urine show strain patterns associated with agonistic and affiliative behaviors in group housed male mice, Mus musculus. *PLOS ONE* **16**, e0251416 (2021).

127. Chen, P. B. *et al.* Sexually Dimorphic Control of Parenting Behavior by the Medial Amygdala. *Cell* **176**, 1206-1221.e18 (2019).

128. Imamura, F., Ito, A. & LaFever, B. J. Subpopulations of Projection Neurons in the Olfactory Bulb. *Frontiers in Neural Circuits* **14**, (2020).

129. Raam, T. & Hong, W. Organization of neural circuits underlying social behavior: A consideration of the medial amygdala. *Current Opinion in Neurobiology* **68**, 124–136 (2021).

130. Keller, D. *et al.* A thalamo-preoptic pathway promotes social grooming in rodents. *Current Biology* S0960982222013847 (2022) doi:10.1016/j.cub.2022.08.062.

131. Barsy, B. *et al.* Associative and plastic thalamic signaling to the lateral amygdala controls fear behavior. *Nat Neurosci* **23**, 625–637 (2020).

132. Dobolyi, A., Cservenák, M. & Young, L. J. Thalamic integration of social stimuli regulating parental behavior and the oxytocin system. *Frontiers in Neuroendocrinology* **51**, 102–115 (2018).

133. Motomura, K. & Kosaka, T. Medioventral part of the posterior thalamus in the mouse. *Journal of Chemical Neuroanatomy* **42**, 192–209 (2011).

134. Kirouac, G. J. The Paraventricular Nucleus of the Thalamus as an Integrating and Relay Node in the Brain Anxiety Network. *Front Behav Neurosci* **15**, 627633 (2021).

135. Penzo, M. A. & Gao, C. The paraventricular nucleus of the thalamus: an integrative node underlying homeostatic behavior. *Trends in Neurosciences* **44**, 538–549 (2021).

136. Burgos-Robles, A., Gothard, K. M., Monfils, M. H., Morozov, A. & Vicentic, A. Conserved features of anterior cingulate networks support observational learning across species. *Neuroscience & Biobehavioral Reviews* **107**, 215–228 (2019).

137. Li, L.-F. *et al.* Dorsal raphe nucleus to anterior cingulate cortex 5-HTergic neural circuit modulates consolation and sociability. 2020.09.21.307280 Preprint at https://doi.org/10.1101/2020.09.21.307280 (2021).

138. Zhang, M., Wu, Y. E., Jiang, M. & Hong, W. Cortical regulation of helping behaviour towards others in pain. *Nature* **626**, 136–144 (2024).

139. Peen, N. F., Duque-Wilckens, N. & Trainor, B. C. Convergent neuroendocrine mechanisms of social buffering and stress contagion. *Hormones and Behavior* **129**, 104933 (2021).

140. Pisansky, M. T., Hanson, L. R., Gottesman, I. I. & Gewirtz, J. C. Oxytocin enhances observational fear in mice. *Nat Commun* **8**, 2102 (2017).

141. Li, L.-F. *et al.* Reduced Consolation Behaviors in Physically Stressed Mandarin Voles: Involvement of Oxytocin, Dopamine D2, and Serotonin 1A Receptors Within the Anterior Cingulate Cortex. *International Journal of Neuropsychopharmacology* **23**, 511–523 (2020).

142. Arias del Razo, R. *et al.* Effects of chronic intranasal oxytocin on behavior and cerebral glucose uptake in juvenile titi monkeys. *Psychoneuroendocrinology* **113**, 104494 (2020).

143. Camerlink, I., Reimert, I. & Bolhuis, J. E. Intranasal oxytocin administration in relationship to social behaviour in domestic pigs. *Physiology & Behavior* **163**, 51–55 (2016).

144. Carter, G. G. & Wilkinson, G. S. Intranasal oxytocin increases social grooming and food sharing in the common vampire bat Desmodus rotundus. *Hormones and Behavior* **75**, 150–153 (2015).

145. Marsh, N., Marsh, A. A., Lee, M. R. & Hurlemann, R. Oxytocin and the Neurobiology of Prosocial Behavior. *Neuroscientist* **27**, 604–619 (2021).

146. Freeman, A. R., Aulino, E. A., Caldwell, H. K. & Ophir, A. G. Comparison of the distribution of oxytocin and vasopressin 1a receptors in rodents reveals conserved and derived patterns of nonapeptide evolution. *Journal of Neuroendocrinology* **32**, e12828

(2020).

147. Sharma, K. *et al.* Sexually dimorphic oxytocin receptor-expressing neurons in the preoptic area of the mouse brain. *PLoS One* **14**, e0219784 (2019).

148. Barrett, L. R., Nunez, J. & Zhang, X. Oxytocin activation of paraventricular thalamic neurons promotes feeding motivation to attenuate stress-induced hypophagia. *Neuropsychopharmacol.* **46**, 1045–1056 (2021).

149. Gur, R., Tendler, A. & Wagner, S. Long-Term Social Recognition Memory Is Mediated by Oxytocin-Dependent Synaptic Plasticity in the Medial Amygdala. *Biological Psychiatry* **76**, 377–386 (2014).

150. Yao, S., Bergan, J., Lanjuin, A. & Dulac, C. Oxytocin signaling in the medial amygdala is required for sex discrimination of social cues. *eLife* **6**, e31373 (2017).

151. Ishimura, K. *et al.* Quantitative analysis of the distribution of serotonin-immunoreactive cell bodies in the mouse brain. *Neuroscience Letters* **91**, 265–270 (1988).

152. Li, L.-F. *et al.* CRF-CRFR1 system within the dorsal medial prefrontal cortex are involved in consolation deficits under acute restraint stress in mandarin voles. *Psychoneuroendocrinology* **132**, 105353 (2021).

153. Kim, B. S. *et al.* Differential regulation of observational fear and neural oscillations by serotonin and dopamine in the mouse anterior cingulate cortex. *Psychopharmacology* **231**, 4371–4381 (2014).

154. Rodrigues Tavares, L. R. *et al.* 5-HT3 receptor within the amygdaloid complex modulates pain hypersensitivity induced by empathy model of cohabitation with a partner in chronic pain condition in mice. *Soc Neurosci* **16**, 534–548 (2021).

155. Cservenák, M. *et al.* A Thalamo-Hypothalamic Pathway That Activates Oxytocin Neurons in Social Contexts in Female Rats. *Endocrinology* **158**, 335–348 (2017).

156. Dimitrov, E. & Usdin, T. B. Tuberoinfundibular peptide of 39 residues modulates the mouse hypothalamic-pituitary-adrenal axis via paraventricular glutamatergic neurons. *J Comp Neurol* **518**, 4375–4394 (2010).

157. Nusbaum, M. P., Blitz, D. M. & Marder, E. Functional consequences of neuropeptide and small-molecule co-transmission. *Nat Rev Neurosci* **18**, 389–403 (2017).

158. Wu, Z., Lin, D. & Li, Y. Pushing the frontiers: tools for monitoring neurotransmitters and neuromodulators. *Nat Rev Neurosci* **23**, 257–274 (2022).

159. Abraira, V. E. & Ginty, D. D. The Sensory Neurons of Touch. *Neuron* **79**, (2013).

160. Horch, K. W., Tuckett, R. P. & Burgess, P. R. A KEY TO THE CLASSIFICATION OF CUTANEOUS MECHANORECEPTORS. *Journal of Investigative Dermatology* **69**, 75–82 (1977).

161. Pitcher, M., Le Pichon, C. E. & Chesler, A. Functional Properties of C-Low Threshold Mechanoreceptors (C-LTMRs) in Nonhuman Mammals. in *Affective Touch and the Neurophysiology of CT Afferents* (eds. Olausson, H., Wessberg, J., Morrison, I. & McGlone, F.) 31–48 (Springer, New York, NY, 2016). doi:10.1007/978-1-4939-6418-5_2.

162. Elias, L. J. & Abdus-Saboor, I. Bridging skin, brain, and behavior to understand pleasurable social touch. *Current Opinion in Neurobiology* **73**, 102527 (2022).

163. Zimmerman, A., Bai, L. & Ginty, D. D. The gentle touch receptors of mammalian skin. *Science* **346**, 950–954 (2014).

164. Li, L. *et al.* The functional organization of cutaneous low-threshold mechanosensory neurons. *Cell* **147**, 1615–1627 (2011).

165. Liu, Q. *et al.* Molecular genetic visualization of a rare subset of unmyelinated sensory neurons that may detect gentle touch. *Nat Neurosci* **10**, 946–948 (2007).

166. Vrontou, S., Wong, A. M., Rau, K. K., Koerber, H. R. & Anderson, D. J. Genetic identification of C fibres that detect massage-like stroking of hairy skin in vivo. *Nature* **493**, 669–673 (2013).

167. Delfini, M.-C. *et al.* TAFA4, a chemokine-like protein, modulates injury-induced mechanical and chemical pain hypersensitivity in mice. *Cell Rep* **5**, 378–388 (2013).

168. Reynders, A. *et al.* Transcriptional Profiling of Cutaneous MRGPRD Free Nerve Endings and C-LTMRs. *Cell Reports* **10**, 1007–1019 (2015).

169. Seal, R. P. *et al.* Injury-induced mechanical hypersensitivity requires C-low threshold mechanoreceptors. *Nature* **462**, 651–655 (2009).

170. McGlone, F., Wessberg, J. & Olausson, H. Discriminative and Affective Touch: Sensing and Feeling. *Neuron* **82**, 737–755 (2014).

171. Mortazavi, S. H., Khaki, S., Moradi, R., Heidari, K. & Vasegh Rahimparvar, S. F. Effects of massage therapy and presence of attendant on pain, anxiety and satisfaction during labor. *Arch Gynecol Obstet* **286**, 19–23 (2012).

172. Nummenmaa, L. *et al.* Social touch modulates endogenous μ-opioid system activity in humans. *NeuroImage* **138**, 242–247 (2016).

173. Perini, I., Olausson, H. & Morrison, I. Seeking pleasant touch: neural correlates of behavioral preferences for skin stroking. *Front Behav Neurosci* **9**, 8 (2015).

174. Tang, Y. *et al.* Social touch promotes interfemale communication via activation of parvocellular oxytocin neurons. *Nature Neuroscience* **23**, 1125–1137 (2020).

175. Weze, C., Leathard, H. L., Grange, J., Tiplady, P. & Stevens, G. Healing by Gentle Touch Ameliorates Stress and Other Symptoms in People Suffering with Mental Health Disorders or Psychological Stress. *Evid Based Complement Alternat Med* **4**, 115–123

(2007).

176. Liu, B. *et al.* Molecular and neural basis of pleasant touch sensation. *Science* **376**, 483–491 (2022).

177. Walker, S. C. *et al.* C-low threshold mechanoafferent targeted dynamic touch modulates stress resilience in rats exposed to chronic mild stress. *European Journal of Neuroscience* **55**, 2925–2938 (2020).

178. Schaffler, M. D. *et al.* A critical role for touch neurons in a skin-brain pathway for stress resilience. 2022.05.23.493062 Preprint at https://doi.org/10.1101/2022.05.23.493062 (2022).

179. Huzard, D. *et al.* The impact of C-tactile low-threshold mechanoreceptors on affective touch and social interactions in mice. *Science Advances* **8**, eabo7566 (2022).

180. Choi, S. *et al.* Parallel ascending spinal pathways for affective touch and pain. *Nature* **587**, 258–263 (2020).

181. Herman, J. P. Regulation of Hypothalamo-Pituitary-Adrenocortical Responses to Stressors by the Nucleus of the Solitary Tract/Dorsal Vagal Complex. *Cell Mol Neurobiol* **38**, 25–35 (2018).

182. Zoccal, D. B., Furuya, W. I., Bassi, M., Colombari, D. S. A. & Colombari, E. The nucleus of the solitary tract and the coordination of respiratory and sympathetic activities. *Frontiers in Physiology* **5**, (2014).

183. Füzesi, T., Daviu, N., Wamsteeker Cusulin, J. I., Bonin, R. P. & Bains, J. S. Hypothalamic CRH neurons orchestrate complex behaviours after stress. *Nat Commun* **7**, 11937 (2016).

184. Kim, J. S. & Iremonger, K. J. Temporally Tuned Corticosteroid Feedback Regulation of the Stress Axis. *Trends Endocrinol Metab* **30**, 783–792 (2019).

185. Marlin, B. J. & Froemke, R. C. Oxytocin modulation of neural circuits for social behavior. *Developmental Neurobiology* **77**, 169–189 (2017).

186. Onaka, T. & Takayanagi, Y. Role of oxytocin in the control of stress and food intake. *Journal of Neuroendocrinology* **31**, e12700 (2019).

187. Walker, S. C., Trotter, P. D., Swaney, W. T., Marshall, A. & Mcglone, F. P. C-tactile afferents: Cutaneous mediators of oxytocin release during affiliative tactile interactions? *Neuropeptides* **64**, 27–38 (2017).

188. Okabe, S., Takayanagi, Y., Yoshida, M. & Onaka, T. Gentle stroking stimuli induce affiliative responsiveness to humans in male rats. *Sci Rep* **10**, 9135 (2020).

189. Okabe, S., Yoshida, M., Takayanagi, Y. & Onaka, T. Activation of hypothalamic oxytocin neurons following tactile stimuli in rats. *Neuroscience Letters* **600**, 22–27 (2015).

190. Yu, H. *et al.* Social touch-like tactile stimulation activates a tachykinin 1-oxytocin pathway to promote social interactions. *Neuron* **110**, 1051-1067.e7 (2022).

191. Stock, S. & Uvnäs-Moberg, K. Increased plasma levels of oxytocin in response to afferent electrical stimulation of the sciatic and vagal nerves and in response to touch and pinch in anaesthetized rats. *Acta Physiologica Scandinavica* **132**, 29–34 (1988).

192. Heinrichs, M., Baumgartner, T., Kirschbaum, C. & Ehlert, U. Social support and oxytocin interact to suppress cortisol and subjective responses to psychosocial stress. *Biological Psychiatry* **54**, 1389–1398 (2003).

193. Morris, M., Callahan, M. F., Li, P. & Lucion, A. B. Central Oxytocin Mediates Stress-Induced Tachycardia. *Journal of Neuroendocrinology* **7**, 455–459 (1995).

194. Ring, R. H. *et al.* Anxiolytic-like activity of oxytocin in male mice: behavioral and autonomic evidence, therapeutic implications. *Psychopharmacology* **185**, 218–225 (2006).

195. Smith, A. S. & Wang, Z. Hypothalamic Oxytocin Mediates Social Buffering of the Stress Response. *Biological Psychiatry* **76**, 281–288 (2014).

196. Tops, M., Van Peer, J. M., Korf, J., Wijers, A. A. & Tucker, D. M. Anxiety, cortisol, and attachment predict plasma oxytocin. *Psychophysiology* **44**, 444–449 (2007).

197. Li, Q. *et al.* Foot massage evokes oxytocin release and activation of orbitofrontal cortex and superior temporal sulcus. *Psychoneuroendocrinology* **101**, 193–203 (2019).

198. Morhenn, V., Beavin, L. E. & Zak, P. J. Massage Increases Oxytocin and Reduces Adrenocorticotropin Hormone in Humans. *Alternative Therapies* **18**, (2012).

199. Uvnäs Moberg, K. & Petersson, M. Physiological effects induced by stimulation of cutaneous sensory nerves, with a focus on oxytocin. *Current Opinion in Behavioral Sciences* **43**, 159–166 (2022).

200. Kiyokawa, Y. & Hennessy, M. B. Comparative studies of social buffering: A consideration of approaches, terminology, and pitfalls. *Neuroscience & Biobehavioral Reviews* **86**, 131–141 (2018).

201. Bieler, M., Xu, X., Marquardt, A. & Hanganu-Opatz, I. L. Multisensory integration in rodent tactile but not visual thalamus. *Sci Rep* **8**, 15684 (2018).

202. Croy, I., Angelo, S. D. & Olausson, H. Reduced pleasant touch appraisal in the presence of a disgusting odor. *PLoS One* **9**, e92975 (2014).

203. Imschloss, M. & Kuehnl, C. Feel the Music! Exploring the Cross-modal Correspondence between Music and Haptic Perceptions of Softness. *Journal of Retailing* **95**, 158–169 (2019).

204. Jousmäki, V. & Hari, R. Parchment-skin illusion: sound-biased touch. *Current Biology* **8**, R190–R191 (1998).

205. Preston, S. D. The origins of altruism in offspring care. *Psychological Bulletin* **139**, 1305–1341 (2013).

206. Royle, N. J., Smiseth, P. T. & Kölliker, M. *The Evolution of Parental Care*. (Oxford University Press, 2012).

207. Burkart, J. M. *et al.* The evolutionary origin of human hyper-cooperation. *Nat Commun* **5**, 4747 (2014).

208. Fang, Y.-Y., Yamaguchi, T., Song, S. C., Tritsch, N. X. & Lin, D. A Hypothalamic Midbrain Pathway Essential for Driving Maternal Behaviors. *Neuron* **98**, 192-207.e10 (2018).

209. Wu, Z., Autry, A. E., Bergan, J. F., Watabe-Uchida, M. & Dulac, C. G. Galanin neurons in the medial preoptic area govern parental behaviour. *Nature* **509**, 325–330 (2014).

210. Numan, M. & Insel, T. R. *The Neurobiology of Parental Behavior*. (Springer, New York, 2003).

211. Wei, Y.-C. *et al.* Medial preoptic area in mice is capable of mediating sexually dimorphic behaviors regardless of gender. *Nat Commun* **9**, 279 (2018).

212. Numan, M. Neural basis of maternal behavior in the rat. *Psychoneuroendocrinology* **13**, 47–62 (1988).

213. Lim, K. Y. & Hong, W. Neural mechanisms of comforting: Prosocial touch and stress buffering. *Hormones and Behavior* **153**, (2023).

214. Kohl, J. *et al.* Functional circuit architecture underlying parental behaviour. *Nature* **556**, 326–331 (2018).

215. vom Saal, F. S. Variation in infanticide and parental behavior in male mice due to prior intrauterine proximity to female fetuses: Elimination by prenatal stress. *Physiology & Behavior* **30**, 675–681 (1983).

216. Chari, T., Griswold, S., Andrews, N. A. & Fagiolini, M. The Stage of the Estrus Cycle Is Critical for Interpretation of Female Mouse Social Interaction Behavior. *Front Behav Neurosci* **14**, 113 (2020).

217. Zeng, P.-Y., Tsai, Y.-H., Lee, C.-L., Ma, Y.-K. & Kuo, T.-H. Minimal influence of estrous cycle on studies of female mouse behaviors. *Front. Mol. Neurosci.* **16**, (2023).

218. Ajayi, A. F. & Akhigbe, R. E. Staging of the estrous cycle and induction of estrus in experimental rodents: an update. *Fertility Research and Practice* **6**, 5 (2020).

219. Byers, S. L., Wiles, M. V., Dunn, S. L. & Taft, R. A. Mouse estrous cycle identification tool and images. *PLoS One* **7**, e35538 (2012).

220. Ekambaram, G. Comparative Study on the Estimation of Estrous Cycle in Mice by Visual and Vaginal Lavage Method. *JCDR* (2017)

doi:10.7860/JCDR/2017/23977.9148.

221. McHenry, J. A. *et al.* Hormonal gain control of a medial preoptic area social reward circuit. *Nat Neurosci* **20**, 449–458 (2017).

222. Pnevmatikakis, E. A. & Giovannucci, A. NoRMCorre: An online algorithm for piecewise rigid motion correction of calcium imaging data. *Journal of Neuroscience Methods* **291**, 83–94 (2017).

223. Zhou, P. *et al.* Efficient and accurate extraction of in vivo calcium signals from microendoscopic video data. *eLife* **7**, e28728 (2018).

224. Kingsbury, L. *et al.* Correlated Neural Activity and Encoding of Behavior across Brains of Socially Interacting Animals. *Cell* **178**, 429-446.e16 (2019).

225. Moffitt, J. R. *et al.* Molecular, Spatial and Functional Single-Cell Profiling of the Hypothalamic Preoptic Region. *Science* **362**, (2018).

226. Mei, L., Osakada, T. & Lin, D. Hypothalamic control of innate social behaviors. *Science* **382**, 399–404 (2023).

227. Láng, T., Dimén, D., Oláh, S., Puska, G. & Dobolyi, A. Medial preoptic circuits governing instinctive social behaviors. *iScience* **27**, (2024).

228. Zhang, G.-W. *et al.* Medial preoptic area antagonistically mediates stress-induced anxiety and parental behavior. *Nature Neuroscience* 1–13 (2021) doi:10.1038/s41593-020-00784-3.

229. Armbruster, B. N., Li, X., Pausch, M. H., Herlitze, S. & Roth, B. L. Evolving the lock to fit the key to create a family of G protein-coupled receptors potently activated by an inert ligand. *Proceedings of the National Academy of Sciences* **104**, 5163–5168 (2007).

230. Mahn, M. *et al.* Efficient optogenetic silencing of neurotransmitter release with a mosquito rhodopsin. *Neuron* **109**, 1621-1635.e8 (2021).

231. Li, X.-Y. *et al.* AGRP Neurons Project to the Medial Preoptic Area and Modulate Maternal Nest-Building. *J Neurosci* **39**, 456–471 (2019).

232. Macbeth, A. H., Stepp, J. E., Lee, H.-J., Young III, W. S. & Caldwell, H. K. Normal maternal behavior, but increased pup mortality, in conditional oxytocin receptor knockout females. *Behavioral Neuroscience* **124**, 677–685 (2010).

233. Hidema, S. *et al.* Oxytocin Receptor-Expressing Neurons in the Medial Preoptic Area Are Essential for Lactation, whereas Those in the Lateral Septum Are Not Critical for Maternal Behavior. *Neuroendocrinology* **114**, 517–537 (2024).

234. Yoshihara, C. *et al.* Calcitonin receptor signaling in the medial preoptic area enables risk-taking maternal care. *Cell Reports* **35**, 109204 (2021).

235. Tsuneoka, Y. *et al.* Oxytocin Facilitates Allomaternal Behavior under Stress in

Laboratory Mice. *eNeuro* **9**, (2022).

236. Stagkourakis, S. *et al.* A Neuro-hormonal Circuit for Paternal Behavior Controlled by a Hypothalamic Network Oscillation. *Cell* **182**, 960-975.e15 (2020).

237. Smiley, K. O., Brown, R. S. E. & Grattan, D. R. Prolactin action is necessary for parental behavior in male mice. *J. Neurosci.* (2022) doi:10.1523/JNEUROSCI.0558-22.2022.

238. Karigo, T. *et al.* Distinct hypothalamic control of same- and opposite-sex mounting behaviour in mice. *Nature* **589**, 258–263 (2021).

239. Bayless, D. W. *et al.* A neural circuit for male sexual behavior and reward. *Cell* **0**, (2023).

240. Aknin, L. B., Van de Vondervoort, J. W. & Hamlin, J. K. Positive feelings reward and promote prosocial behavior. *Curr Opin Psychol* **20**, 55–59 (2018).

241. Curry, O. S. *et al.* Happy to help? A systematic review and meta-analysis of the effects of performing acts of kindness on the well-being of the actor. *Journal of Experimental Social Psychology* **76**, 320–329 (2018).

242. Mason, P. Lessons from helping behavior in rats. *Current Opinion in Neurobiology* **68**, 52–56 (2021).

243. Moll, J. *et al.* Human fronto-mesolimbic networks guide decisions about charitable donation. *Proc Natl Acad Sci U S A* **103**, 15623–15628 (2006).

244. Sáez, I., Zhu, L., Set, E., Kayser, A. & Hsu, M. Dopamine Modulates Egalitarian Behavior in Humans. *Current Biology* **25**, 912–919 (2015).

245. Sun, F. *et al.* Next-generation GRAB sensors for monitoring dopaminergic activity in vivo. *Nat Methods* **17**, 1156–1166 (2020).

246. Dai, B. *et al.* Responses and functions of dopamine in nucleus accumbens core during social behaviors. *Cell Reports* **40**, 111246 (2022).

247. Tao, C. *et al.* The medial preoptic area mediates depressive-like behaviors induced by ovarian hormone withdrawal through distinct GABAergic projections. *Nat Neurosci* 1–12 (2023) doi:10.1038/s41593-023-01397-2.

248. DeNardo, L. A. *et al.* Temporal evolution of cortical ensembles promoting remote memory retrieval. *Nat Neurosci* **22**, 460–469 (2019).

249. Yang, T. *et al.* Hypothalamic neurons that mirror aggression. *Cell* **186**, 1195-1211.e19 (2023).

250. Mayer, H. S. *et al.* Effects of maternal experience on pup-induced activation of maternal neural circuits in virgin mice. *Hormones and Behavior* **141**, 105129 (2022).

251. Adelman, J. S. & Martin, L. B. Vertebrate sickness behaviors: Adaptive and integrated neuroendocrine immune responses. *Integrative and Comparative Biology* **49**, 202–214 (2009).

252. Lopes, P. C. & König, B. Wild mice with different social network sizes vary in brain gene expression. *BMC Genomics* **21**, 506 (2020).

253. Andrews, P. L. R. & Horn, C. C. Signals for nausea and emesis: Implications for models of upper gastrointestinal diseases. *Auton Neurosci* **125**, 100–115 (2006).

254. Biesmans, S. *et al.* Systemic Immune Activation Leads to Neuroinflammation and Sickness Behavior in Mice. *Mediators of Inflammation* **2013**, 271359 (2013).

255. Sun, W. *et al.* Reviving-like prosocial behavior in response to unconscious or dead conspecifics in rodents. *Science* **387**, eadq2677 (2025).

256. Sun, F., Wu, Y. E. & Hong, W. A neural basis for prosocial behavior toward unresponsive individuals. *Science* **387**, eadq2679 (2025).

257. Lasselin, J. *et al.* Comparison of bacterial lipopolysaccharide-induced sickness behavior in rodents and humans: Relevance for symptoms of anxiety and depression. *Neuroscience & Biobehavioral Reviews* **115**, 15–24 (2020).

258. Kiesecker, J. M., Skelly, D. K., Beard, K. H. & Preisser, E. Behavioral reduction of infection risk. *Proceedings of the National Academy of Sciences* **96**, 9165–9168 (1999).

259. Behringer, D. C., Butler, M. J. & Shields, J. D. Ecological and physiological effects of PaV1 infection on the Caribbean spiny lobster (*Panulirus argus* Latreille). *Journal of Experimental Marine Biology and Ecology* **359**, 26–33 (2008).

260. Fairbanks, B. M., Hawley, D. M. & Alexander, K. A. No evidence for avoidance of visibly diseased conspecifics in the highly social banded mongoose (Mungos mungo). *Behav Ecol Sociobiol* **69**, 371–381 (2015).

261. Willette, A. A., Lubach, G. R. & Coe, C. L. Environmental context differentially affects behavioral, leukocyte, cortisol, and interleukin-6 responses to low doses of endotoxin in the rhesus monkey. *Brain Behav Immun* **21**, 807–815 (2007).

262. Loehle, C. Social Barriers to Pathogen Transmission in Wild Animal Populations. *Ecology* **76**, 326–335 (1995).

263. Stockmaier, S., Bolnick, D. I., Page, R. A. & Carter, G. G. Sickness effects on social interactions depend on the type of behaviour and relationship. *Journal of Animal Ecology* **89**, 1387–1394 (2020).

264. Boillat, M. *et al.* The Vomeronasal System Mediates Sick Conspecific Avoidance. *Current Biology* **25**, 251–255 (2015).

265. Weiss, J. *et al.* Sensing and avoiding sick conspecifics requires Gαi2+ vomeronasal

neurons. *BMC Biology* **21**, 152 (2023).

266. Edwards, J. C. The effects of *Trichinella spiralis* infection on social interactions in mixed groups of infected and uninfected male mice. *Animal Behaviour* **36**, 529–540 (1988).

267. Kwon, J.-T. *et al.* An amygdala circuit that suppresses social engagement. *Nature* **593**, 114–118 (2021).

268. Franco, N. H., Gerós, A., Oliveira, L., Olsson, I. A. S. & Aguiar, P. *ThermoLabAnimal* – A high-throughput analysis software for non-invasive thermal assessment of laboratory mice. *Physiology & Behavior* **207**, 113–121 (2019).

269. van der Vinne, V. *et al.* Continuous and non-invasive thermography of mouse skin accurately describes core body temperature patterns, but not absolute core temperature. *Sci Rep* **10**, 20680 (2020).

270. Kozak, W., Conn, C. A. & Kluger, M. J. Lipopolysaccharide induces fever and depresses locomotor activity in unrestrained mice. *Am J Physiol* **266**, R125-135 (1994).

271. Piirsalu, M. *et al.* Treatment With Lipopolysaccharide Induces Distinct Changes in Metabolite Profile and Body Weight in 129Sv and Bl6 Mouse Strains. *Front. Pharmacol.* **11**, (2020).

272. Zhang, F.-X. *et al.* Evaluating proxies for motion sickness in rodent. *IBRO Neuroscience Reports* **15**, 107–115 (2023).

273. Ding, W., Weltzien, H., Peters, C. & Klein, R. Nausea-induced suppression of feeding is mediated by central amygdala Dlk1-expressing neurons. *Cell Rep* **43**, 113990 (2024).

274. Benbow, T. *et al.* Peripheral N-methyl-d-aspartate receptor activation contributes to monosodium glutamate-induced headache but not nausea behaviours in rats. *Sci Rep* **12**, 13894 (2022).

275. Machuca-Márquez, P. *et al.* Vestibular CCK signaling drives motion sickness–like behavior in mice. *Proceedings of the National Academy of Sciences* **120**, e2304933120 (2023).

276. Liu, Y.-L., Malik, N., Sanger, G. J., Friedman, M. I. & Andrews, P. L. R. Pica—A model of nausea? Species differences in response to cisplatin. *Physiology & Behavior* **85**, 271–277 (2005).

277. Qian, K., Liu, J., Cao, Y., Yang, J. & Qiu, S. Intraperitoneal injection of lithium chloride induces lateralized activation of the insular cortex in adult mice. *Mol Brain* **14**, 71 (2021).

278. Shrum, B. *et al.* A robust scoring system to evaluate sepsis severity in an animal model. *BMC Research Notes* **7**, 233 (2014).

279. Savage, J. C., St-Pierre, M.-K., Hui, C. W. & Tremblay, M.-E. Microglial Ultrastructure in the Hippocampus of a Lipopolysaccharide-Induced Sickness Mouse Model. *Front. Neurosci.* **13**, (2019).

280. Stolzenberg, D. S. & Rissman, E. F. Oestrogen-Independent, Experience-Induced Maternal Behaviour in Female Mice. *Journal of Neuroendocrinology* **23**, 345–354 (2011).

281. Martín-Sánchez, A. *et al.* Wired for motherhood: induction of maternal care but not maternal aggression in virgin female CD1 mice. *Frontiers in Behavioral Neuroscience* **9**, (2015).

282. Stolzenberg, D. S. & Mayer, H. S. Experience-dependent mechanisms in the regulation of parental care. *Frontiers in Neuroendocrinology* **54**, 100745 (2019).

283. de Waal, F. B. M. Putting the altruism back into altruism: the evolution of empathy. *Annu Rev Psychol* **59**, 279–300 (2008).

284. Chen, Q., Panksepp, J. B. & Lahvis, G. P. Empathy Is Moderated by Genetic Background in Mice. *PLOS ONE* **4**, e4387 (2009).

285. Symonds, M. R. E. & Blomberg, S. P. A Primer on Phylogenetic Generalised Least Squares. in *Modern Phylogenetic Comparative Methods and Their Application in Evolutionary Biology: Concepts and Practice* (ed. Garamszegi, L. Z.) 105–130 (Springer, Berlin, Heidelberg, 2014). doi:10.1007/978-3-662-43550-2_5.

286. Kingsbury, L. & Hong, W. A Multi-Brain Framework for Social Interaction. *Trends Neurosci* **43**, 651–666 (2020).